# Temporal and spatial variations of cyanobacteria in Karori Reservoir, Wellington

A thesis
submitted in partial fulfillment
of the requirements for the degree
of
**Master of Science in Biological Science**
at
**The University of Waikato**
by
**Matthew James Prentice**


THE UNIVERSITY OF
WAIKATO
*Te Whare Wānanga o Waikato*

---

The University of Waikato
2008

# Abstract

The Lower Karori Reservoir (LKR) is a small, monomictic lake of 2.34 ha situated in the Karori Wildlife Sanctuary (KWS), Wellington. Over the past decade cyanobacterial blooms have become a common occurrence in this water body. In 2005 *Anabaena planktonica* was detected for the first time in the LKR and this species now forms dense blooms during summer. These blooms are problematic as they reduce aesthetic appeal and have resulted in odour problems for visitors to this high profile wildlife sanctuary. The objectives of this study were to identify key physical, chemical and biological variables influencing phytoplankton dynamics in the LKR and to use ecological models to investigate plausible management options. The key parameters investigated, that may cause bloom formation were; summer stratification, high nutrient levels, and the food web effects of a large population of European perch (*Perca fluviatilis*).

High resolution sampling was carried out every six hours over a 72 hour period during pre-bloom, bloom and post-bloom periods in 2006/7 to elucidate short term temporal and spatial variations in biological and physico-chemical parameters. Quantitative polymerase chain reaction (QPCR) was used to enumerate *A. planktonica* populations, allowing a large number of samples to be simultaneously evaluated. Algal densities were also estimated using conventional phytoplankton enumeration and chlorophyll *a* analysis. Water samples were collected for nutrient analysis at discrete depths and profiles were taken for temperature, dissolved oxygen and photosynthetic active radiation. Secchi depth and pH were also measured. Weekly or fortnightly phytoplankton and zooplankton samples and physical variables have been collected at LKR since September 2005 as part of an independent sampling program carried out by the KWS, Waikato University and Cawthron Institute. In this project the 2-year data set was used to assist with analysis of lake processes and for validation of the hydrodynamic-ecological model DYRESM-CAEDYM. Between 12 and 15 February, 2007, electric fishing was undertaken within the LKR. A total of 3,946 *P. fluviatilis* were removed and the effects on phytoplankton and zooplankton concentrations were investigated. To increase knowledge of the physiology of *A.*

*planktonica*, laboratory experiments were undertaken using cultures subjected to a range of different light intensities and temperature regimes

The phytoplankton assemblage of the LKR shows very distinct temporal variations. Summer stratification occurred in the LKR for ~4 months each summer. During these periods *A. planktonica* comprised up to 99.9% of the surface phytoplankton population. During isothermy chlorophytes, bacillariophytes and small flagellated dinophytes are co-dominant in the phytoplankton assemblage. The results of the QPCR showed distinct diurnal vertical movement of *A. planktonica*, with the highest cell concentrations occurring at 1900 hours at the surface. Ammonium ($NH_4$-N) is the dominant species of inorganic nitrogen during periods of stratification, while nitrate ($NO_3$-N) is generally dominant during times of isothermy. Phosphate concentrations at surface and depth remained at low levels throughout the sampling period. The large surface populations of *A. planktonica*, are probably responsible for the elevated total nitrogen concentrations in surface waters during stratified periods. There appeared to be some short term effects of the *P. fluviatilis* removal with an increase in large crustaceans (e.g., *Daphnia* sp.) and a reduction in *A. planktonica* densities observed in the months following the *P. fluviatilis* removal. Only a small proportion of the total *P. fluviatilis* population was removed and it is unlikely that the effects will be long-lasting without subsequent removal steps. However, it seems likely that *P. fluviatilis* is one of the factors contributing to cyanobacterial blooms and management of this fish species should be considered in future lake restoration plans. Growth experiments indicated *A. planktonica* grow over a wide range of light intensities and temperatures, although highest growth rates were generally associated with higher temperatures (25 °C) and light intensities (60 - 140 μmol $m^{-2}$ $s^{-1}$).

Ecological and hydrodynamic trends within the LKR over a two year period were simulated with adequate success using the model DYRESM-CAEDYM. Management scenarios simulated using DYRESM-CAEDYM suggest implementation of an artificial destratification system in the LKR may be the most practical and effective means of controlling *A. planktonica* blooms. The addition of

an artificial aeration system emitting air at a rate of approximately 50 $l^{-1}$ $s^{-1}$ should result in an isothermal system. Without summer stratification some of the physiological features of *A. planktonica* (e.g., buoyancy regulation and nitrogen-fixation) that give it a competitive advantage over other phytoplankton species will be reduced.

# Acknowledgements

I would like to thank my supervisor Professor David Hamilton and co-supervisor Dr Susie Wood for their expertise, advice and encouragement throughout this project. Thank you both for field assistance and valuable help in writing this thesis. Thank you Professor David Hamilton for assistance in the application of the model DYRESM-CAEDYM and Dr Susie Wood for algal identification and enumeration, QPCR analysis and culture experiments.

I thank Keith Calder and the staff of the Karori Wildlife Sanctuary for their friendly reception, assistance and support of my study. I also specifically thank Ron Goudswaard for his assistance on multiple occasions (rain, hail or shine) in collecting field data and for all other miscellaneous tasks he assisted with. Matu Booth is acknowledged for his assistance in sample collection at 0100 hours in February.

I thank Associate Professor Brendan Hicks for organising and implementing the perch removal between 12 and 15 February 2007, which I was able to make use of as part of this study. Also, Dr Ian Duggan is thanked for identification and enumeration of zooplankton samples and assistance with the application of CCA. Professor Craig Cary provided occasional scientific advice and expertise.

I thank Dr Andreas Rueckert for his assistance with QPCR analysis and use the *A. planktonica* probe, Dr Barry O'Brien for his assistance with microscopy and Bruce Patty for assistance with nutrient analysis. I also thank Lee Laboyrie, Alex Ring and Warrick Powrie for technical and field assistance.

I am indebted to Deniz Özkundakci and Austin Zhang for their assistance with nutrient analysis and Dennis Trolle, Chris McBride, Ditte Nielsen and Anders Nielsen for assistance with modelling. I also thank Wendy Paul for assistance with algal identification and enumeration, Bram Mulling for culture experiments, Richard O'Rorke for field assistance between 4 and 7 June 2007 and Grant Tempero for proof reading this work.

The University of Waikato is acknowledged for financial assistance through that of a Masters Research Scholarship, a Research Study Award and the Vivienne Cassie-Cooper Award.

Finally I would like to thank my family, Mark, Jenni, Ben and Zoe for their love and encouragement and also assistance with field work preparation and collection. And God.

# Table of Contents

# List of Figures

# List of Tables

# 1 Introduction

## *1.1 Eutrophication*

Eutrophication is the enhancement of the natural processes of biological production in rivers, lakes and reservoirs, caused by excess inputs of nitrogen and phosphorus (Chorus & Bartram, 1999). Over the last few decades, many previously oligotrophic waterbodies in New Zealand and around the world have become significantly eutrophied due to anthropogenic actions. This has led to considerable changes in the physical, chemical and biological parameters of affected lakes and reservoirs, and has resulted in increased incidences of phytoplankton blooms (Paerl, 1988; Oliver & Ganf, 2000; Anderson *et al.*, 2002).

Europhication is associated with increased productivity, simplification of biotic communities at all trophic levels, and a reduction in the ability organisms to adapt to enhanced nutrient loading (Wetzel, 2001). In most instances the phytoplankton community becomes dominated by cyanobacteria (Carmichael, 1995). As a result cyanobacterial dominance in lakes and reservoirs is commonly regarded as the ultimate phase of eutrophication (Dokulil & Teubner, 2000).

## *1.2 Cyanobacteria*

Cyanobacteria (cyanophyceae or blue-green algae) belong to the Kingdom Bacteria, Class Cyanoprokaryota. This class includes about 150 genera and approximately 2,000 species (Carmichael, 2001). Cyanobacteria may grow as single cells, filaments or colonies. At least 40 species are known to produce toxic substances known as cyanotoxins (Paerl, 1988; Hitzfeld *et al.*, 2000; Carmichael, 2001). Cyanobacteria produce a variety cyanotoxins, which may be categorized based on their function into; hepatotoxins, neurotoxins and cytotoxins (Hitzfeld *et al.*, 2000).

The predominant forms of nitrogen in aquatic habitats are dinitrogen gas, and to a lesser extent nitrate and ammonium. Most cyanobacterial species can use nitrate,

nitrite and ammonium as a nitrogen source for growth (Guerrero & Lara, 1987). Some species may also fix dinitrogen under inorganic nitrogen-depleted conditions (Paerl, 1988; Oliver & Ganf, 2000; Paerl *et al.*, 2001) by converting atmospheric dinitrogen gas into ammonium (Reynolds & Walsby, 1975; Paerl, 1988; Tandeau de Marsac & Houmard, 1993). This is achieved through specialized cells known as heterocytes, which are formed via the differentiation of vegetative cells under nitrogen limited conditions.

In addition to the ability to fix nitrogen under nitrogen depleted conditions, some species may also take up phosphorus in excess of their cellular requirements and store it for later use in phosphorus depleted conditions (Reynolds & Walsby, 1975; Dokulil & Teubner, 2000).

Many cyanobacteria species possess gas vacuoles, giving them the ability to regulate their buoyancy and control their position in the water column (Hitzfeld *et al.*, 2000). As a result these species have the ability to regulate their cell density and rapidly move up and down vertical light, temperature and nutrient gradients within a stratified water column (Paerl, 1988; Oliver, 1994; Oliver & Ganf, 2000). Rising and sinking rates in buoyant cyanobacteria have been demonstrated to be of the order of 50 m $day^{-1}$ for *A. circinalis* (Reynolds, 1972) and up to 140 m $day^{-1}$ for *Microcystis aeruginosa* (Reynolds & Walsby, 1975). The main environmental factor which affects buoyancy regulation in gas vacuolate cyanobacteria is light, with the availability of carbon, nitrogen and phosphorus affecting the response to light intensity (Tandeau de Marsac & Houmard, 1993). Cell buoyancy can be regulated in two ways. First the degree of gas vacuolation may be modified by collapsing of gas vesicles due to increased turgor pressure due to photosynthesis or by a reduction in gas vesicle synthesis (Oliver, 1994; Oliver & Ganf, 2000). Secondly by altering the extent to which carbohydrates are accumulated as ballast in the cell through photosynthesis and their reduction through respiration to a less dense protein (Oliver, 1994; Oliver & Ganf, 2000). This results in the cell accumulating carbohydrate under favorable light conditions, causing them to become less buoyant and to descend in the water column to the nutrient rich hypolimnion. Here as carbohydrate stores are used

up, they again become positively buoyant and return to surface waters. Advantages caused by buoyancy regulation include the reduction in sedimentation loss (Reynolds & Walsby, 1975; Reynolds, 1984), occupation of photosynthetically active radiation (PAR) and carbon dioxide ($CO_2$) rich surface layers during the day (Reynolds, 1972; Humphries & Lyne, 1988), and access to limiting resources, such as nitrogen and phosphorus, in vertically stratified waters at night (Ganf & Oliver, 1982).

Under conditions unfavorable for bloom maintenance (e.g., reduction in water temperature, water column mixing, grazing pressure) all major nitrogen-fixing cyanobacteria can morphologically and physiologically differentiate vegetative cells into resting spores known as akinetes. Akinetes resting in the sediment may be activated as the conditions become optimal and thus provide significant inocula for the development of pelagic cyanobacterial populations (Paerl, 1988).

Many cyanobacteria have high temperature optima for growth, around 25 °C (Robarts & Zohary, 1987) and also lower light energy requirements (Tilzer, 1987) in relation to other phytoplankton phyla. Most cyanobacteria harvest light primarily through unique structures known as phycobilisomes (Tilzer, 1987; Tandeau de Marsac & Houmard, 1993). In cyanobacteria, efficiency in light harvesting and energy transfer by phycobilisomes is close to 100%, and significantly higher than any pigments used by photosynthetic eukaryotes, allowing cyanobacteria to absorb light more efficiently over a wider range of wavelengths than other phytoplankton (Tandeau de Marsac & Houmard, 1993; Glazer *et al.*, 1994). These adaptations make them highly suited to the elevated temperatures of the epilimnion during stratification, and enable them to out-compete other phyla in low light conditions.

Cyanobacteria have superior uptake kinetics of organic carbon in relation to other phytoplankton phyla (Shapiro, 1973; 1997). Therefore under bloom conditions, when $CO_2$ levels can be considerably reduced, positively buoyant cyanobacteria are at an advantage over other phytoplankton taxa as they can intercept atmospheric $CO_2$, directly at the air-water interface or via atmospheric diffusion into surface waters (Paerl, 1988). Under inorganic carbon limited conditions, some cyanobacteria, such

as *Anabaena* sp. and *Microcystis* sp., are able to utilize bicarbonate directly by actively transporting bicarbonate across cell membranes using a "proton pump", or by converting bicarbonate to $CO_2$, using the enzyme carbonic anhydrase (Paerl, 1988; Badger *et al.*, 2002). As a result of their superior $CO_2$ uptake kinetics, cyanobacteria may reduce concentrations of carbon to a level in which only they may continue to photosynthesize (Shapiro, 1973; 1997). This adaptation makes cyanobacteria efficient competitors at high pH levels which are often characteristic of eutrophic systems.

## *1.3 Cyanobacterial blooms*

Algal blooms are generally accumulations of a single species in excess of l0,000 cells $ml^{-1}$, and where this species makes up as much as 95-99% of the phytoplankton biomass (Paerl, 1988). Cyanobacteria blooms have many detrimental effects including; water discoloration and reduced transparency, decreased biodiversity, increased primary production, and oxygen depletion, which may result in unpleasant odours and fish deaths (Walsby, 1994; Dokulil & Teubner, 2000; Carmichael, 2001). Toxic blooms may also have debilitating effects for humans and animals using the water for domestic, industrial and recreational uses (Chorus & Bartram, 1999; Dokulil & Teubner, 2000; Hitzfeld *et al.*, 2000).

Blooms are generally associated with stratification and the resultant decline in mixing intensity, as well as adequate supply of nutrients in the epilimnion. Under these conditions cyanobacteria often exert competitive dominance over other phytoplankton due to their ability to regulate buoyancy via gas vesicles.

### 1.3.1 Environmental factors permitting cyanobacterial dominance

Cyanobacterial blooms are the result of a complex interaction of a multitude of chemical, physical and biological factors including; warm weather, increased thermal stratification, enhanced PAR, enhanced nutrient levels from runoff and sediment releases in the hypolimnion due to anoxia and interactions with other trophic levels.

As a result, the synergistic impacts of physical, chemical and biological conditions dictate bloom frequencies and magnitudes in lentic systems (Fogg, 1969; Reynolds & Walsby, 1975). The combination of conditions most likely to lead to cyanobacterial blooms in freshwater environments is discussed immediately below.

Warm weather, resulting in vertical thermal stratification of the water column plays an important part in the dominance of cyanobacterial populations by favoring accumulation of cyanobacteria at depths optimal for growth (Reynolds & Walsby, 1975). Such depths vary on a daily basis, depending on the interaction of PAR at the surface and nutrients at depth (Paerl, 1988). Elevated PAR levels at the surface and elevated nutrient levels in the hypolimnion favour cyanobacteria. This regime allows buoyant cyanobacteria to orient themselves near the water surface during daylight hours with elevated light intensity and then migrate to nutrient-rich hypolimnetic waters during potentially photoinhibitory midday or aphotic nighttime hours (Paerl, 1988).

Light intensity and spectral composition in an aquatic environment change significantly with depth due to absorption and scattering by particles and coloured components in water (Kirk, 1994; Walsby, 1994; Oliver & Ganf, 2000). As a result, light intensity decreases exponentially with depth and selective removal of wavelengths causes shifts in the spectral distribution within the water column (Oliver & Ganf, 2000). As net growth of algae only occurs if they spend sufficient time above the depth where photosynthesis compensates for respiratory losses, buoyant cyanobacteria near the water surface may outcompete other phytoplankton (Walsby, 1994). Additionally gas vacuolate cyanobacteria may also modify the spectral distribution of light through reduced light penetration, and thus shade out other phytoplankton lower in the water column (Havens *et al.*, 1998; Robson & Hamilton, 2004).

In addition to the above physical and chemical conditions, biotic interactions between trophic levels play a significant role in cyanobacterial bloom formation (Dokulil & Teubner, 2000). Algal-bacterial synergism can be important as it may cause positive

impacts on phycosphere nutrient cycling, thus affecting nutrient availability (Dokulil & Teubner, 2000). Algal-micrograzer synergism may cause nutrient availability to increase among cyanobacteria. The structure and composition of micrograzing zooplankton and fish populations may affect cyanobacteria abundance, where absence or reduced numbers could enable proliferation of cyanobacteria (Paerl, 1988; Dokulil & Teubner, 2000).

## *1.4 Biomanipulation*

Zooplanktivorous fish are known to selectively consume large zooplankton and, as a result, shift zooplankton community structure toward dominance by smaller species. Such changes are often associated with a shift in the phytoplankton community structure toward dominance by cyanobacteria (Smith & Lester, 2006). In the past, efforts to limit the adverse effects associated with these cyanobacterial blooms and lake degradation have generally concentrated on reducing nutrient inputs, known as "bottom-up" control (Schindler, 1974).

Although workable in theory, "bottom-up" control may be difficult, as in many situations, external loadings are not easily controlled or internal loadings, associated with the bottom sediments, are released during summer as the hypolimnion becomes anoxic (Jeppesen *et al.*, 2005). Because of some of the inherent difficulties associated with "bottom-up" control, the idea of manipulating food webs, known as "top-down" control, as proposed by Shapiro *et al.* (1975) and later expanded upon by Carpenter *et al.* (1985), as a lake restoration technique has become increasingly popular among aquatic restoration ecologists (Prokopkin *et al.*, 2006).

Biomanipulation of a food web or "top-down" control as a means of controlling cyanobacterial populations is based on the "trophic cascade hypothesis" (Gulati & van Donk, 2002). By increasing biomass of piscivorous fish and/or reducing abundance of zooplanktivorous fish there will be an increase in the abundance of large zooplankton and, in turn, a reduction in the abundance of cyanobacteria and

other phytoplankton (Hansson *et al.*, 1998; Lammens, 1999; Gulati & van Donk, 2002).

Recently, the effects of successful food web manipulations have been demonstrated on a variety water bodies, with an improvement in water quality (e.g., Benndorf, 1990; Meijer *et al.*, 1994; Annadotter *et al.*, 1999; Gulati & van Donk, 2002). In most cases the use of "top down" control has been used in association with a reduction in the nutrient inputs (Annadotter *et al.*, 1999) and/or reducing the internal cycling of nutrients during anoxic conditions in stratified lakes (Gulati & van Donk, 2002).

## *1.5 Quantitative polymerase chain reaction*

Quantitative (or real-time) polymerase chain reaction (QPCR) was developed in the 1990s (Wilhelm & Pingoud, 2003), and is a molecular based technique permitting the quantitative detection of specific DNA sequences within a sample (Rinta-Kanto *et al.*, 2005). QPCR uses real-time detection to measure the change in product concentration at certain points during each PCR cycle (Coyne *et al.*, 2005). The increase in product concentration is measured as an increase in fluorescence emission (Heid *et al.*, 1996) generated by either cleavage of a fluorescent reporter dye from a template-specific fluorescent oligonucleotide (Taqman) probe or by a DNA intercalating dye (e.g. SYBR Green; Coyne *et al.*, 2005). By recording the amount of fluorescence emission at each cycle, it is possible to monitor the PCR reaction during the exponential phase (de Bruin *et al.*, 2003). QPCR has been used in a range of applications from human and veterinary microbiology to detection of algae, bacteria and viruses in environmental samples.

Detection of microbes in environmental samples using QPCR has several advantages over traditional techniques (e.g., microscope enumeration) including; improved specificity and sensitivity, faster turn around times and high–throughput capability (Schober & Kurmayer, 2006; Rueckert *et al.*, 2008). Applications of QPCR for phytoplankton communities have generally focused on the investigation of genetic

biodiversity within a population (e.g., Larsen *et al.*, 2001), identification and enumeration of problematic species (e.g., Rinta-Kanto *et al.*, 2005) and identification and quantification of enzymes involved in the biosynthesis of toxins (e.g., Kurmayer & Kutzenberger, 2003; Vaitomaa *et al.*, 2003). The ease of use, sensitivity and advantages over traditional laborious microscopic methods and other non-specific PCR based methods has seen QPCR assays incorporated into routine monitoring programmes (e.g., Skovhus *et al.*, 2004; Rinta-Kanto *et al.*, 2005).

In this project a Taqman QPCR assay (Rueckert *et al.*, 2008) was used to quantify the dominant cyanobacteria species (*A. planktonica*) in a large number of samples collected from the Lower Karori Reservoir (LKR).

## *1.6 Temperature and light growth experiments*

Factors accounting for long- and short- term spatial and temporal variation of phytoplankton in lentic systems are often associated with their photosynthetic responses to an array of environmental conditions. Subsequent changes in photosynthetic rate play in integral part in the net growth of the phytoplankton under specific conditions (Coles & Jones, 2000).

In natural communities, light intensity and temperature can limit biomass through their control over net growth rate of the phytoplankton community (Wofsy, 1983). The magnitude of the response may be parameterised under controlled conditions in the laboratory with a photosynthesis versus irradiance curve (*P-I* curve or *P-E* curve) as proposed by Jassby and Platt (1976). As a result, changes in the parameters defining the *P-I* curve reflect changes in environmental conditions. Changes in the *P-I* curve are examined through variations in the initial slope and the saturation plateau of the *P-I* curve (Babin *et al.*, 1994). A *P-I* curve has three distinct regions. In the first light limited phase growth is uncoupled with light, with growth continuing until a plateau is reached. The second phase is the light saturated phase where no further increase in light will enhance growth. The final phase is that of photoinhibition

where additional increases in light lead to reduced growth as a result of photochemical damage (Pokorný & Květ, 2004).

To study the *P–I* relationship, samples are incubated over a range of light intensities for a period of time, sometimes at different constant temperatures (Macedo *et al.*, 2002). Varied responses by different phytoplankton have been observed under varying temperatures (e.g., Song *et al.*, 1998; Coles & Jones, 2000), light intensities (e.g., Coles & Jones, 2000; Macedo *et al.*, 2002; Dyble, 2006) and nutrient regimes (e.g., Song *et al.*, 1998).

There is a lack of data on the bloom forming species *A. planktonica*, which is dominant in the LKR. This study assessed *A. planktonica* growth rates under a limited number of different light intensities and temperature regimes.

## *1.7 Modelling*

Models of lake ecosystems vary in complexity from simple mass balance models to highly parameterized simulation models, including coupled hydrodynamic and ecological processes (e.g., Bruce *et al.*, 2006). The ecological model DYRESM-CAEDYM allows assessment of interactions amongst forcing variables and their subsequent effects on controlling phytoplankton bloom dynamics (Chan & Hamilton, 1998). The need for such models has arisen largely as a result of increased eutrophication, and the subsequent increase in phytoplankton blooms in lakes worldwide (Hamilton & Schladow, 1996).

This study makes use of a specific new version of the vertically resolved one-dimensional coupled ecological and hydrodynamic model 'Dynamic Reservoir Simulation Model - Computational Aquatic Ecosystem Dynamics Model' (DYRESM-CAEDYM) developed at the Centre of Water Research at the University of Western Australia.

DYRESM is a one-dimensional hydrodynamic model which simulates vertical distribution of temperature, salinity and density over depth and time in lakes and reservoirs (Gal *et al.*, 2003; Yeates & Imberger, 2004). DYRESM is a process based model therefore does not require extensive calibration of model parameters (Yeates & Imberger, 2004) though recent versions have demonstrated that extensive calibration may be required (D. Hamilton, pers. comm.). DYRESM is based on a Lagrangian layer structure which simulates the water body as a series of horizontally uniform layers of varying thickness. Layer thicknesses vary as the layers are moved vertically in response to volume changes as a result of differences in inflow and outflow volumes (Gal *et al.*, 2003; Bruce *et al.*, 2006). The main processes modeled by DYRESM are surface heat, mass and momentum transfers, mixed layer dynamics, hypolimnetic mixing, benthic boundary layer mixing, inflows and outflows, all of which are achieved by the use of local meteorological data and/or a series of computational algorithms (Bruce *et al.*, 2006).

DYRESM can either be run individually or coupled with an ecological model such as CAEDYM for studies involving biological and/or chemical processes. CAEDYM uses a series of differential equations to simulate dissolved oxygen, several species of total and dissolved nitrogen and phosphorus, as well as several groups of phytoplankton, zooplankton, fish and other aquatic life (Robson & Hamilton, 2004). The model responds to environmental forcing and ecological interactions for each Lagrangian layer represented by the DYRESM model (Bruce *et al.*, 2006).

DYRESM-CAEDYM is used in this study to simulate temporal and vertical dynamics of phytoplankton within the LKR. Employment of the model DYRESM-CAEDYM provides the opportunity to investigate the relationships between physical, chemical and biological parameters in water bodies over different time scales from sub-daily to inter-annual (Lewis *et al.*, 2004; Yeates & Imberger, 2004). This is advantageous as a sub-daily time step enables enhanced resolution of photosynthetic processes, allowing seasonal trends to be more accurately resolved (Yeates & Imberger, 2004).

As each water body has unique qualities the output generated by DYRESM-CAEDYM on the growth rates of cyanobacteria under changing environmental conditions may assist in assessing management options and evaluating the effectiveness of a proposed water quality management plan (Lewis *et al.*, 2004). The model simulations in this study are used to aid in the development of strategies to assist in the control of cyanobacterial communities in the LKR.

## *1.8 Lower Karori Reservoir*

In 1874 construction of the LKR was completed, providing the first comprehensive water supply scheme for Wellington City (Morrison, 1986; Lynch, 1995). It had a total capacity of approximately 150 million litres (Burch, 1997). Construction of the Upper Karori Reservoir (UKR) followed in the years 1908 to 1911. With a capacity of approximately 225 million litres, the UKR was created to supplement the Wellington water supply provided in part by the LKR (Burch, 1997).

In 1979 the UKR was declared unsafe (Burch, 1997), and in 1992 it was decommissioned and partially emptied following engineers' findings that it did not have "sufficient factors of safety" to cover the possibility of an earthquake on the Wellington faultline which runs through both reservoirs (Wood, 2005). In 1998 upon the completion of a new enclosed water supply reservoir for Wellington at Johnsonville, the LKR was also decommissioned and withdrawn from Wellington's water supply system (Wood, 2005). Unlike the UKR, the LKR was maintained for water storage as it was considered safe provided it did not have to withstand additional water pressure or overtopping if the upper dam were to collapse (Wood, 2005).

In 1996 the Karori Sanctuary Trust began converting the upper and lower reservoirs and their 252 ha surrounding catchment into what is now known as the Karori Wildlife Sanctuary (KWS; Gunn *et al.*, 2000). The sanctuary is enclosed within an 8.6 km predator-proof fence, specifically designed to exclude non-native mammals (Smith, 2005; Wood, 2005). In 2000 a multi-species eradication programme was

completed with all non-native mammals being removed (Smith, 2005). Re-introductions of native flora and fauna followed (Wood, 2005). The goal of the project is to restore the area to a state which resembles, as closely possible, the conditions pre-human arrival (Gunn *et al.*, 2000).

Both brown trout (*Salmo trutta*) and European perch (*Perca fluviatilis*) are resident within the LKR, with *S. trutta* also found in the UKR. *Perca fluviatilis* were introduced in the LKR in 1878, and since then have become the dominant fish species (Smith & Lester, 2006; 2007). Under natural conditions *P. fluviatilis* will undergo two ontogenic shifts throughout their lifetime, beginning as juveniles feeding on pelagic zooplankton, then shifting to benthic invertebrates and finally shifting to a diet mainly consisting of fish (Smith, 2005). Despite the potential for attaining large size *P. fluviatilis* populations in New Zealand are characterized by large populations of small sized fish (Smith & Lester, 2006). This is probably due to the lack of any natural predators (Persson *et al.*, 2000), high intraspecific competition (Persson *et al.*, 2000), and a lack of food sources (Magnhagen & Heibo, 2004). Under these conditions, stunted populations of small fish will result, leading to an increased time in the initial stages of their ontogeny and resulting in increased and sustained predatory pressure on the zooplankton community. Smith and Lester (2006) used mesocosms to show that *P. fluviatilis* were likely to be a contributing factor to cyanobacterial blooms in the LKR, and suggested that a *P. fluviatilis* eradication within the LKR would result in a reduction of cyanobacterial blooms and an increase in water clarity.

The LKR is a warm monomictic lake with a mean depth of 8.2 m, maximum depth of over 20 m and a 252 ha catchment consisting of mixed regenerating shrub-hardwood forest (Lynch, 1995; Smith, 2005). Cyanobacterial blooms caused by *Anabaena* species have occurred in the LKR since the summer of 1996/7 (Wood, 2005), with the first severe cyanobacterial bloom occurring during the summer of 2000/1 (Smith & Lester, 2006; 2007). Since this time the dominant *Anabaena* species have changed. Wood (2005) noted that *A. lemmermannii* and *A. circinalis* were the dominant bloom-forming species in 2005, and have since been succeeded by *A.*

*planktonica*. Since the arrival *A. planktonica*, concentrations of *A. circinalis* are significantly lower and *A. lemmermannii* has not been observed since March 2006. *A. planktonica* has become the dominant bloom forming species and has been found to comprise of up to 99.9% of the surface phytoplankton (Cawthron Institute/Waikato University, unpubl. data). In January 2003, when *A. lemmermannii* and *A. circinalis* were the dominant bloom-forming species, the cyanotoxin anatoxin-a was detected in a sample from the LKR (Wood *et al.*, 2006).

Cyanobacterial blooms have a number of associated detrimental effects on the KWS including visual degradation, odour problems and causing possible health risks to humans and wildlife (Smith, 2005). Both Karori reservoirs have in the past been used to store water from other locations prior to it being distributed to Wellington water supply. Water from Morton Dam (Wainuiomata) was originally pumped to both reservoirs. Interestingly, this dam has been documented as having experienced blooms of *Anabaena* spp. between 1947 and 1966 (Vidal & Frieda Maris-McArthur, 1973) and may have been the original source of the *Anabaena* sp.

Based on the physiology of the *Anabaena* sp., physico-chemical variables and other trophic interactions within the reservoir, it seems likely that bloom frequency and magnitude may be attributed to a complex suite of biological, physical and chemical interactions working in synergy. Historic data gathered by Smith (2005), Wood (2005), and a 2-year data set maintained by Cawthron Institute and Waikato University, as well as high resolution sampling undertaken in this project will be used a gain a further understanding on bloom dynamics within the LKR.

## *1.9 Aims and Objectives*

The objective of this study is to identify key physical, chemical and biological variables influencing phytoplankton dynamics in the LKR.

This overarching objective is addressed through the following aims:

(1) To use high resolution sampling to understand phytoplankton dynamics in the LKR.

(2) To use QPCR to rapidly enumerate cyanobacterial (*Anabaena planktonica*) concentrations in a large number of samples.

(3) To use laboratory-based culture experiments to gather physiological information on *A. planktonica*. This information is used in the models to ensure that they are specific to the species present in the LKR.

(4) To predict temporal and spatial phytoplankton dynamics within the LKR. This will be achieved by incorporating site specific data into the model DYRESM-CAEDYM.

(5) To assess for a possible trophic cascade effect of a European perch (*Perca fluviatilis*) removal on both zooplankton and phytoplankton assemblages by assessing pre- and post-removal data.

(6) To develop strategies to assist in the control of cyanobacterial communities in the LKR. Management options will be based on collected data and DYRESM-CAEDYM simulation outputs.

# 2 Materials and Methods

## *2.1 Study site*

The Lower Karori Reservoir (LKR; 41°17′33.25″S, 174°45′05.69″E) is located in the inner Wellington suburb of Karori (Gunn *et al.*, 2000; Smith & Lester, 2007). The reservoir has a mean depth of 8.2 m and a maximum depth of over 20 m (Smith, 2005). The reservoir has an area of 2.34 ha (Hicks *et al.*, 2007), with a catchment of approximately 252 ha predominantly covered in a regenerating mixed shrub-hardwood forest (Lynch, 1995). The reservoir has a single inflow entering at the southern end from the UKR and a single outflow exiting at the northern end (Fig. 2.1.1).

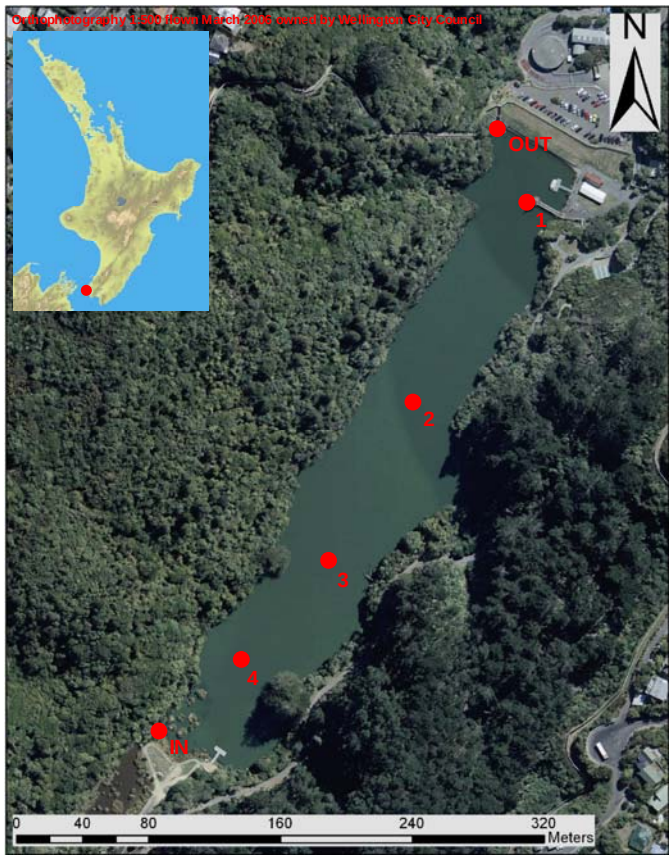


**Figure 2.1.1:** The Lower Karori Reservoir study site, with the inflow (IN) labeled at the southern end, the outflow (OUT) at the northern end and lake sampling sites denoted by 1, 2, 3 and 4.

## *2.2 Phytoplankton composition and environmental variables*

### 2.2.1 Field data collection

A long term sampling regime has been carried out by Cawthron Institute and Waikato University since 5 September 2005. Sampling includes temperature and dissolved oxygen profiles, nutrients (ammonium, nitrate, phosphate, total nitrogen, and total phosphorus), phytoplankton and zooplankton (Methods; Appendix I). This data set was made available for my study to assist with analysis of lake processes and for model validation.

Sampling undertaken in this study was carried out at approximately 0100, 0800, 1300 and 1900 hours over a 72 hour period during pre-bloom (6 – 9 December 2006), bloom (9 – 12 February 2007) and post-bloom (4 – 7 June 2007) periods. Each sampling involved the gathering of a suite of physical, chemical and biological variables from the valve tower, (Site 1; Fig. 2.1.1) at depths of 0, 5, 10 and 15 m using a Schindler-Patellas trap. Additionally, in the early morning at approximately 0800 hours the same suite of variables was collected at three equally spaced sites along the reservoir (Sites 2, 3, 4; Fig. 2.1.1). Samples on the transect were collected at 0 m and at depths of 7 m at Site 2, 8 m at Site 3 and 5 m at Site 4. Samples were collected at the inflow and outflow at the time of transect sampling.

Conductivity, fluorescence, temperature, photosynthetically active radiation (PAR) and dissolved oxygen levels were recorded vertically through the water column using a SBE 19 plus SEACAT profiler (Sea-Bird Electronics Inc.), with additional sensors mounted for dissolved oxygen (Sea-Bird Electronics Inc.), PAR (Licor Inc.), beam transmittance (Sea-Bird Electronics Inc.), and chlorophyll fluorescence (Chelsea Instruments Ltd.).

Secchi depth was measured using a 20 cm diameter Secchi disk and an underwater viewing chamber (Davies-Colley, 1988). The pH was measured and recorded using a handheld pH meter (Eutech Instruments & Oakton Instruments).

Water sub-samples for QPCR analysis were transferred to sterile 50 ml Falcon tubes. Water sub-samples for total nutrient analysis were transferred to clean 15 ml Falcon tubes. Water sub-samples for dissolved nutrient analysis were filtered on site using a syringe tip attached to the end of a 60 ml syringe and transferred to clean 15 ml Falcon tubes. Chlorophyll *a* analysis was undertaken by filtering a known quantity of water though a GC50 0.45 µm glass fibre filter (Advantec). The filter was then wrapped in tinfoil. All samples were put on ice in a chilli-bin before being transferred to a freezer and stored at -20 °C until analysed.

Water samples for microscopic algal identification and enumeration were stored in clean 50 ml polycarbonate containers and treated immediately with 1 % Lugols iodine (10% (w/v) potassium iodine, 5% (w/v) iodine, 10% (v/v) acetic acid).

As of 18 May 2006, water temperature was logged every 30 minutes at 2 m intervals from the water surface to the reservoir bottom with thermistors (Stowaway Tidbits) attached to a rope at the valve tower. Water temperature was also logged at the inflow. Tidbits were downloaded on an approximate bi-monthly basis using BoxCar Pro 4.3 (Onset Computer Corporation, 2002).

## 2.2.2 Analysis

### 2.2.2.1 Secchi Disk readings

Euphotic Depth ($z_{eu}$) was approximated using Secchi Disk values using equation 2.1.

$$z_{eu} = SDV \cdot 2 \quad \textbf{(2.1)}$$

where $SDV$ is the Secchi Disk value in $m^{-1}$.

### 2.2.2.2 Seacat profiler data

Data for temperature, PAR and dissolved oxygen were recorded using a SBE 19 plus SEACAT profiler (Sea-Bird Electronics Inc.) and these data were exported into

Microsoft Excel using the Sea-Bird Electronics software. Profiles for temperature and dissolved oxygen were plotted using Microsoft Excel and thermocline depth was quantified according to Hoare & Spigel (1987), using equation 2.2.

$$z_t = \max\left(\frac{\Delta T}{\Delta z}\right) \quad \textbf{(2.2)}$$

Where $T$ is the temperature of water and $z$ is water depth.

The Wedderburn number (Equation 2.3) was used to quantify the extent of the metalimnion displacement (Spigel & Imberger, 1987):

$$W = \frac{\Delta\rho g h^2}{\rho_0 {u_*}^2 L} \quad \textbf{(2.3)}$$

where $\Delta\rho$ is the density difference between the surface mixing layer and the hypolimnion in kg $m^{-3}$, $g$ is gravitational acceleration in m $s^{-2}$, $h$ is surface mixed layer thickness in $m^{-1}$, $\rho_0$ is the reference density of water in kg $m^{-3}$, $u_*$ is the water friction velocity due to wind stress in m $s^{-1}$ and $L$ is lake length at the bottom of the surface mixing layer in the direction of the wind in $m^{-1}$.

The light attenuation coefficient ($K_d$) was determined for samples taken in daylight based on the PAR readings recorded by the SBE 19 plus SEACAT profiler (Sea-Bird Electronics Inc.) by determining light at 0 and 5 m and entering the values into equation 2.4, rearranged from Beer's law in equation 2.5.

$$K_d = \frac{\ln(I(0)) - \ln(I(z))}{z} \quad \textbf{(2.4)}$$

$$K_d = \frac{-\ln\left(\frac{I(z)}{I(0)}\right)}{z} \quad \textbf{(2.5)}$$

where $K_d$ is the light attenuation coefficient, I(0) is the PAR immediately below the surface and I($z$) is the PAR at a depth and $z$ is the depth at which I($z$) was taken.

#### 2.2.2.3 Phytoplankton identification and enumeration

Phytoplankton species concentration and composition were estimated by counting and identifying a sub-sample settled in a Utermöhl settling chamber (Utermöhl, 1958) viewed under an inverted microscope (CKX41, Olympus, Wellington, New Zealand). For each sample a single transect was counted at either 200x or 400x magnification. Species for which less than 45 cells per transect were counted were then counted over half a chamber. Cyanobacteria were identified to species level and other phytoplankton to genus level. Heterocytes present in *Anabaena* spp. were counted. To aid in the identification of phytoplankton taxa the following texts were employed: Prescott (1978), Entwisle *et al.* (1997), Moore (2000) and John *et al.* (2002).

#### 2.2.2.4 Dissolved and filtered nutrients

Filtered nutrients were analysed on a Lachat QuickChem® Flow Injection Analyser (FIA+ 8000 Series, Zellweger Analytics, Inc.). Ammonium ($NH_4$-N) was analysed using Lachat QuickChem® Method 10-107-06-2-C (Prokopy, 1992). Nitrite ($NO_2$-N) was analysed using Lachat QuickChem® Method 10-107-04-1-A (Wendt, 2000) and nitrate ($NO_3$-N) through subtracting $NO_2$-N values from $NO_x$ values post analysis. Phosphate ($PO_4$-P) was analysed using Lachat QuickChem® Method 10-115-01-1-A (Diamond, 2000).

Total nitrogen (TN) and total phosphorus (TP) were digested using a persulphate digestion method (Ebina *et al.*, 1983) before analysis on the Lachat QuickChem® Flow Injection Analyser as for $NO_3$-N and $PO_4$-P using the QuickChem® Methods 10-107-04-1-A (Wendt, 2000) and 10-115-01-1-A (Diamond, 2000), respectively.

Milli-Q water was used in preparing all standards and reagents. Stock standards were prepared from analytical reagent-grade chemicals, and stored in clean bottles at 4 °C. Working standards were prepared by diluting stock standards with Milli-Q water.

Before each batch of samples were analysed, calibration standards were run and calibrated on the Lachat QuickChem® Flow Injection Analyser and software (Omnion 3.0, Lachat Instuments). Four checking standards were used every 30 samples.

#### 2.2.2.5 Quantitative polymerase chain reaction (QPCR)

The QPCR Taqman probe and primers used is this study were designed by Rueckert *et al.* (2007). The primers and probe are specific for *A. planktonica* and target a hyper-variable region of the long intergenic transcribed spacer region. The assay uses the addition of an internal standard as described in Coyne *et al.*, (2005). It involves the addition of a known concentration of exogenous plasmid DNA (pGEM-32, Promega) into the lysis buffer to act as an internal standard. Since the target DNA is extracted in the presence of the internal standard, inherent variability in extraction efficiencies and the presence of inhibitors equally affect both the target and standard. The concentration of target DNA is then measured by QPCR using target-specific primers and a Taqman probe and then corrected by QPCR determination of the internal standard copy number. The introduction of an exogenous internal standard during the extraction phase also reduces variability due to human error (Coyne *et al.*, 2005).

The samples for QPCR were thawed and 10 ml sub-samples taken for the December and June sampling periods. These were transferred into sterile 15 ml Falcon tubes. Samples were centrifuged for 15 minutes at 3,200 rpm (Jouan CR 4-11, Saint-Nazaire, France). The upper 9 ml of the supernatant was decanted and the remaining solution and pellet vortexed and transferred into a 2 ml eppendorf tube. Samples were then centrifuged for 5 minutes at 13,200 rpm in a benchtop centrifuge (Eppendorf 5415R, Germany). A 1 ml sub-sample of samples taken in February was centrifuged for 5 minutes at 13,200 rpm in a benchtop centrifuge (Eppendorf 5415R, Germany). The remaining supernatant was then removed by sterile pipetting and the samples frozen at -20 °C. Cyanobacteria in pellets were disrupted by addition of 45 µl of lysis formulation (0.5% Triton X-100 (v/v), 50 mM dithiothreitol, 0.5 M Tris-HCl pH 7.5 (Rasmussen *et al.*, 2008)), PGEM (14 ng) was added to each sample in a

1.5 ml eppendorf tube. Samples were centrifuged for 5 seconds at 13,200 rpm (Eppendorf 5415R, Germany), vortexed briefly, centrifuged again for 5 seconds at 13,200 rpm (Eppendorf 5415R, Germany) and finally placed in a thermomixer comfort (Eppendorf, Germany) for 10 minutes at 70 °C and 450 rpm to lyse the cells. Samples were stored at -20 °C until analysis.

The frozen processed samples were thawed and vortexed, and diluted 1:10 with Milli-Q water. Diluted samples were then centrifuged for 5 seconds at 6,400 rpm (Eppendorf 5415R, Germany), vortexed briefly and centrifuged for 5 seconds at 6,400 rpm (Eppendorf 5415R, Germany), and stored on ice.

The QPCR was performed with a Rotor-Gene 6000 (Corbett, Life Sciences, Australia) in 0.1 ml PCR tubes using a 72-well rotor. QPCR for *A. planktonica* and the internal pGEM reference standard were performed for each sample in duplicate in two separate reactions.

The *A. planktonica* assay consisted of a 12.5 µl reaction volume containing; 6 mM $MgCl_2$, 0.2 mM dNTPs (Roche Diagnostics, New Zealand), 1× PCR reaction buffer, 0.5 units of Platinum *Taq* DNA polymerase (Invitrogen, New Zealand), 450 nM forward primer (5´-GGT ATA TTC CTT TTG AAT TTT GCC TTT TGA-3´), 150 nM reverse primer 23S30R (5´-CHT CGC CTC TGT GTG CCW AGG T-3´), 200 nM probe (5´-ACA GAC ATG AGA GTG TTT CGT G-3´; Rueckert *et al.*, 2008; Integrated DNA Technology, USA), 0.8 µg non-acetylated BSA (Sigma, New Zealand) and 2 µl of environmental sample lysate. The *A. planktonica* TaqMan probe was synthesized with a FAM-reporter dye at the 5´-end and a Black Hole Quencher 2 at the 3´-end. PCR cycling used the following conditions: 95 °C for 2 min and 45 cycles of 95 °C for 7 seconds and 60 °C for 40 seconds.

The QPCR amplifying the internal reference standard (pGEM-32, Promega) utilized 300 nM forward primer M13f (5´-CCC AGT CAC GAC GTT GTA AAA CG-3´), 900 nM reverse primer pGEMr (5´-TGT GTG GAA TTG TGA GCG GA-3´) and 200 nM TaqMan probe (5´-CAC TAT AGA ATA CTC AAG CTT GCA TGC CTG CA-

3´; Coyne *et al.* (2005); Integrated DNA Technology, USA). The pGEM TaqMan probe was synthesized with a Cy5-reporter dye at the 5´-end and a Black Hole Quencher 2 at the 3´-end. QPCR cycling conditions were as described above.

Negative extraction and positive and negative PCR controls were included in each PCR run to check for contamination. Each run also included a calibrator sample (Sample 1; December, Day 1 (6 December 2006), Site 1, 0 m). Determination of cell abundance was performed using the comparative $C_T$ method according to Coyne *et al.* (2005), whereby unknown samples are compared to a calibrated sample containing a known abundance of the target organism determined by conventional enumeration under a microscope. Using the calibrator sample, the *A. planktonica* cell abundances for remaining samples are calculated according to equation 2.6 (the comparative $C_T$ method):

$$Cells\ ml^{-1} = E^{-\Delta\Delta Ct} \cdot C_{calibrator} \quad \textbf{(2.6)}$$

where $E$ is the amplification efficiencies for both assays, $C_{calibrator}$ is the volume of cells ml$^{-1}$ in the calibrator sample. The amplification efficiency calculated from the slope of regression line of the *A. planktonica* and pGEM assays is 1.98 (Rueckert *et al.*, 2008). $\Delta\Delta Ct$ was calculated as in equation 2.7.

$$\Delta\Delta Ct = \Delta Ct_{unknown} - \Delta Ct_{calibrator} \quad \textbf{(2.7)}$$

where $\Delta Ct_{unknown}$ is the change of the fraction cycle number of the unknown sample and $\Delta Ct_{calibratort}$ is the change of the fraction cycle number of the calibrator sample. The change in the fraction cycle number was calculated as in equation 2.8.

$$\Delta Ct = Ct_{target} - Ct_{pGEM} \quad \textbf{(2.8)}$$

where $Ct_{target}$ is the fractional cycle number of the target of the target species and $Ct_{pGEM}$ is the fractional cycle number of pGEM.

#### 2.2.2.6 Chlorophyll *a*

Chlorophyll *a* samples were analysed using the method described in Arar & Collins (1997). Samples were ground into a slurry with 10 ml of 90% acetone buffered with magnesium carbonate acetone, and then poured into a 15 ml Falcon tube to seep in the dark. After approximately 24 hours the slurry was centrifuged (Jouan B4i, Saint-Nazaire, France) at 3,300 rpm for 10 minutes and fluorescence from an aliquot pre and post application of 10 µl of 10% HCl measured using a 10-AU Fluorometer (Turner Designs).

The following equations were used to calculate the chlorophyll *a* concentration in the in the extract solution analysed (equation 2.9) and the chlorophyll *a* concentration in the whole water sample (equation 2.10).

$$C_{E,c} = F_s\left(r/r-1\right)\left(R_b - R_a\right) \quad \textbf{(2.9)}$$

where $C_{E,c}$ is the chlorophyll *a* concentration (µg $l^{-1}$) in the in the extract solution analysed, $F_s$ is the response factor for the sensitivity setting (0.132), $r$ is the before-to-after acidification ratio, $R_b$ is the fluorescence of the sample extract before acidification and $R_a$ is the sample extract after acidification.

$$C_{s,c} = \frac{C_{s,c} \cdot EV \cdot DF}{SV} \quad \textbf{(2.10)}$$

where $C_{s,c}$ is the chlorophyll *a* concentration (µg $l^{-1}$) in the whole water sample, $EV$ is the extract volume, $DF$ is the dilution factor and $SV$ is the sample volume.

### 2.2.3 Statistics

Correlation matrices of air temperature, a suite of physico-chemical variables and phytoplankton assemblage values were generated using STATISTICA (v. 7.0). $P$ values of less than 0.05 were considered significant.

Canonical Correspondence Analysis (CCA; Clarke & Ainsworth, 1993) was used to relate temporal variation of the phytoplankton assemblage to physico-chemical variables. All combined variables were removed prior to analysis to reduce information redundancy (Hall & Smoll, 1992) and analysis distortion (Pielou, 1984). Phytoplankton taxa that occurred on six or less instances of the 23 were excluded. Environmental variables used were standardized to a zero mean and unit variance. Phytoplankton data were log-transformed as part of the analysis on CANOCO (v. 4.5; ter Braak & Similauer, 1997).

Using STATISTICA, an analysis of variance (ANOVA) was used to test for any significant changes in the zooplankton assemblage pre- and post- *P. fluviatilis* removal. Only months with data available in both years were used, so as to reduce the effects of seasonality on the analysis. $P$ values $< 0.05$ were considered significant.

The preliminary analysis demonstrated there to be no variation in physico-chemical variables with respect to time within each sampling period (i.e., December, February and June). Therefore data at each discrete time were considered replicates so as to test vertical spatial variation with increased degrees of freedom. ANOVAs were completed to test variation of several biotic and abiotic variables with respect to depth within each month. All data was log transformed and obvious outliers omitted. Data was tested to the assumptions of ANOVA by using the Brown-Forsythe test to test for homogenous variances and the Shapiro-Wilk test to test for normal distribution. ANOVA $P$ values of $< 0.05$ were considered significant. Correlation matrices of physico-chemical variables against the phytoplankton assemblage were generated using STATISTICA.

## *2.3 Biomanipulation*

Between 12 and 15 February 2007 an intensive fish removal was carried out in the LKR using a combination of netting and boat electrofishing as described in Hicks *et al.* (2007). Netting was carried out using a combination of stretched-mesh gill nets, 2

mm mesh minnow traps, 5 mm mesh fyke nets, and opera house nets. Electrofishing was carried out using a 4.5 m long electrofishing boat. All fish caught were weighed and fork length measured, with introduced species removed and native species replaced (Hicks *et al.*, 2007). My part in the removal involved weighing and measuring of fish and assistance in setting and lifting nets, and more broadly, to assess its effects on the trophic structure of LKR.

## *2.4 Temperature and light growth experiments*

MLA media was made as described in Bolch & Blackburn (1996; Appendix II). Under a laminar flow, 200 ml MLA media and 1 ml of *A. planktonica* culture were added to sterilized 250 ml flasks. Treatments were undertaken in triplicate.

Four light intensities were tested; 20, 40, 60 and 140 μmol $m^{-2}$ $s^{-1}$. These intensities were a similar range to those used by Song *et al.* (1998) for *Microcystis* sp. experiments and Dyble *et al.* (2006) for *Cylindrospermopsis raciborskii* assays. Light intensity for each treatment was controlled by wrapping the desired number of layers of waxed lined paper around a wire frame surrounding each set of flasks. Treatments were incubated at constant temperature on a 12h:12h light:dark cycle in a growth cabinet (Contherm, BioSyn 6000CP, Wellington, New Zealand).

Three temperatures were tested; 10, 20 and 25 °C. These treatments were incubated at 140 μmol $m^{-2}$ $s^{-1}$ on a 12h:12h light dark cycle in a growth cabinet (Contherm, BioSyn 6000CP, Wellington, New Zealand).

Samples were collected on day zero, immediately after the cultures were prepared, and then every three to four days for the 60 and 140 μmol $m^{-2}$ $s^{-1}$ and 20 and 25 °C treatments and every seven days for the 20 and 40μmol $m^{-2}$ $s^{-1}$ and 10 °C treatments. On these days flasks were removed from their housing and incubator, and under the laminar flow gently agitated for approximately 15 seconds. Sub-samples (1.5 $ml^{-1}$) were taken and 20 μl Lugols iodine added. Each sample was inverted several times, before being stored in the dark until analysed. The pH of each sub-sample was

measured using 4.5-10 pH strips (J.T. Baker, Germany). Each treatment was terminated after 4 months.

The 1.5 ml sample was settled in a Utermöhl settling chamber (Utermöhl, 1958) and the *A. planktonica* concentrations enumerated under an inverted microscope (CKX41, Olympus, Wellington, New Zealand). Depending on the estimated concentration, each sample was counted in a single transect at either 200x or 400x. If the count did not exceed 100 cells then a half chamber count was completed. Heterocytes present were counted. Samples with extremely high *A. planktonica* concentrations were diluted 1:4 or 1:10 with Milli-Q water before settling.

Growth rates ($r_n$) were parameterised as in Reynolds (1997), using the equation 2.11.

$$r_n = \ln\left[N(T_2)/N(T_1)\right]/(T_2 - T_1) \quad \textbf{(2.11)}$$

where $N(T_1)$ is the cell concentration in cells $ml^{-1}$ at time $T_1$, $N(T_2)$ is the cell concentration at time $T_2$, and $T_2 - T_1$ is the time difference.

## *2.5 Modelling and bloom control strategies*

### 2.5.1 Meteorological data

Daily meteorological data (Fig. 2.4.1) was collected from several sources and stations within the Wellington area. Daily rainfall was obtained from a rain gauge within the Karori Wildlife Sanctuary. Daily means of hourly measurements of air temperature and wind speed were obtained from the geographically closest weather station (Wellington, Kelburn Aws, 41°17′06.00″S, 174°46′04.80″E) operated by NIWA. Relative humidity and daily means of hourly dry bulb were obtained from the Kelburn site to calculate mean daily water vapour pressure (T.V.A., 1972) using equation 2.12.

$$e_a = (h/100)\exp[2.303((a \cdot q_D/(q_D + b)) + c)] \quad \textbf{(2.12)}$$

where $e_a$ is the vapour pressure in hPa, $h$ is the relative humidity of air as a percentage, $q_D$ is the dry bulb air temperature in °C and $a$ (7.5), $b$ (237.3) and $c$ (0.7858) are coefficients for over-water calculations.

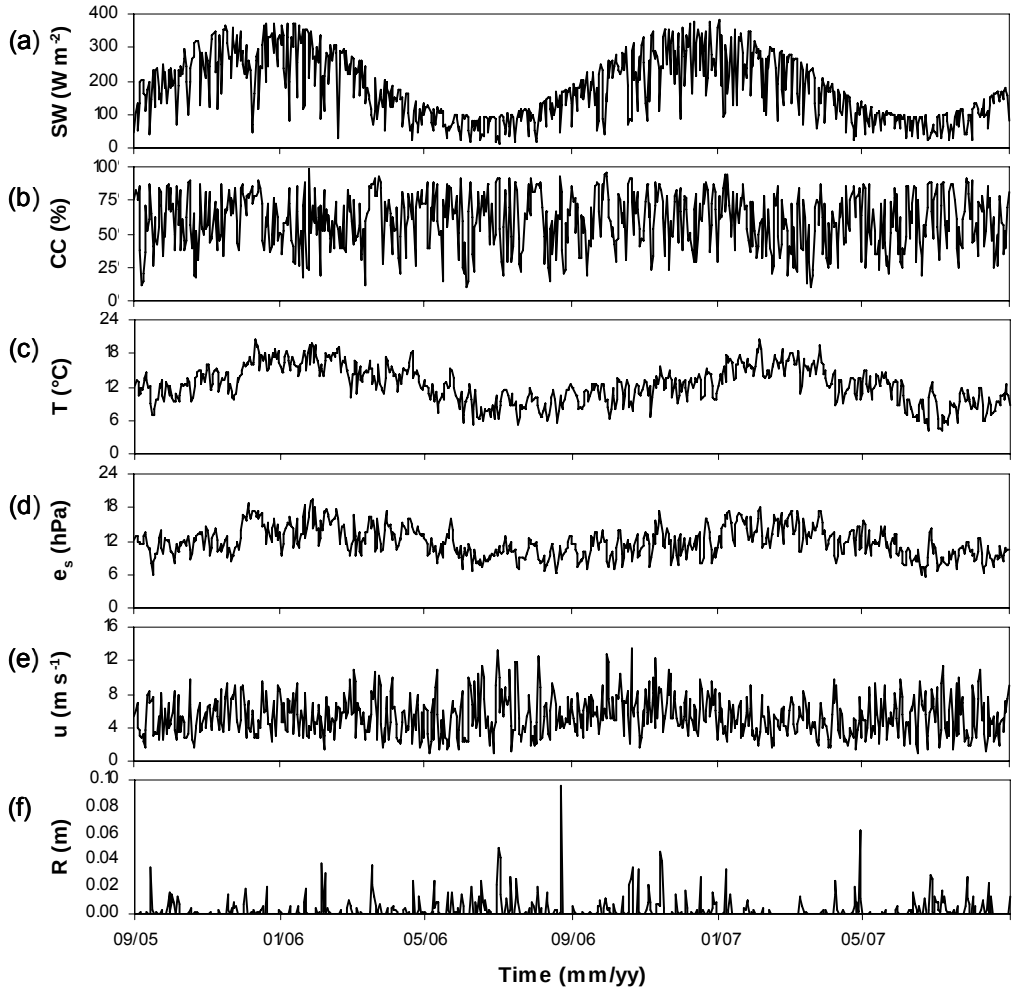


**Figure 2.5.1:** Meteorological data used as daily input for the DYRESM-CAEDYM model, including (a) total short wave radiation, (b) mean cloud cover, (c) mean temperature, (d) mean vapour pressure, (e) mean wind speed at a height 10 m above the lake and (f) total rainfall.

Daily totals of shortwave radiation were collected from the NIWA operated site, Blenheim Research Ews (41°29′56.08″S, 173°57′46.26″E). Daily means of cloud cover were collected from the NIWA site at Wellington Airport (Wellington Airport, 41°19′19.20″S, 174°48′14.40″E).

### 2.5.2 Inflow and outflow volume

Two inflows were assigned to the model, inflow one pertaining to the stream entering the reservoir from the Upper Karori Reservoir (UKR) and inflow two to the ungauged surface flows entering the reservoir. Due to a lack of direct inflow data, both inflows were assigned as daily means of hourly changes, in the monitored height of the UKR. Inflow one was directly related to the changes in the UKR height, multiplied by the surface area of the reservoir to give a daily inflow volume from the UKR. Inflow two was related to inflow one by the scaling of the relative catchment areas for the two systems.

Daily outflows were calculated, as in equation 2.13, from a daily water budget consisting of variables that included inflow one and inflow two as determined above, and rainfall and evaporation as daily values over the lake surface area.

$$\frac{\partial V}{\partial t} = V_{in} - V_{out} \quad \textbf{(2.13)}$$

where $V_{in}$ is the volume of the combined inflows (inflows and rain) and $V_{out}$ is the volume of the combined outflows (outflows and evaporation).

Evaporation was calculated by converting the change in mass in the surface layer due to latent heat flux (equation 2.14) into a daily value as $m^{-3}$ $d^{-1}$.

$$\Delta M^{(/h)} = \frac{-Q_{lh}.A_N}{L_V} \quad \textbf{(2.14)}$$

where $Q_{lh}$ is latent heat flux in (W $m^{-2}$), $A_N$ is the surface area of the surface layer in $m^{-2}$ and $L_V$ is the latent heat of vaporisation for water (2,258,000 J $kg^{-1}$).

The latent heat flux was calculated as in Fischer *et al*. (1979) in equation 2.15. The surface temperature for the model period was estimated by correlating half hourly daily mean temperature logger data (Stowaway Tidbits) over the period 18 May 2006

– 11 May 2007 with seven day mean air temperature data ($r^2$ = 0.845) taken from the Kelburn Aws station.

$$Q_{lh} = \min\left(0, \frac{0.622}{P} C_L \cdot \rho_A \cdot L_E \cdot U_a \left(e_a - e_s\left(T_s\right)\right)\Delta t\right) \quad \textbf{(2.15)}$$

where $P$ is the atmospheric pressure in hPa, $C_L$ is the latent heat transfer coefficient ($1.3\text{x}10^{-3}$) for wind speed at the reference height of 10 m, $\rho_A$ the density of air in kg $m^{-3}$, $L_E$ the latent heat of evaporation of water ($2.453\text{x}10^6$ J $kg^{-1}$), $U_a$ is the wind speed in m $s^{-1}$ at the reference height of 10 m, $e_a$ the vapour pressure of the air in hPa, and $e_s$ $(T_S)$ the saturated vapour pressure at the water surface temperature in hPa. It is assumed that $Q_{lh} \leq 0$, is so no condensation effects are considered.

The saturated vapour pressure was estimated using the Magnus-Tetens formula (T.V.A., 1972) as in equation 2.16.

$$e_s\left(T_s\right) = \exp\left[2.3026\left(\frac{7.5 \cdot T_s}{T_s + 237.3} + 0.7858\right)\right] \quad \textbf{(2.16)}$$

where $T_s$ is the water surface temperature in °C and $e_s$ the vapor pressure in hPa.

With the water level assumed constant and inflows, rainfall, evaporation known the residual was designated as the outflow.

### 2.5.3 Inflow water quality

Inflow water temperature was logged by a temperature logger (Stowaway Tidbits) every 30 minutes between 18 May 2006 and 3 June 2007. Mean daily data was used to estimate inflow water temperature over the modelling period by correlating it with seven daily mean air temperature data ($r^2$ = 0.820) taken from the Kelburn Aws station. Inflow two was also assigned the same temperature. For both inflows, dissolved oxygen concentrations were assumed to be at saturation and estimated from the calculated daily water temperatures. Nutrients (total nitrogen, ammonium, nitrate,

total phosphorus and phosphate) for each of the inflows were based on mean values taken during December, February and June.

### 2.5.4 Phytoplankton

The dynamics of two phytoplankton phyla were simulated in the model; *A. planktonica* representing cyanobacteria and *Staurastrum* sp., chlorophyta. Parameters were based on literature values from various sources. Initial lake water column concentrations for each group were calculated by multiplying their proportion of the total cell count with the chlorophyll *a* measurement.

### 2.5.5 Model validation and calibration

In this study the model DYRESM-CAEDYM was run on daily output time step between 5 September 2005 and 4 September 2006 for calibration and between 5 September 2005 and 29 October 2007 for validation. Model output was set at 0900 hours daily. Field data used for calibration and validation of the model was obtained from the Cawthron Institute and Waikato University 2-year data set commencing on 9 September 2005. The model output was validated and calibrated against 0, 5, 10 and 14 m data for temperature and dissolved oxygen and 0 and 15 m data for nutrients and chlorophyll *a*. Concentrations of the cyanobacteria *A. planktonica* and the chlorophyte *Staurastrum* sp. were validated against their relative chlorophyll *a* contribution.

### 2.5.6 Management scenarios

Five scenarios were modeled using DYRESM-CAEDYM. Scenario one involved the implementation of an artificial aeration system throughout the LKR. The system involved 20 bubblers emitting a total of 50 l $s^{-1}$ of air coinciding with when the reservoir would normally have been stratified (15 September – 15 March). Each bubbler was placed 0.5 m from the bottom and consisted of four ports that produced a total of 2.5 l $s^{-1}$ of air. Scenarios two through four examined the effects of limiting

internal nutrient loads by sediment capping, i.e., setting sediment nutrient releases to zero. Scenario two involved limiting the release of phosphate from the sediment. In scenario three ammonium release was limited and in scenario four both phosphate and ammonium limited. The final scenario involved modelling the effects of a reduced residence time. The residence time was reduced from approximately one year to only 5 days to approximate the residence time prior to 2000 (Hicks *et al.*, 2007).

# 3 Results

## *3.1 Long term trends*

### 3.1.1 Meteorology

Air temperature followed a typical annual cycle, with temperatures ranging from 4.2 °C to 20.7 °C over the period of 5 September 2005 through 12 December 2007. Temperatures peaked approximately one month later over the summer of 2006/7 compared with 2005/6 (Fig. 3.1.1). Elevated air temperatures over summer generally coincided with a reduction in wind speed, especially over the summer of 2006/7 in which a larger relative disparity between air temperature and wind speed occurred compared with the previous summer.

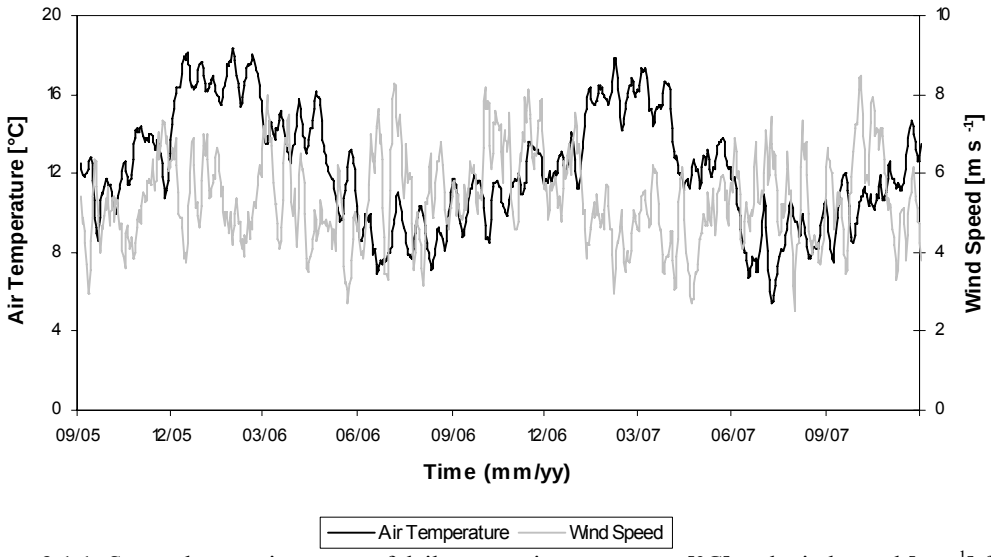


**Figure 3.1.1:** Seven day moving mean of daily mean air temperature [°C] and wind speed [m $s^{-1}$] from the Kelburn meteorological station between 5 September 2005 and 12 December 2007.

### 3.1.2 Thermal structure and dissolved oxygen

Water temperatures within the LKR ranged from 7.3 °C (3 July 2006 and 16 July 2007) to 20.8 °C (30 January 2006) in the surface mixed layer and 7.6 °C (16 July 2007) to 14.6 °C at depth (28 March 2006; Fig. 3.1.2a). The reservoir was thermally stratified from late October 2005 to late March 2006, mid November 2006 through

mid April 2007, and had begun to stratify once again in early November 2007 (Fig. 3.1.1). During these periods the reservoir had a strong temperature gradient between 10 and 16 m. Over the summer of 2005/6 the thermocline penetrated deeper into the water column than in 2006/7 (Fig. 3.1.2a), possibly due to the higher wind speeds recorded over the summer of 2005/6 (Fig. 3.1.1). Surface water temperature (0 m) was positively correlated with daily mean air temperature ($r = 0.834$, $P < 0.001$) and the seven day running mean of air temperature ($r = 0.915$, $P < 0.001$)

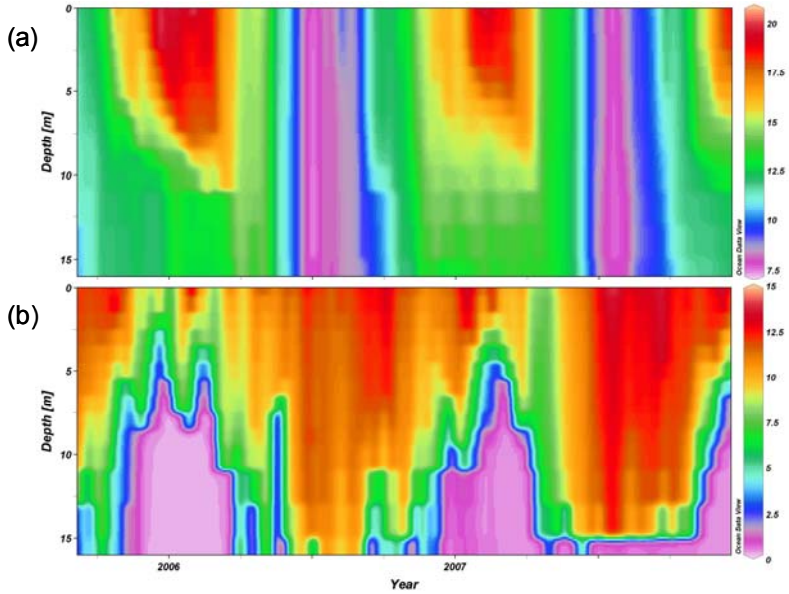


**Figure 3.1.2:** Profiles of (a) temperature and (b) dissolved oxygen measured approximately weekly from the Valve Tower (Site 1) between 5 September 2005 and 12 December 2007.

The hypolimnion was anoxic (< 1 mg $l^{-1}$) from 29 November 2005 through 20 March 2006, 4 December 2006 through 10 April 2007 and again beginning on 12 November 2007 (Fig. 3.1.2b). The lower depths (~16 m) of the reservoir remained in an almost permanent state of anoxia throughout the period of isothermy between the summers of 2006/7 and 2007/8. Surface waters (0 and 1 m) generally remained well oxygenated (> 9 mg $l^{-1}$) throughout periods of thermal stratification and isothermy. However, these occasionally dropped to as low as 6.47 mg $l^{-1}$ during the period of thermal stratification in 2005/6 and again during the breaking down of thermal stratification between 10 and 30 April 2007. Throughout periods of isothermy in 2006 and 2007, the water column remained high in dissolved oxygen with levels

typically 8 -14 mg $l^{-1}$ between 0 and 14 m depth. Dissolved oxygen levels at depth (14 m) were negatively correlated with surface water temperature ($r$ = -0.870, $P$ < 0.001).

The thermocline was considerably more stable over the summer of 2005/6 compared to 2006/7 (Fig. 3.1.3). In 2005/6 the thermocline depth ranged between 6 and 9 m and was generally at about 9 m throughout stratification. This also coincided with a relatively strong thermocline, ranging between 1.1 and 3.3 °C $m^{-1}$. In 2006/7 the thermocline depth ranged from 4 to 12 m, although spent most of its time in the vicinity of 6 m. During this period the water column experienced several overturns on 11 December 2005 and between 8 January and 15 January 2006. Thermocline strength ranged between 0.6 and 1.6 °C $m^{-1}$, considerably lower than that of the previous year.

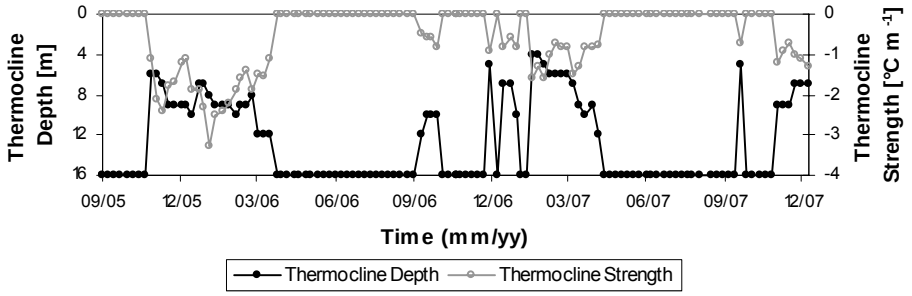


**Figure 3.1.3:** (a) Thermocline depth and (b) thermocline strength at the Valve Tower (Site 1).

Wedderburn values were generally greater than 1 (Fig. 3.1.4), and approximately 40 % of these values were greater than 10. This is indicative of limited upwelling and a highly stable state. Days which demonstrated values of less than 1 were 21 November 2005, 7 March 2006 and 13 September 2006. This indicates a high chance of upwelling and were generally associated with the beginning or ending of a stratification event. The summer of 2005/6 exhibited a greater number of extreme high values than the following year, indicating there was higher stability of the water column.

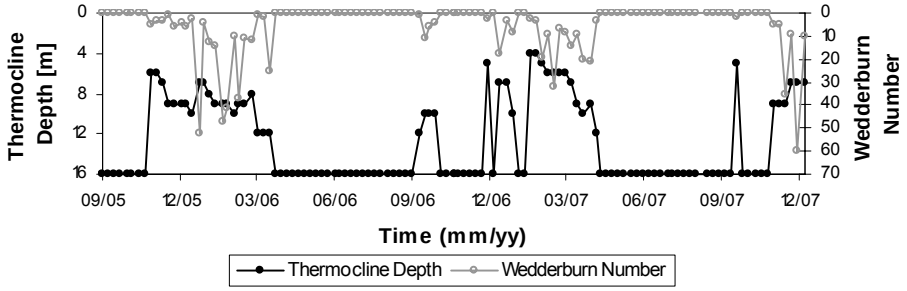


**Figure 3.1.4:** (a) Thermocline depth and (b) Wedderburn number at the Valve Tower (Site 1).

### 3.1.3 Nutrients and chlorophyll *a*

Nutrient concentrations at the surface (0 m) and depth (14 m) generally increased during anoxic conditions induced by summer stratification. Large peaks of ammonium ($NH_4$-N), total nitrogen (TN) and total phosphorus (TP) on 6 December 2006 may be associated with a deeper sample collection depth from an infrequently mixed deeper layer, in relation to adjacent samples (Hicks *et al*. 2007). Such infrequently mixed deeper layers were observed on dissolved oxygen profiles below approximately 15 m since late 2006 (Fig. 3.1.2b).

Ammonium was the dominant species of inorganic nitrogen during periods of stratification, while nitrate ($NO_3$-N) is generally dominant during times of isothermy (Fig. 3.1.5a, 3.1.5b). Variation between surface and deep concentrations of ammonium coincided with thermally stratified conditions and resultant anoxia, whereby deep (14 m) concentrations were negatively correlated with dissolved oxygen concentrations at the corresponding depth ($r$ = -0.466, $P$ = 0.025). Surface concentrations of total nitrogen were positively correlated with surface chlorophyll *a* ($r$ = 0.688, $P$ < 0.001) and *A. planktonica* concentrations ($r$ = 0.764, $P$ < 0.001).

Phosphate ($PO_4$-P) concentrations at surface and depth remained at low levels throughout the sampling period (Fig. 3.1.5d). The relatively low resolution of nutrient concentrations prior to the change of analytical lab on 4 July 2006, from the Greater Wellington Regional Council Water Quality Testing Lab to the

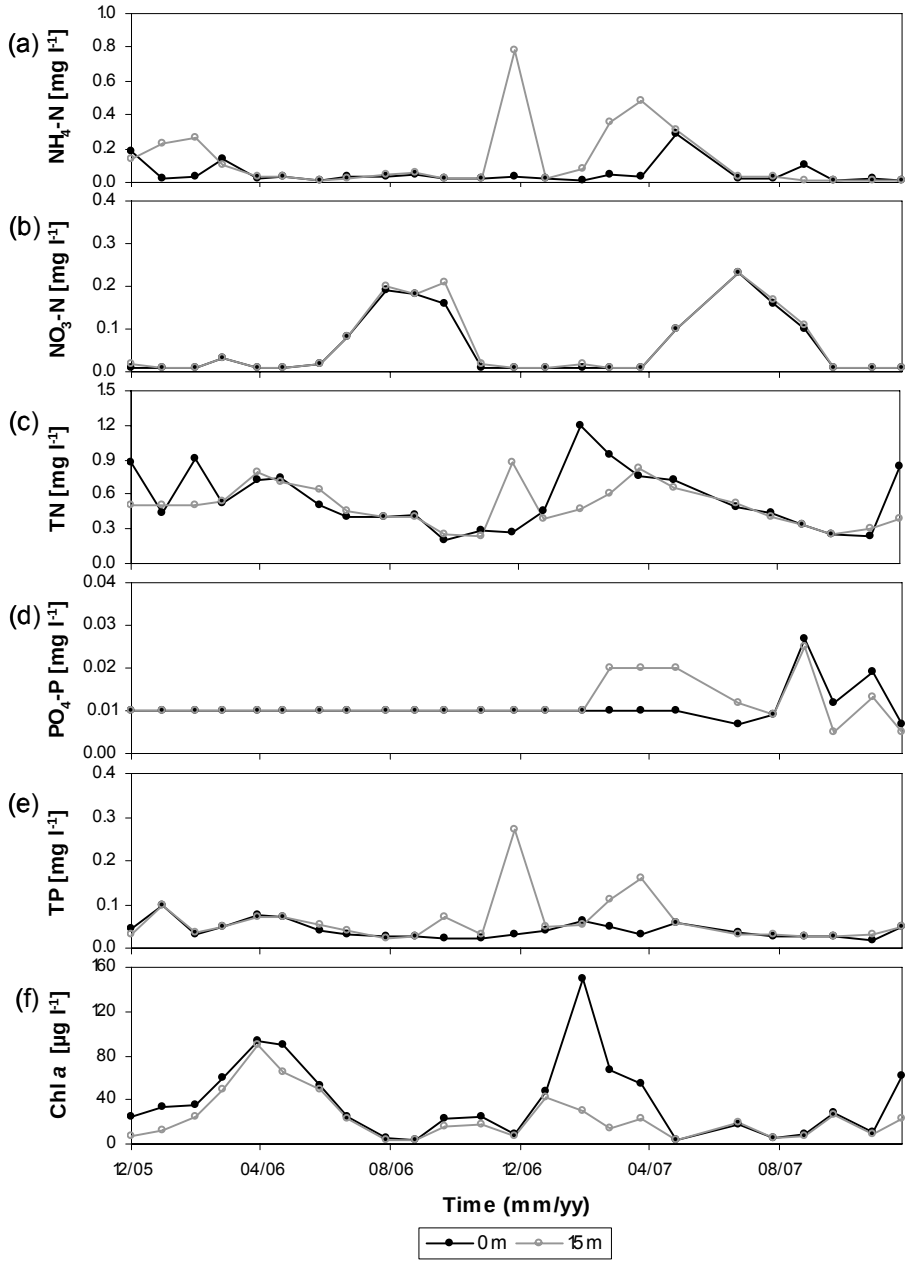


**Figure 3.1.5:** Surface (0 m) and depth (15 m) measurements of (a) ammonium, (b) nitrate, (c) total nitrogen, (d) phosphate, (e) total phosphorus and (f) chlorophyll *a* measured monthly from the Valve Tower (Site 1) between 12 December 2005 and 4 December 2007.

Environmental Laboratory Services Ltd, made any detection of phosphate trends in the earlier period implausible. Surface total phosphorus tends to follow a similar annual cycle to that of total nitrogen (Fig 3.1.5c; Fig. 3.1.5e), whereby total phosphorus levels at the surface tended to coincide with the peaks and troughs of chlorophyll *a* concentrations (Fig 3.1.5e; Fig 3.1.5f). Deeper (14 m) concentrations

of total phosphorus show increases over surface concentrations on 2 October 2006, 6 March 2007 and 4 April 2007.

Chlorophyll *a* follows a seasonal trend (Fig. 3.1.5f) with concentrations especially at the surface, increasing dramatically over summer during thermal stratification. Surface samples are positively correlated with surface temperature ($r = 0.503$, $P = 0.012$). Concentrations increased earlier in the 2005/6 summer compared with summer of 2006/7 and remained elevated for a longer period when compared with summer of 2005/6. This appears to coincide with the delayed onset of increased air temperature during the summer of 2006/7 (Fig. 3.1.1).

### 3.1.4 Phytoplankton assemblage

The phytoplankton assemblage of the LKR shows very distinct temporal variation. Cyanobacteria, in particular *A. planktonica*, dominate during summer under stratified conditions. These are replaced briefly by other phytoplankton taxa as the reservoir returns to isothermal conditions in April or May (Fig. 3.1.6; Fig. 3.1.7). Cyanobacteria are the dominant phytoplankton phyla within the reservoir (Fig. 3.1.6), accounting for 86.2% of the total phytoplankton cell densities in reservoir surface samples from 24 October 2005 to 4 December 2007. Due to their predominance in the phytoplankton taxa, surface cyanobacterial samples are positively correlated with total phytoplankton counts ($r = 0.945$, $P < 0.001$) and chlorophyll *a* ($r = 0.817$, $P < 0.001$) at the surface.

While cyanobacteria heavily dominate the phytoplankton phyla composition, *A. planktonica* dominates the cyanobacteria, accounting for 95.8% of the total cyanobacterial concentrations from reservoir surface samples. *Anabaena planktonica* surface concentrations are strongly positively correlated with cyanobacterial surface concentrations ($r = 0.999$, $P < 0.001$), total phytoplankton counts ($r = 0.942$, $P < 0.001$) and chlorophyll *a* ($r = 0.815$, $P < 0.001$). *Anabaena planktonica*

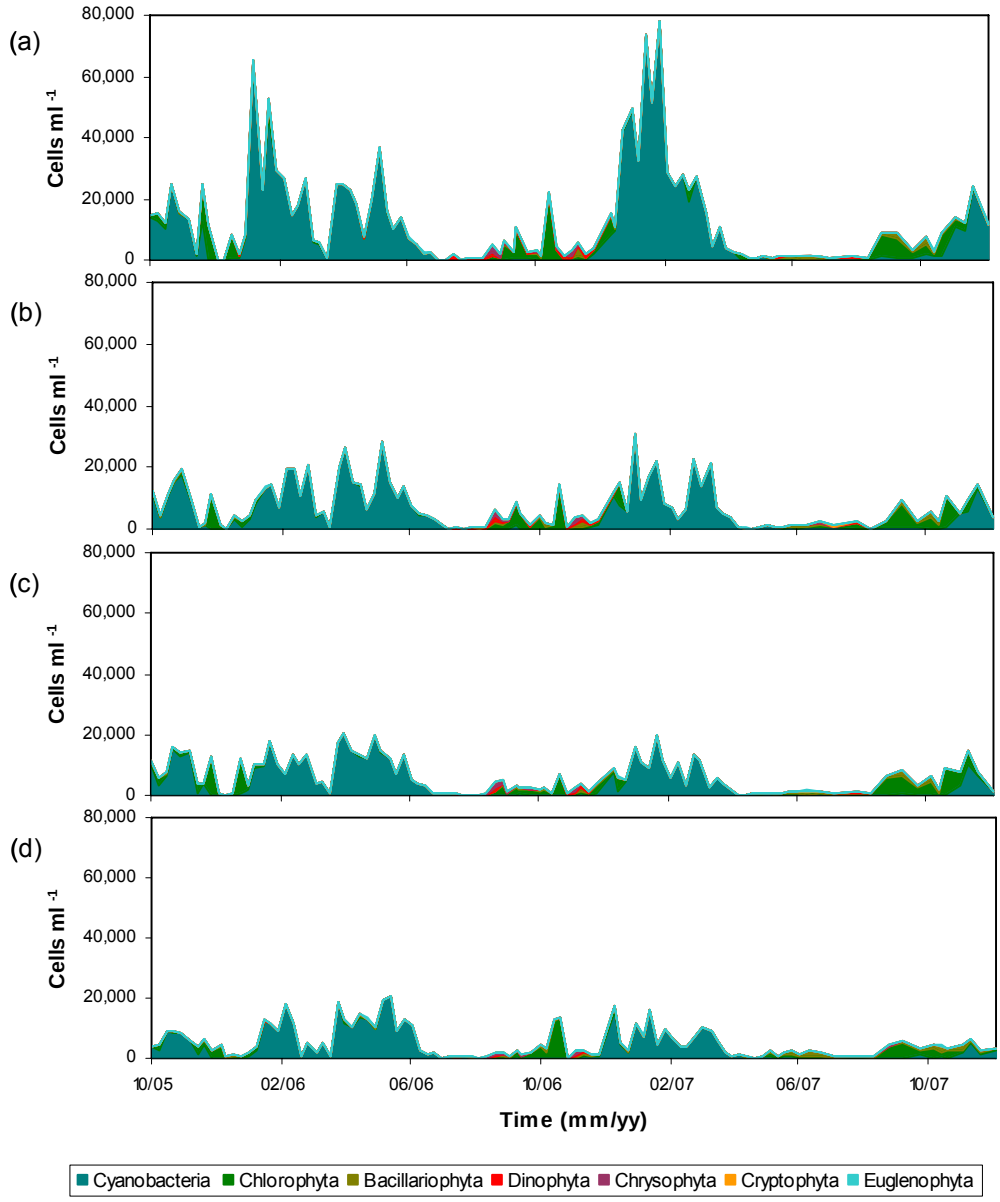


**Figure 3.1.6:** Composition of phytoplankton phyla at depths (a) 0 m, (b) 5 m, (c) 10 m and (d) 15 m from the Valve Tower (Site 1) between 24 October 2005 and 12 December 2007.

concentrations, as with chlorophyll *a*, increased later over the 2006/7 summer period, and remained at bloom levels for a shorter period compared with the previous year, 2005/6. However, maximal surface concentrations reached a higher level compared with 2006/7, peaking at 63,800 cells $ml^{-1}$ on 30 January 2006 and 78,400 cells $ml^{-1}$ on 19 February 2007. A larger disparity between surface (0 m) and depth (15 m) samples also occurred in 2006/7, possibly due to the elevated wind speeds associated and increased water column mixing in 2005/6 (Fig. 3.1.1).

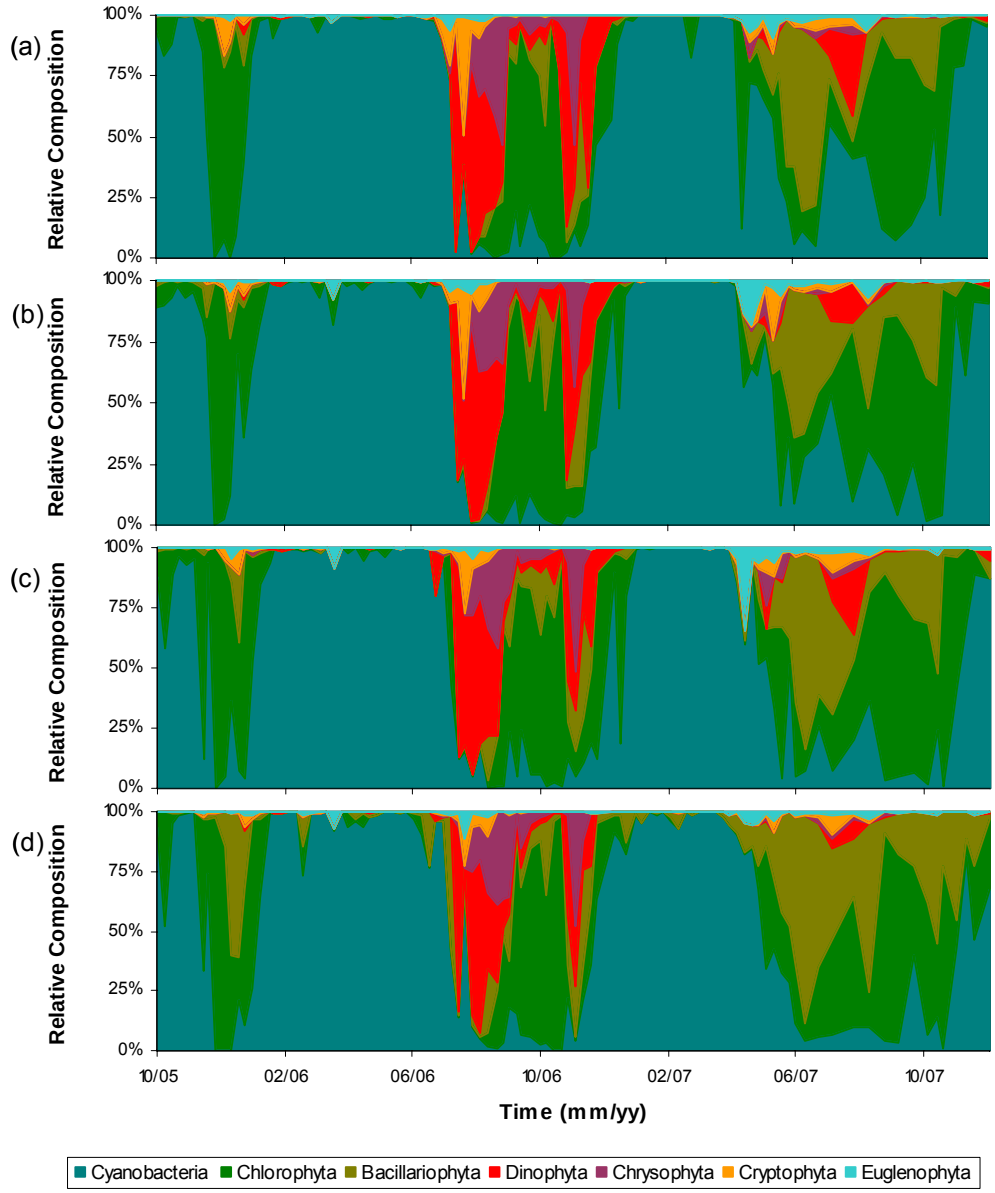


**Figure 3.1.7:** Relative composition of phytoplankton phyla at depths (a) 0 m, (b) 5 m, (c) 10 m and (d) 15 m from the Valve Tower (Site 1) between 24 October 2005 and 12 December 2007.

Phytoplankton assemblages were more homogenous with respect to depth during isothermal conditions (Fig. 3.1.6), compared with times of stratification when abundances of specific taxa were an order of magnitude greater at the surface compared to depth (15 m). During periods of isothermy *Staurastrum* sp., *Closterium* sp., *Dictyosphaerium* sp., *Eudorina* sp. and *Volvox* sp. amongst the chlorophytes, *Aulacoseira* sp. amongst the bacillariophytes and small flagellated dinophytes comprised the majority of the phytoplankton assemblage. This changed from year to

year, with chlorophytes and dinophytes dominating the winter of 2006 and chlorophytes and bacillariophytes the winter of 2007 (Fig. 3.1.7).

*Anabaena planktonica* concentrations and heterocytes per vegetative cell followed a noticeable seasonal pattern that appeared to be related to the total inorganic nitrogen concentrations (TIN = $NH_4$-N + $NO_3$-N; Fig. 3.1.8). As TIN becomes depleted at the surface the number of heterocytes per vegetative cell increases, which is followed by substantial increases in *A. planktonica* cell densities.

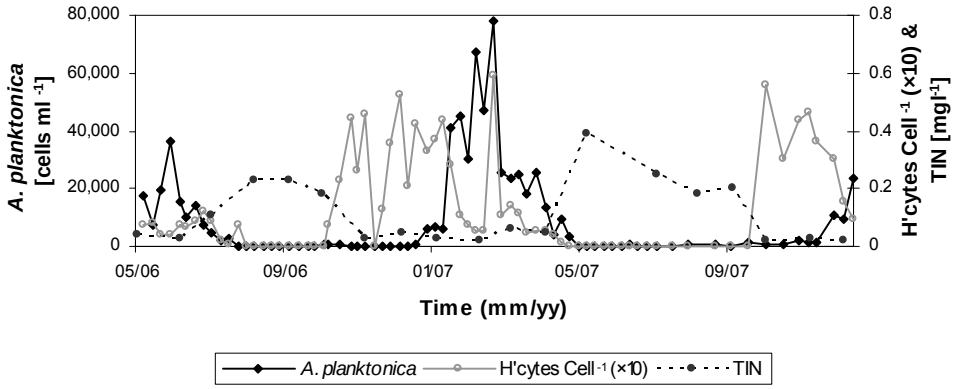


**Figure 3.1.8:** *Anabaena planktonica* concentrations, number of heterocytes per *A. planktonica* cell and total inorganic nitrogen (TIN = $NH_4$-N + $NO_3$-N) concentrations at 0 m between 2 May 2006 and 12 December 2007.

## 3.1.5 Statistical analysis of environmental influences on phytoplankton

Canonical correspondence analysis (CCA) was used to infer relationships between the phytoplankton assemblage and physico-chemical variables with respect to time. The CCA produced eigenvalues of 0.253 and 0.114 for axis 1 and 2 respectively (Fig. 3.1.9). Axis 1 had a species-environment correlation of 0.889 and axis 2, 0.882. Both axes combined explained a total of 38.2 % of the species data variance and 73.3 % of the species environment correlation variance (Table 3.1). Individually, axis 1 explained 26.3 % of the species data variance and 50.5 % of the species-environment correlation variance, while axis 2 explained only 11.9 % of the species data variance and 22.8 % of the species-environment correlation variance (Table 3.1).

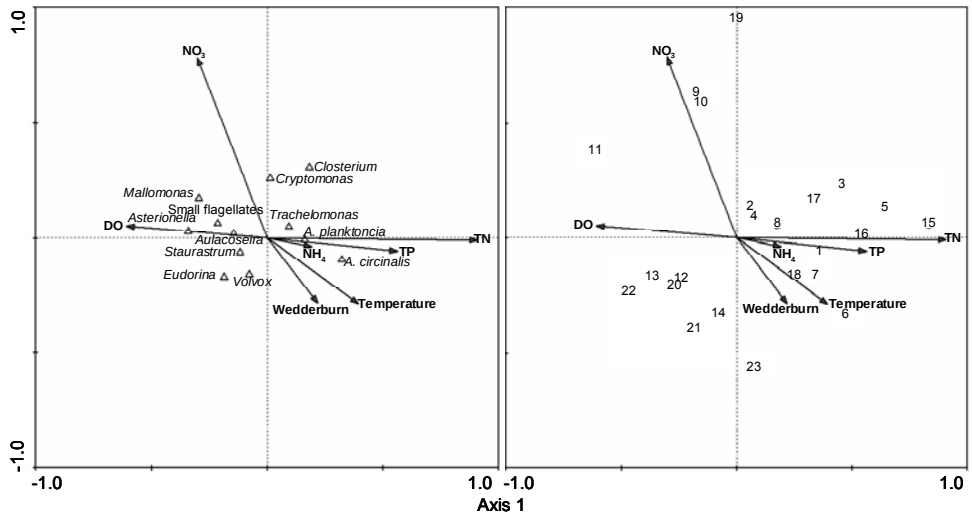


**Figure 3.1.9:** CCA ordination of phytoplankton taxa with respect to physico-chemical environmental variables at the surface (0 m) in the Lower Karori Reservoir, showing physico-chemical variables with (a) phytoplankton taxa and (b) sample numbers.

**Table 3.1** Results of CCA ordination using 7 abiotic variables and 12 phytoplankton taxa.

| | Axis 1 | Axis 2 | Axis 3 | Axis 4 |
|---|---|---|---|---|
| Eigenvalues | 0.253 | 0.114 | 0.057 | 0.036 |
| Species-environment correlations | 0.889 | 0.882 | 0.649 | 0.691 |
| Cumulative percentage variance | | | | |
| of species data | 26.3 | 38.2 | 44.1 | 47.9 |
| of species-environment correlation | 50.5 | 73.3 | 84.7 | 91.9 |

Samples taken during thermally stratified conditions were predominantly positively correlated (located on the right side of the ordination) with axis 1, with 8 of the 12 samples taken during stratified conditions found on the right side of the ordination (Fig. 3.1.9; Table 3.2). Of the four samples associated with stratified conditions, but placed on the left side of the ordination, three were recorded during the first two months of stratification (samples 13, 14 and 22) and one during a short term stratification event in October (sample 11). Associated with the negative side of the ordination, and subsequently negatively correlated with axis 1, were samples generally related with isothermal conditions or weak stages of stratification (Fig. 3.1.9; Table 3.2). Species associated with stratified conditions, such as *A. planktonica* and *A. circinalis*, are located on the positive side of axis 1. Conversely taxa predominantly associated with isothermal conditions such as the chrysophyte *Mallomonas* sp., the chlorophyte *Staurastrum* sp. and the bacillariophye *Asterionella* sp., are located on the negative side of axis 1.

**Table 3.2** Key to sample numbers for the CCA ordination.

| No. | Date | Stratified (S) or Isothermal (I) | No. | Date | Stratified (S) or Isothermal (I) |
|---|---|---|---|---|---|
| 1 | 12/12/2005 | S | 13 | 06/12/2006 | S |
| 2 | 09/01/2006 | S | 14 | 04/01/2007 | S |
| 3 | 09/02/2006 | S | 15 | 08/02/2007 | S |
| 4 | 07/03/2006 | S | 16 | 06/03/2007 | S |
| 5 | 10/04/2006 | I | 17 | 04/04/2007 | S |
| 6 | 02/05/2006 | I | 18 | 07/05/2007 | I |
| 7 | 07/06/2006 | I | 19 | 04/07/2007 | I |
| 8 | 03/07/2006 | I | 20 | 04/09/2007 | I |
| 9 | 07/08/2006 | I | 21 | 01/10/2007 | I |
| 10 | 04/09/2006 | I | 22 | 07/11/2007 | S |
| 11 | 02/10/2006 | S | 23 | 04/12/2007 | S |
| 12 | 06/11/2006 | I | | | |

Axis 1 is highly positively correlated with total nitrogen and total phosphorus and negatively correlated with dissolved oxygen (Fig. 3.1.9). The CCA ordination, forward selection and Monte Carlo permutation (Table 3.3) demonstrated that total nitrogen was the most important environmental factor in the analysis and therefore the most important variable contributing to temporal phytoplankton variation in the LKR. Total nitrogen explained a total of 21 % of the phytoplankton variation. Although dissolved oxygen, nitrate and total phosphorus had Lambda 1 values of 10 % or more, much of this variation had already been explained, as evidenced by the lower Lambda A values (Table 3.3).

**Table 3.3** Results for forward selection and Monte Carlo permutation tests using seven physico-chemical variables and 12 phytoplankton taxa.

| | Lambda 1 | Lambda A | *P*-value |
|---|---|---|---|
| Total Nitrogen | 0.21 | 0.21 | 0.002 |
| Dissolved Oxygen | 0.11 | 0.04 | 0.200 |
| Nitrate | 0.10 | 0.09 | 0.014 |
| Total Phosphorus | 0.10 | 0.02 | 0.666 |
| Temperature | 0.07 | 0.05 | 0.100 |
| Ammonium | 0.04 | 0.05 | 0.162 |
| Wedderburn Number | 0.03 | 0.04 | 0.296 |

## *3.2 High Resolution temporal and vertical variation*

### 3.2.1 Thermal structure and dissolved oxygen

In the December sampling period, temperature and dissolved oxygen varied considerably in the uppermost 8 m of the water column (Fig. 3.2.1a). It is possible that is partly due to the Seacat profiler coming into contact with the dam wall at approximately from 4 to 11.5 m and thus affecting the accuracy of some of the probe

readings around these depths. The uppermost 4 m of the water profile appears to show the most variation in temperature and dissolved oxygen levels in LKR throughout the December sampling. Surface (0.5 m) temperature ranged between 15.4 and 17.7 °C over the December sampling period, with the maximum temperature associated with the 1300 hours sampling time, corresponding approximately to the daily solar solstice. Surface dissolved oxygen levels also varied considerably over the 72 h period, with a range of 8.0 to 10.1 mg $l^{-1}$. Temperature and dissolved oxygen profiles also seem to hint at a possible deepening of the surface mixed layer over the final 24 hours of sampling. Here, profiles taken on 8 December 2006 at 0800, 1300, 1900 and 0100 hours the following day show that the surface mixed layer was deepened, from approximately 4 to 8 m in depth. 8 December 2006 had the fifth lowest total solar radiation and the eighth highest hourly mean wind speed of any day in December.

The problem of the Seacat profiler coming into contact with the dam wall was resolved by February when additional profiles were undertaken. At this time there was a shallow surface mixed layer of approximately 3 m (Fig. 3.2.1b), with the remainder of the profile showing little variation in temperature and dissolved oxygen over the sampling period. Surface temperatures ranged between 19.3 and 21.3 °C, and dissolved oxygen between 7.4 and 9.9 mg $l^{-1}$, with the warmest and most oxygen rich waters associated with 1900 hours sampling, following sustained diurnal illumination.

Samples in June showed the reservoir had returned to a state of isothermy with homogenous profiles of temperature and dissolved oxygen recorded throughout the depth profile for the duration of the sampling period (Fig. 3.2.1). Individual profiles of temperature varied by less than 0.5 °C and dissolved oxygen by less than 0.15 mg $l^{-1}$.

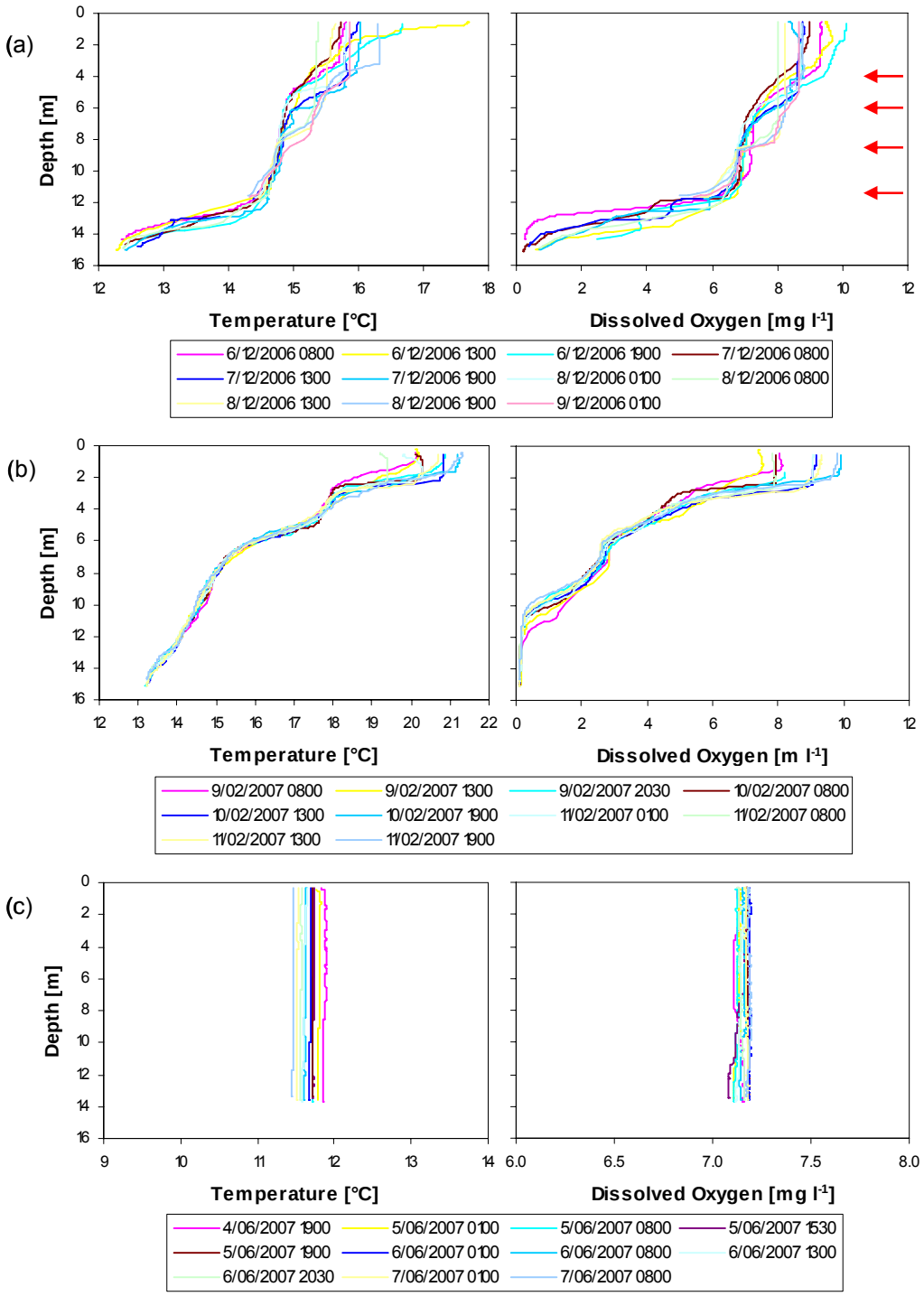


**Figure 3.2.1:** Temporal variation of temperature and dissolved oxygen at the Valve Tower (Site 1) between 6 and 9 December 2006, 9 and 12 February 2007 and 4 and 7 June 2007. Red arrows represent areas in the profile in which the Seacat profiler came into contact with the dam wall, which may have affected probe readings.

The euphotic depth (Table 3.4) was considerably lower in February, compared with pre-bloom conditions in December and post-bloom conditions in June. This relationship was also noticeable in terms of the light attenuation coefficient (Table 3.4), which was considerably higher during bloom conditions compared with pre- and post- bloom conditions. No noticeable variation was observed in the euphotic depth and light attenuation coefficient within each 24 h cycle. The depth of the thermocline (Table 3.4) varied considerably over the three day period in December, increasing from approximately 3.5 m on day 1 to 7.5 m on day 3, with a corresponding reduction in thermocline strength (Table 3.4). Both thermocline depth and strength remained relatively stable over the three day period in February.

**Table 3.4** Variations in euphotic depth, light attenuation coefficient and thermocline depth and strength with day and time

| | Day 1 | | | | Day 2 | | | | Day 3 | | | |
|---|---|---|---|---|---|---|---|---|---|---|---|---|
| | **0800** | **1300** | **1900** | **0100** | **0800** | **1300** | **1900** | **0100** | **0800** | **1300** | **1900** | **0100** |
| December | | | | | | | | | | | | |
| Depth of the Euphotic Zone, $Z_{eu}$ [m] | 4.6 | 5.6 | 4.2 | na | 5.8 | 4.8 | 5.8 | na | 5.2 | 5.6 | 4.6 | na |
| Light Attenuation Coefficient, $K_d$ [$m^{-1}$] | 0.9 | 0.6 | 0.9 | na | 0.8 | 0.8 | 0.9 | na | 0.8 | 0.7 | 0.9 | na |
| Depth of Thermocline, $z_t$ [m] | 3.7 | 3.2 | 3.9 | 5.0 | 3.3 | 5.3 | 5.7 | 5.0 | 7.1 | 7.6 | 7.5 | 8.1 |
| Strength of Thermocline, $\Delta t/\Delta d$ [°C $m^{-1}$] | 0.5 | 0.4 | 0.4 | 0.8 | 0.3 | 0.4 | 0.9 | 0.7 | 0.3 | 0.3 | 0.2 | 0.3 |
| February | | | | | | | | | | | | |
| Depth of the Euphotic Zone, $Z_{eu}$ [m] | 1.4 | 2.2 | 1.2 | na | 1.0 | 0.8 | 0.8 | na | 1.0 | 1.0 | 1.0 | na |
| Light Attenuation Coefficient, $K_d$ [$m^{-1}$] | nd | nd | 3.2 | na | 3.9 | 3.5 | 3.3 | na | 3.3 | 2.5 | 3.0 | na |
| Depth of Thermocline, $z_t$ [m] | 5.5 | 4.9 | 6.0 | ns | 5.8 | 5.7 | 5.4 | 5.6 | 5.7 | 5.3 | 5.6 | ns |
| Strength of Thermocline, $\Delta t/\Delta d$ [°C $m^{-1}$] | 1.1 | 1.3 | 1.6 | ns | 1.7 | 1.3 | 1.3 | 1.4 | 1.3 | 1.5 | 1.4 | ns |
| June | | | | | | | | | | | | |
| Depth of the Euphotic Zone, $Z_{eu}$ [m] | 6.8 | 6.4 | na | na | 6.6 | 6.4 | na | na | 7.0 | 6.6 | na | na |
| Light Attenuation Coefficient, $K_d$ [$m^{-1}$] | 0.7 | 0.8 | na | na | 0.8 | 0.8 | na | na | 0.8 | 0.8 | na | na |
| Depth of Thermocline, $z_t$ [m] | na | na | na | na | na | na | na | na | na | na | na | na |
| Strength of Thermocline, $\Delta t/\Delta d$ [°C $m^{-1}$] | na | na | na | na | na | na | na | na | na | na | na | na |

na, not applicable; nd, not determined; ns, not sampled

## 3.2.2 pH

During the December sampling period the pH remained relatively homogenous throughout the water column (Fig. 3.2.2). However, depth samples taken on 8 December 2006 at 0800, 1300, 1900 and 9 December at 0100 hours may indicate the beginning of thermal stratification as decreases in pH in 0, 5, and 10 m samples from the previous day appear to coincide with deepening of the surface mixed layer (Fig. 3.2.1). February samples showed differences in pH with depth and a possible mixing event from 11-12 February when 0 and 5 m samples and the 10 and 15 m samples were similar. June samples showed pH to be homogenous at all depths over the 72

hour sampling period. ANOVA tests found that pH varied significantly with depth during December ($F_{3, 43} = 15.7$, $P < 0.001$) and February ($F_{3, 40} = 88.2$, $P < 0.001$).

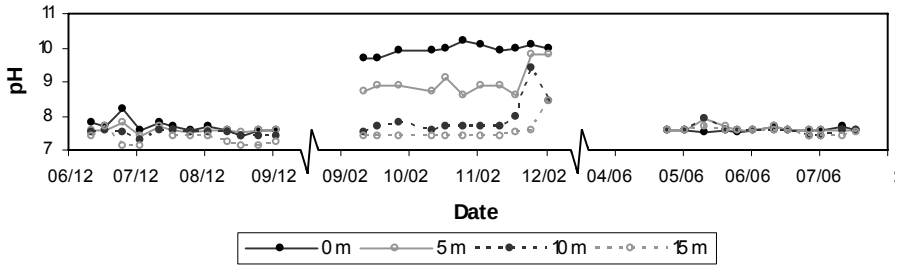


**Figure 3.2.2:** Temporal variation of pH at 0, 5, 10 and 15 m depth, measured at the Valve Tower (Site 1) between 6 and 9 December 2006, 9 and 12 February 2007 and 4 and 7 June 2007.

### 3.2.3 Nutrients and chlorophyll *a*

Concentrations of ammonium were low at all depths over the three sampling periods (December, February and June), with the general exception of depth (15 m) samples in February and to a lesser extent in December (Fig. 3.2.3a). Ammonium concentrations varied significantly with depth in December ($F_{3, 43} = 66.9$, $P < 0.001$) and February ($F_{3, 40} = 101.3$, $P < 0.001$). Nitrate concentrations show large increases in June. Nitrate only varied significantly with depth in February ($F_{3, 40} = 15.8$, $P < 0.001$). During December and February ammonium is the main constituent of TIN, while in June nitrate dominates the TIN. Concentrations of total nitrogen increased at the surface (0 m) and at depth (15 m) during February compared with samples at 5 and 10 m. Total nitrogen varied significantly with depth during December ($F_{3, 44} = 14.4$, $P < 0.001$) and February ($F_{3, 40} = 33.5$, $P < 0.001$).

Concentrations of phosphate, in agreement with the long-term dataset, are very low. Similar to ammonium, phosphate concentrations are elevated at 15 m, relative to other depths. Phosphate varied significantly with depth during December ($F_{3, 40} = 28.9$, $P < 0.001$) and February ($F_{3, 40} = 7.0$, $P < 0.001$). Total phosphorus showed a similar temporal pattern to total nitrogen, with elevated concentrations at depth during December and at surface and depth during February. High concentrations detected at 15 m depth during the first 24 hours of sampling in February were

removed as outliers in the ANOVA, with the resultant analysis showing that total phosphorus varied significantly with depth during December ($F_{3, 43} = 26.9$, $P < 0.001$) and February ($F_{3, 36} = 26.3$, $P < 0.001$).

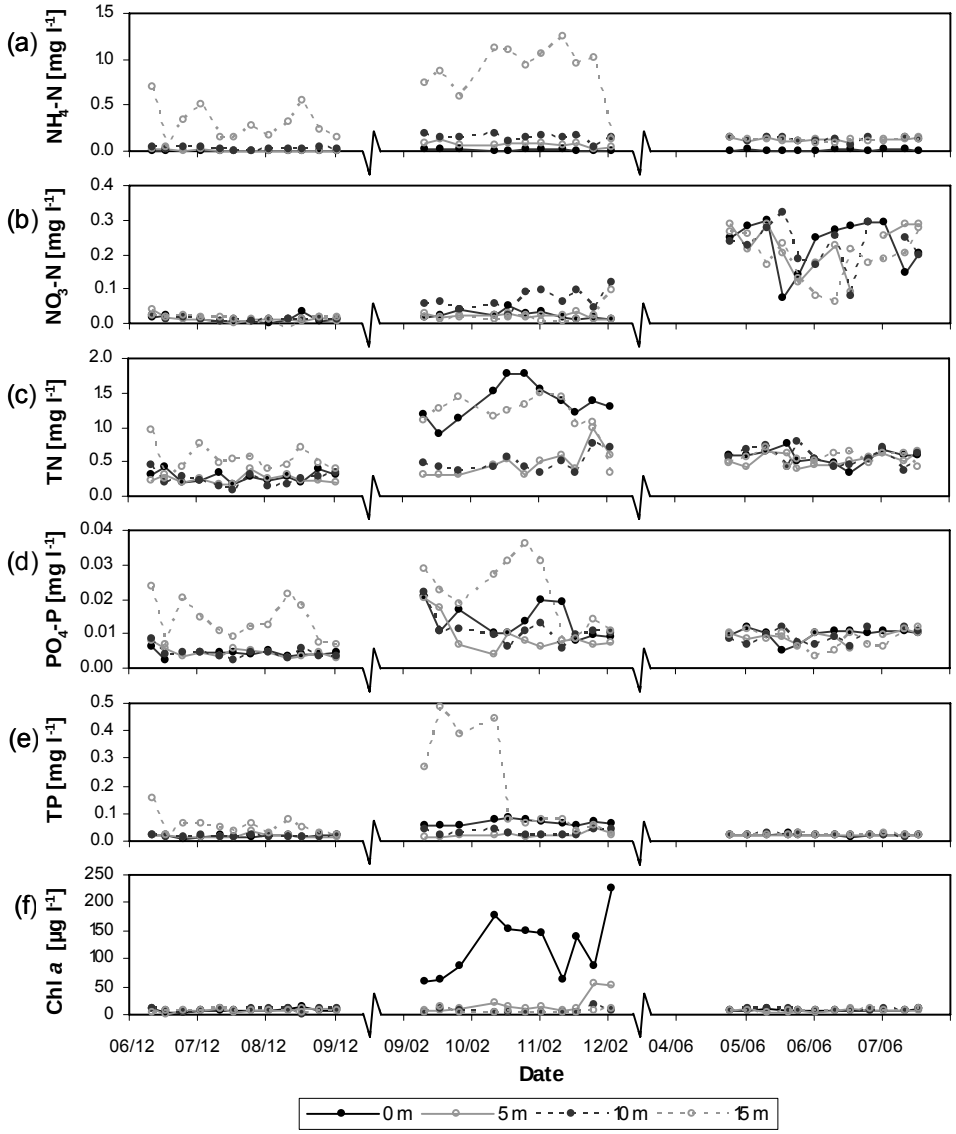


**Figure 3.2.3:** Temporal variation of (a) nitrate, (b) ammonium, (c) total nitrogen, (d) phosphate, (e) total phosphorus and (f) chlorophyll *a* at 0, 5, 10 and 15 m depth, measured at the Valve Tower (Site 1) between 6 and 9 December 2006, 9 and 12 February 2007 and 4 and 7 June 2007.

Chlorophyll *a* concentrations were homogenous at all depths during December and June, but there were significant differences at the surface compared with those at 5, 10 and 15 m depth in February ($F_{3, 40} = 69.2$, $P < 0.001$).

### 3.2.4 Phytoplankton assemblage

Phytoplankton taxa varied noticeably with depth during December and February, coinciding with stratified conditions. During December, samples were dominated by cyanobacteria, bacillariophytes and chlorophytes. In February, cyanobacterial concentrations were in excess of 80,000 cells $ml^{-1}$ at the surface and concentrations of chlorophytes, bacillariophytes and euglenophytes were low. Cyanobacterial densities in February decreased markedly with depth, although this group remained the dominant taxon at all depths.

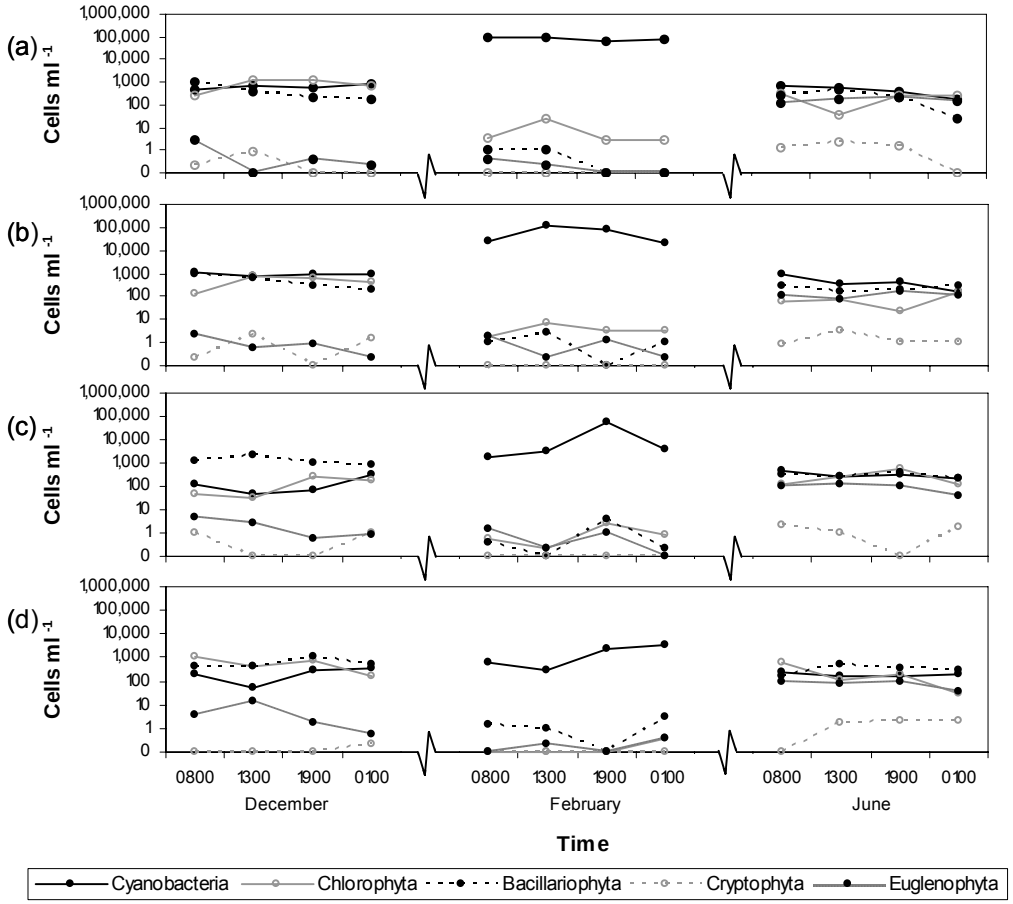


**Figure 3.2.4:** Temporal variation of phytoplankton at (a) 0 m, (b) 5 m, (c) 10 m and (d) 15 m measured at the Valve Tower (Site 1) between 0800 hours 8 December 2006 and 0100 hours 9 December 2006, 0800 hours 11 February 2007 and 0100 hours 12 February 2007 and 0800 hours 6 June 2007 and 0100 hours 7 June 2007.

June concentrations were similar to those seen in December, although euglenophytes made up a considerable proportion of the assemblage along with cyanobacteria,

bacillariophytes and chlorophytes. Cryptophytes were recorded during December and June but did not exceed concentrations of 2.2 and 3.0 cells $ml^{-1}$ respectively at any depth.

## *3.3 High resolution horizontal spatial variation*

### 3.3.1 Thermal structure and dissolved oxygen

On 7 December 2007 Sites 3 and 4, located at the southern end, were approximately 1 °C warmer over the upper 2 m than Sites 1 and 2 at a similar time of day (Fig. 3.3.1a). Dissolved oxygen showed little or no spatial variation between sites over the December sampling period. As with 9 December 2007, temperature and dissolved oxygen profiles taken on 9 February showed similar increases within the surface mixed layer along the transect, otherwise little variation was noted between sites (Fig. 3.3.1b). There was little variation in temperature and dissolved oxygen in June profiles (Fig 3.3.1c).

June concentrations were similar to those seen in December, although euglenophytes made up a considerable proportion of the assemblage along with cyanobacteria, bacillariophytes and chlorophytes. Cryptophytes were recorded during December and June but did not exceed concentrations of 2.2 and 3.0 cells $ml^{-1}$ respectively at any depth.

Euphotic depth and light attenuation (Table 3.5) showed little spatial variation between 6 and 8 December. The thermocline depth and strength (Table 3.5) also showed little variation, although a trend of deepening of the thermocline from 6 December (Day 1) to 8 December (Day 3) was evident. In February, light attenuation coefficients generally increased from Site 1 to Site 4 on 9 February (Day 1) and reduced from Site 1 to Site 4 on 10 February (Day 2) and 11 February (Day 3). Euphotic depth and the light attenuation coefficient showed no noticeable spatial variation in June.

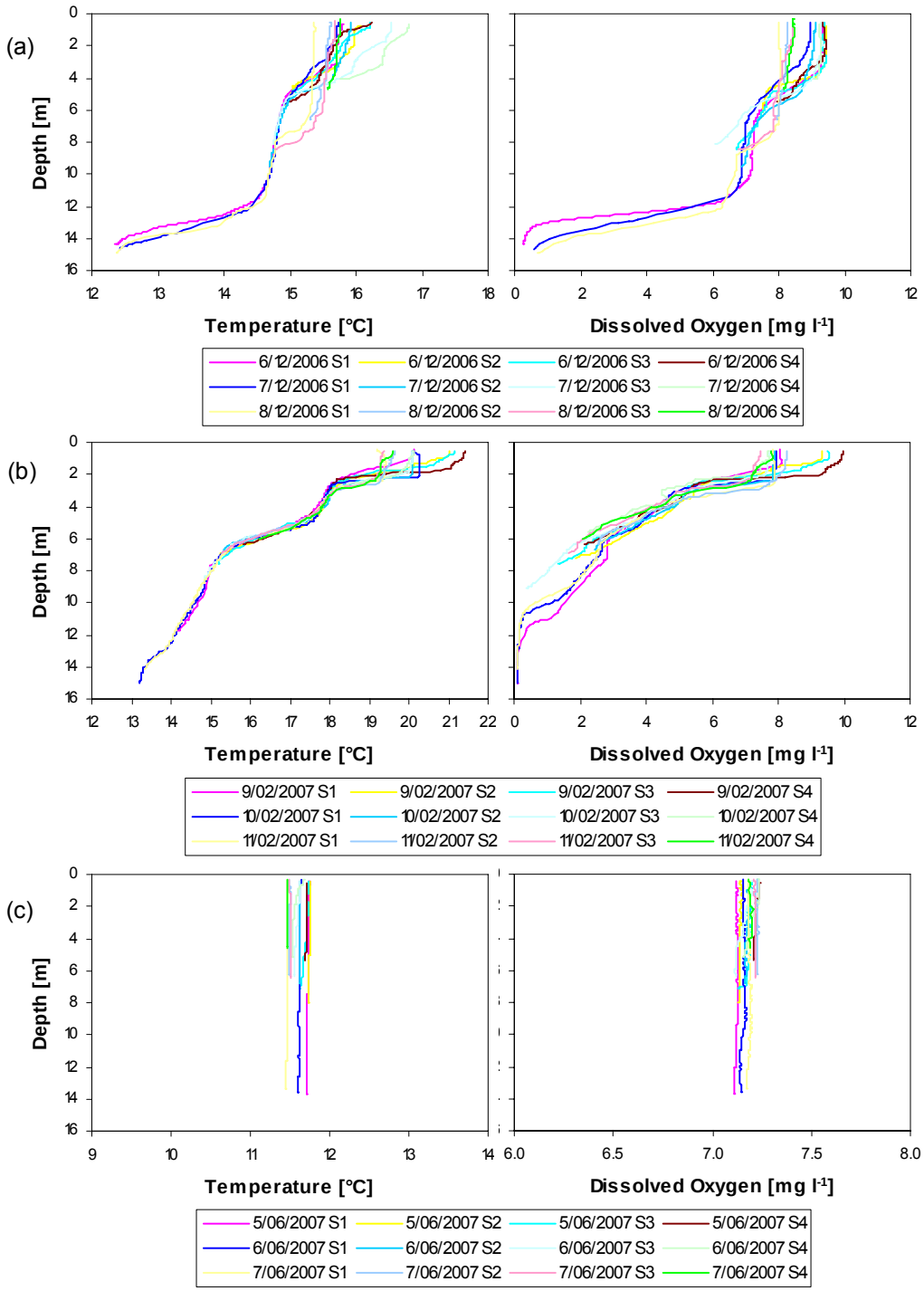


**Figure 3.3.1:** Spatial variation of temperature and dissolved oxygen between Sites 1, 2, 3 and 4 between 6 and 9 (a) December 2006, (b) 9 and 12 February 2007, (c) 4 and 7 June 2007.

**Table 3.5** Variations in euphotic depth, light attenuation coefficient and thermocline depth and strength with day and site.

| | Day 1 | | | | Day 2 | | | | Day 3 | | | |
|---|---|---|---|---|---|---|---|---|---|---|---|---|
| | **S1** | **S2** | **S3** | **S4** | **S1** | **S2** | **S3** | **S4** | **S1** | **S2** | **S3** | **S4** |
| December | | | | | | | | | | | | |
| Depth of the Euphotic Zone, $Z_{eu}$ [m] | 4.6 | 4.8 | 4.8 | 4.8 | 5.8 | 5.6 | 5.8 | 5.8 | 5.2 | 5.0 | 5.0 | 4.8 |
| Light Attenuation Coefficient, $K_d$ [$m^{-1}$] | 0.9 | 0.7 | 0.8 | 0.6 | 0.8 | 0.8 | 0.8 | 0.8 | 0.8 | 0.7 | 0.8 | 0.8 |
| Depth of Thermocline, $z_t$ [m] | 3.7 | 4.0 | 4.4 | nd | 3.3 | 5.1 | 4.5 | nd | 7.1 | nd | 6.1 | nd |
| Strength of Thermocline, $\Delta t/\Delta d$ [°C $m^{-1}$] | 0.5 | 0.6 | 0.5 | nd | 0.3 | 0.4 | 0.7 | nd | 0.3 | nd | 0.5 | nd |
| February | | | | | | | | | | | | |
| Depth of the Euphotic Zone, $Z_{eu}$ [m] | 1.4 | 1.0 | 1.0 | 0.8 | 1.0 | 1.0 | 1.0 | 1.0 | 1.0 | 1.0 | 1.0 | 1.0 |
| Light Attenuation Coefficient, $K_d$ [$m^{-1}$] | nd | 3.2 | 3.3 | 3.8 | 3.6 | 3.3 | 3.1 | 2.7 | 3.1 | 2.3 | 2.0 | 2.5 |
| Depth of Thermocline, $z_t$ [m] | 5.5 | 6.0 | 5.4 | nd | 5.8 | 5.5 | 5.7 | nd | 5.7 | 6.0 | 5.6 | nd |
| Strength of Thermocline, $\Delta t/\Delta d$ [°C $m^{-1}$] | 1.1 | 1.2 | 1.1 | nd | 1.7 | 1.6 | 1.8 | nd | 1.3 | 1.4 | 1.3 | nd |
| June | | | | | | | | | | | | |
| Depth of the Euphotic Zone, $Z_{eu}$ [m] | 6.6 | 6.8 | 6.2 | 7.0 | 6.6 | 5.8 | 6.0 | 6.4 | 7.0 | nd | 7.0 | 7.6 |
| Light Attenuation Coefficient, $K_d$ [$m^{-1}$] | 0.8 | 0.7 | 0.7 | 0.6 | 0.8 | 0.8 | 0.8 | 0.8 | 0.8 | 0.7 | 0.7 | 0.9 |
| Depth of Thermocline, $z_t$ [m] | na | na | na | na | na | na | na | na | na | na | na | na |
| Strength of Thermocline, $\Delta t/\Delta d$ [°C $m^{-1}$] | na | na | na | na | na | na | na | na | na | na | na | na |

na, not applicable; nd, not determined

## 3.3.2 pH

Within each of the three periods; December, February and June, samples demonstrated no variation of pH between sites at the surface, although inflow pH in February was considerably lower than surface values (Fig. 3.3.2). December and June pH measurements did not vary significantly with depth. In contrast, surface and depth samples taken during February differed by approximately 2 pH units at all sites.

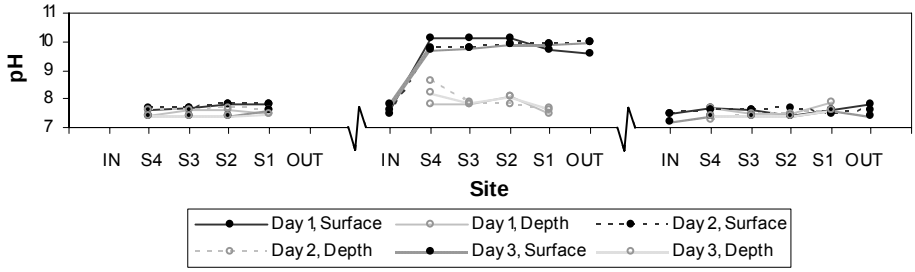


**Figure 3.3.2:** Variation of pH at surface (0 m) and depth (Site 1, 10 m; Site 2, 7 m; Site 3, 8 m; Site 4, 5 m), measured at the inflow (IN) Site 4 (S4), Site 3 (S3), Site 2 (S2), Site 1 (S1) and the outflow (OUT) between 6 and 9 December 2006, 9 and 12 February 2007 and 4 and 7 June 2007.

## 3.3.3 Nutrients and chlorophyll *a*

Ammonium concentrations were low in surface and depth samples throughout December, although concentrations on the first day at depth are elevated at Sites 1 and 2, possibly due to slightly deeper sampling depth (Fig. 3.3.3). Concentrations of

nitrate, total nitrogen, phosphate, total phosphorus and chlorophyll *a* were relatively spatially homogenous, both vertically and horizontally, between December 6 and 9.

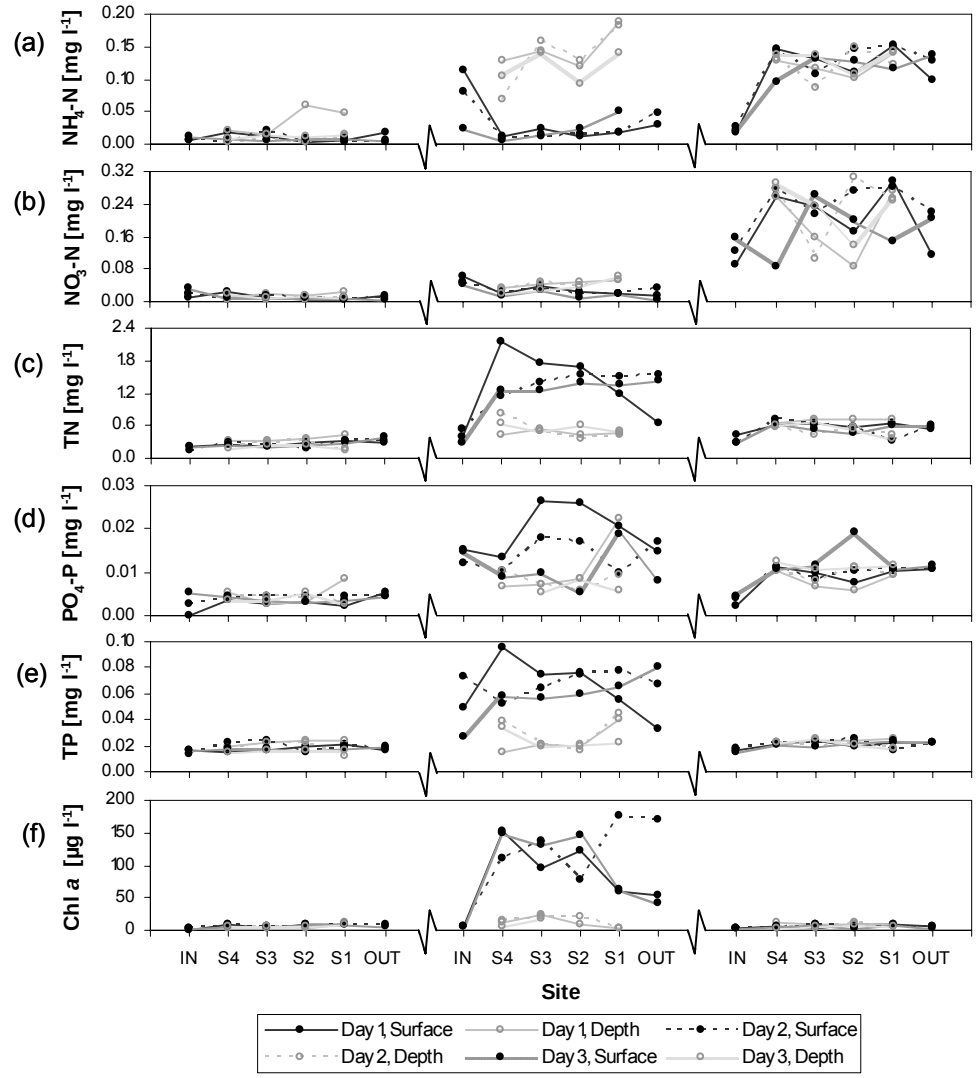


**Figure 3.3.3:** Variation of (a) nitrate, (b) ammonium, (c) total nitrogen, (d) phosphate, (e) total phosphorus and (f) chlorophyll *a* at surface (0 m) and depth (Site 1, 10 m; Site 2, 7 m; Site 3, 8 m; Site 4, 5 m), measured at the inflow (IN) Site 4 (S4), Site 3 (S3), Site 2 (S2), Site 1 (S1) and the outflow (OUT) between 6 and 9 December 2006, 9 and 12 February 2007 and 4 and 7 June 2007.

During February there was greater variation of ammonium with depth, although some of this variation could be attributable to unintentional small variations in sample depth (Fig 3.3.3). Interestingly, total phosphorus and total nitrogen appear to increase at the surface from Site 1 to Site 4 on 9 February (Day 1) and conversely decrease on 9 and 10 February (Days 2 and 3). On day 1 a similar spatial trend occurs with

chlorophyll *a*, but not on days 2 and 3. During February, nutrient and chlorophyll *a* inflow values varied considerably compared with those from Sites 1, 2, 3, 4 and the outflow.

During June, ammonium, nitrate, total nitrogen, phosphate, total phosphorus and chlorophyll *a* were all highly vertically and horizontally homogenous (Fig. 3.3.3).

## *3.4 Quantitative PCR*

The results of the QPCR results clearly showed temporal (Fig. 3.4.1) and spatial variation (Fig. 3.4.2) of *A. planktonica* within LKR, especially during February. *Anabaena planktonica* concentrations in December (Fig. 3.4.1a) were ~ 500 cells $ml^{-1}$. Although samples show no distinct variation with respect to time over this period, concentrations tend to be slightly elevated at 0 m and 5 m. There was a significant increase in *A. planktonica* abundance between December and February. During February concentrations were noticeably higher at the surface (0 m). Additionally, there was a distinct surface temporal variation of *A. planktonica* concentrations. The concentrations increased from 0800 hours to a peak at 1900 hours and had declined again by 0100 hours. Samples at depths of 5, 10 and 15 m showed no distinct temporal variation, although at 0800 hours they were similar to or at higher concentrations than surface samples. Samples in June (Fig. 3.4.1) showed *A. planktonica* concentrations to be both temporally and vertically spatially homogenous with depth.

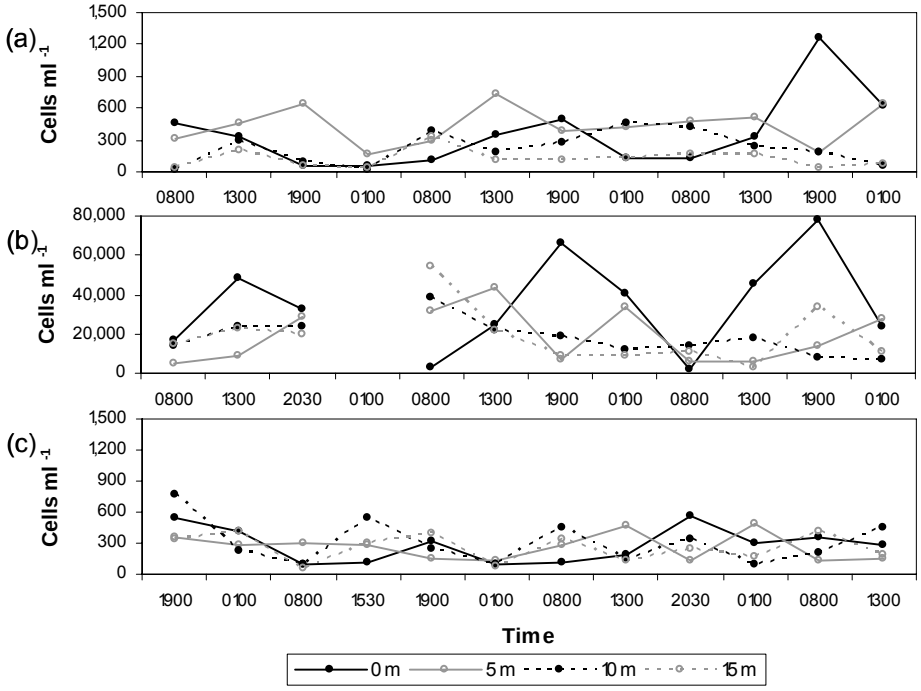


**Figure 3.4.1:** Temporal variation of *Anabaena planktonica* determined using QPCR at the Valve Tower (Site 1) in (a) December, (b) February and (c) June. Note different scale in b compared with a and c.

Each day sampled, 8 December, 11 February and 7 June demonstrated the inflow to be free from *A. planktonica*. It also suggested that surface samples of *A. planktonica* increase in a horizontal direction from the south end (at the inflow) to the northern end (at the outflow). This is especially noticeable on 11 February (Fig 3.4.2b), when concentrations increase from 600 cells $ml^{-1}$ at Site 4, to 1,100 cells $ml^{-1}$ at Site 3, 6,700 cells $ml^{-1}$ at Site 2, and 17,100 cells $ml^{-1}$ at Site 1, and reach concentrations of 28,500 cells $ml^{-1}$ at the outflow. Depth samples (Site 1, 10 m; Site 2, 7 m; Site 3, 8 m; Site 4, 5 m) were relatively horizontally homogenous over each day; 8 December, 11 February and 7 June.

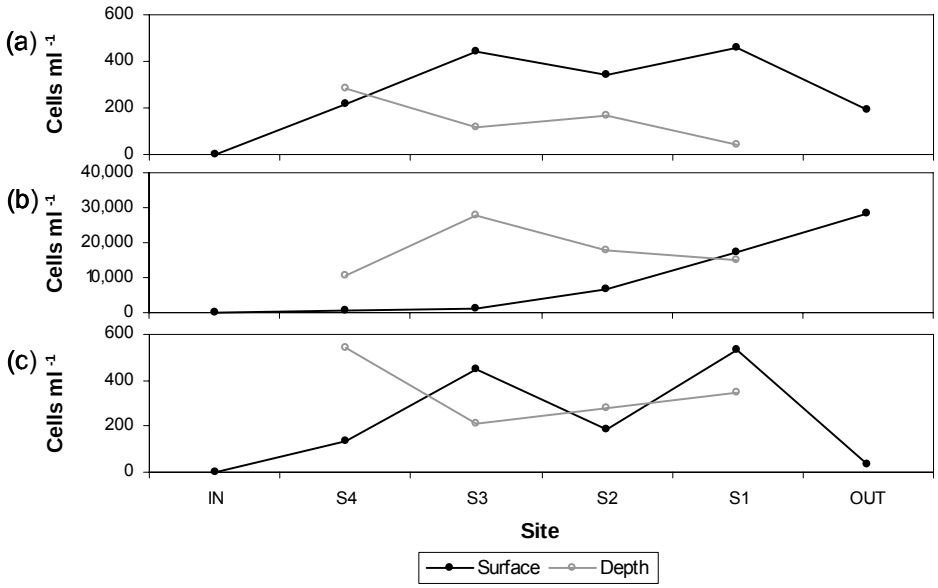


**Figure 3.4.2:** Spatial variation of *Anabaena planktonica* determined using QPCR between the inflow (IN), Site 4 (S4), Site 3 (S3), Site 2 (S2), Site 1 (S1) and the outflow (OUT) on (a) 8 December, (b) 11 February and (c) 7 June. Note different scale in b compared with a and c.

## *3.5 Biomanipulation*

Between 12 and 15 February 2007 3,946 *Perca fluviatilis* (European perch) and one brown trout (*Salmo trutta*) were caught and removed, while two longfin eels (*Anguilla dieffenbachia*) and one koura (*Paranephrops planifrons*) were caught and replaced in the reservoir. A further four shortfin eels and one koura were caught and replaced, and one brown trout caught and removed in the wetland at the northern end of the reservoir. Based on fork length, three age classes of *P. fluviatilis* were estimated between lengths of 25 and 160 mm, with the remaining fish over 160 mm in length at least three years in age. Hicks *et al.* (2007) estimates there to be approximately 20,000 to 22,000 *P. fluviatilis* within the LKR, of which 80% are comprised by age-0 and age-1 individuals.

On 26 February 2007, 11 days following the removal of *P. fluviatilis* a large drop in *A. planktonica* concentration (51.4%) and a marked increase in zooplankton concentration (63.6%) were observed (Fig. 3.5.1) compared with the pre-removal counts (12 February 2007). The month immediately following the *P. fluviatilis* removal (Fig. 3.5.2) showed a noticeable reduction in the rotifer population and a

subsequent increase in large-bodied crustaceans (e.g., *Daphnia* sp.). Since this time the rotifer population has rebounded and large bodied crustaceans have again decreased, while copepods concentrations have increased relative to their pre-removal concentrations. *Anabaena planktonica* concentrations, reduced immediately following *P. fluviatilis* removal and remained at low abundance during isothermal conditions. However, these appear to be increasing again as the system becomes stratified (November 2007).

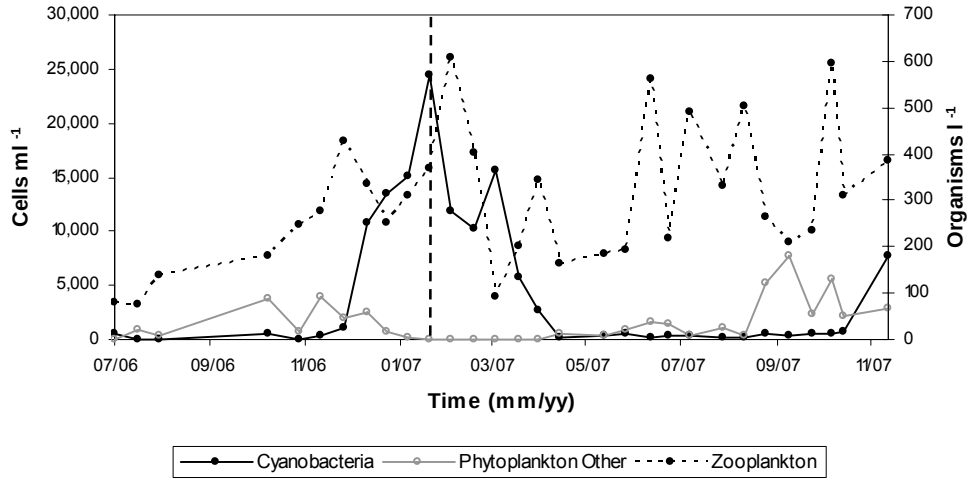


**Figure 3.5.1:** Cyanobacteria (pooled 0, 5, 10 and 15 m samples), phytoplankton (excluding cyanobacteria; pooled 0, 5, 10 and 15 m samples; left vertical axis) and zooplankton (pooled 5, 10 and 15 m samples; right vertical axis). Vertical black hatched line denotes *Perca fluviatilis* removal between 12 and 15 February 2007.

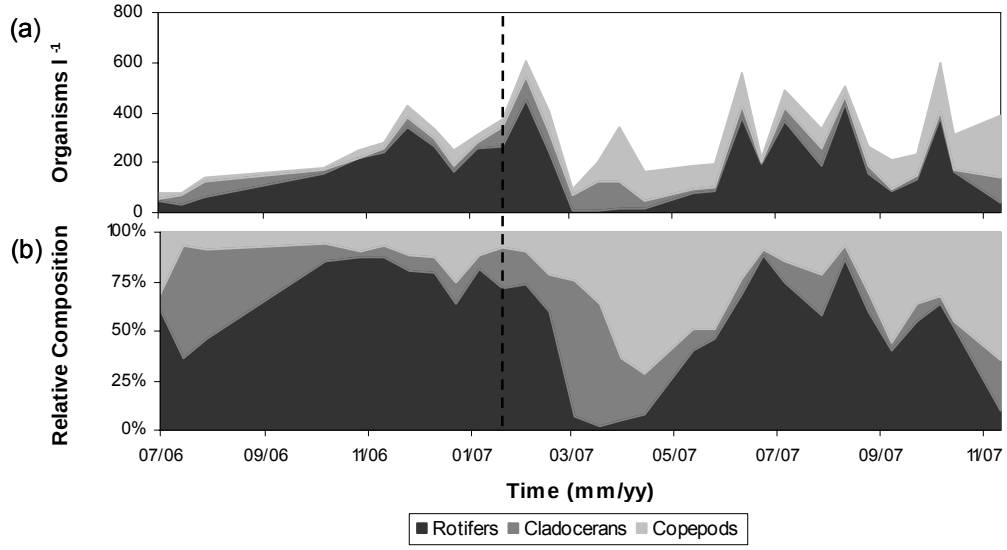


**Figure 3.5.2:** (a) Absolute and (b) relative composition and succession of zooplankton taxa from a pooled sample taken from depths of 5, 10 and 15 m from the Valve Tower (Site 1) between 24 July 2006 and 4 December 2007. Vertical black hatched line denotes *Perca fluviatilis* removal between 12 and 15 February 2007.

An ANOVA test comparing periods (24 July and 18 December) of pre- and post- *P. fluviatilis* removal showed that the zooplankton population had increased significantly ($F_{1, 15} = 5.6$, $P = 0.032$) following *P. fluviatilis* removal (Table 3.6). Although the zooplankton community increased significantly, copepods were the only group for which the result was statistically significant ($F_{1, 15} = 11.6$, $P = 0.004$).

**Table 3.6** ANOVA demonstrating changes in zooplankton abundance as a result of the *Perca fluviatilis* removal. SD is standard deviation. * denotes $P < 0.05$ and ** $P < 0.01$.

| | Pre-Removal | | Post-Removal | | *P*-value |
|---|---|---|---|---|---|
| | Mean | SD | Mean | SD | |
| Rotifers | 156.5 | 117.1 | 210.2 | 134.6 | 0.407 |
| Cladocerans | 26.3 | 21.4 | 36.2 | 29.3 | 0.458 |
| Copepods | 21.3 | 15.1 | 109.5 | 66.5 | 0.004 ** |
| Total | 204.1 | 124.9 | 355.9 | 133.6 | 0.032 * |

## *3.6 Temperature and light growth experiments*

Growth rates, μ ($K_e$), of *A. planktonica* increased with increasing light intensity (Table 3.7). *Anabaena planktonica* growth rates were 0.17 day$^{-1}$ at light intensities of 140 and 60 μmol m$^{-2}$ s$^{-1}$. Growth rates slowed considerably when irradiance was decreased from 60 to 40 μmol m$^{-2}$ s$^{-1}$, and were lowest at the lowest light intensity tested; 20 μmol m$^{-2}$ s$^{-1}$ (Table 3.7).

The different light intensities also had a marked effect on the final concentration of *A. planktonica* in the stationary phase (Fig. 3.6.1; Fig. 3.6.2). Maximal densities were recorded at 140 µmol $m^{-2}$ $s^{-1}$ with concentrations exceeding 700,000 cells $ml^{-1}$. Cell concentrations in the 20 and 40 µmol $m^{-2}$ $s^{-1}$ cases only reached 20,000 cells $ml^{-1}$ in the stationary phase.

**Table 3.7** Growth rates and doubling times of *Anabaena planktonica* at 20, 40, 60 and 140 µmol $m^{-2}$ $s^{-1}$.

| Light Intenisty [µmol $m^{-2}$ $s^{-1}$] | Growth Rate, µ ($K_e$) [$d^{-1}$] | Doubling Time [$d^{-1}$] |
|---|---|---|
| 20 | 0.08 | 12.1 |
| 40 | 0.10 | 9.8 |
| 60 | 0.17 | 5.8 |
| 140 | 0.17 | 6.0 |

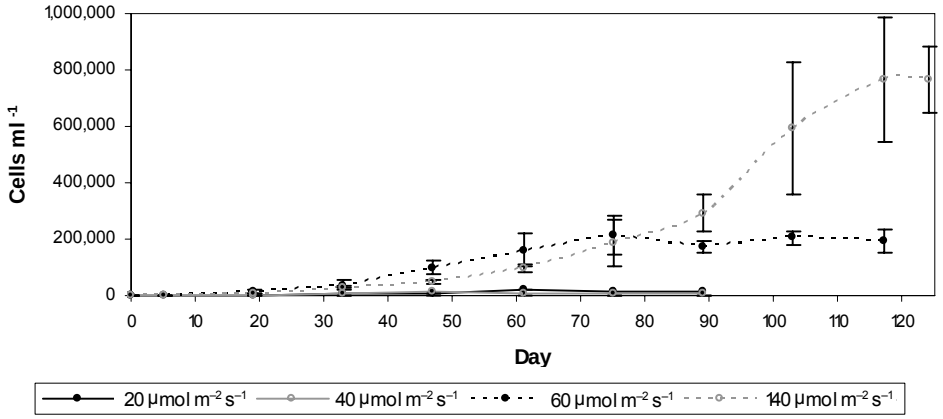


**Figure 3.6.1:** Growth curves for *Anabaena planktonica* at light intensities of 20, 40, 60 and 140 µmol $m^{-2}$ $s^{-1}$. Error bars indicate one standard deviation.

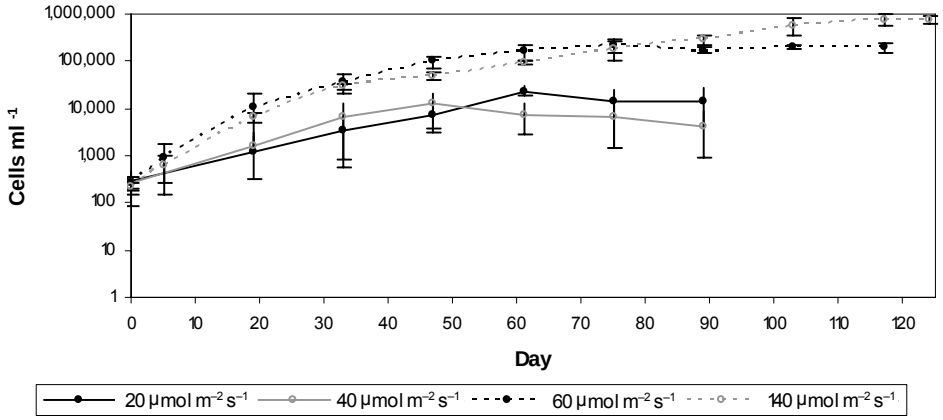


**Figure 3.6.2:** Growth curves for *Anabaena planktonica* at light intensities of 20, 40, 60 and 140 µmol $m^{-2}$ $s^{-1}$, plotted on a $\log_{10}$ scale. Error bars indicate one standard deviation.

Growth rates of *A. planktonica* also varied with temperature (Table 3.8). The highest growth rates (0.25 $day^{-1}$) were recorded at 25 °C. Interestingly, the growth rates at temperatures of 10 and 20 °C (0.17 $day^{-1}$) did not differ as expected.

Temperature also had a substantial effect on the concentration of *A. planktonica* in the stationary phase (Fig. 3.6.3; Fig. 3.6.4), although not to the same extent as observed for light intensity. The highest concentrations (> 700,000 cells $ml^{-1}$) were recorded at 20 °C. Cultures at 25 °C grew at the fastest rate during the exponential phase but also reached the stationary phase sooner than the other treatments. Treatments at 10 and 20 °C spent a longer time in the exponential phase, but grew at a slower rate. Due to time and resource constraints, the experiment had to be cut off before the 10 °C treatment had reached the stationary phase. For an unknown reason large variations were recorded in the 10 °C replicates, denoted by high standard deviations.

**Table 3.8** Growth rates and doubling times of *Anabaena planktonica* at 10, 20 and 25 °C.

| Temperature [°C] | Growth Rate, μ ($K_e$) [$d^{-1}$] | Doubling Time [$d^{-1}$] |
|---|---|---|
| 10 | 0.14 | 7.1 |
| 20 | 0.17 | 6.0 |
| 25 | 0.25 | 4.0 |

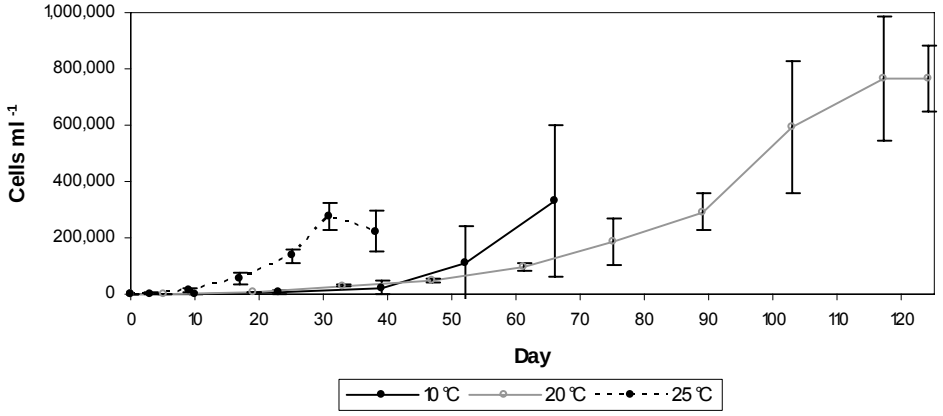


**Figure 3.6.3:** Growth curves for *Anabaena planktonica* at light intensities of 10, 20 and 25 °C. Error bars indicate one standard deviation.

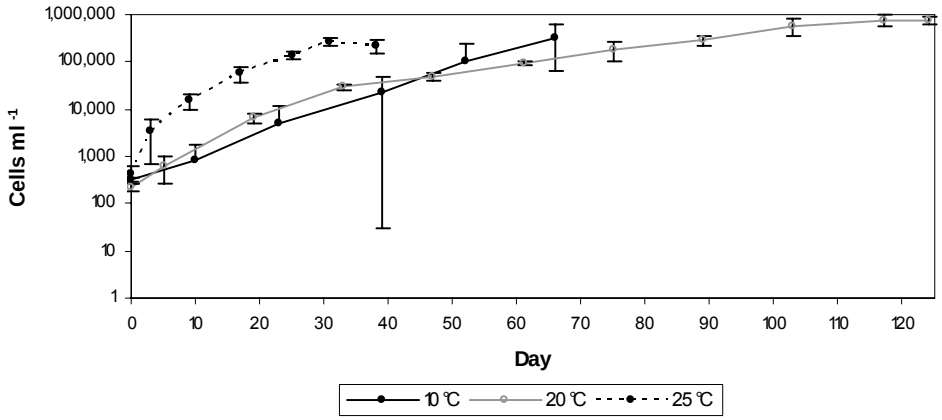


**Figure 3.6.4:** Growth curves for *Anabaena planktonica* at light intensities of 10, 20 and 25 °C, plotted on a $\log_{10}$ scale. Error bars indicate one standard deviation.

## *3.7 Modelling and bloom control strategies*

### 3.7.1 Temperature

Water column temperature was well approximated by the hydrodynamic model, DYRESM, both over time and space (Table 3.9; Fig 3.7.1). The timing and duration of stratification was demonstrated accurately over both years, although the model predicted the surface waters to cool at a slightly faster rate following stratification compared with the observed data (Fig 3.7.1; Fig. 3.7.2). There was also some difficulty simulating mixing events just prior to and after stratification. Here the model overestimated the degree at which warm water was partitioned vertically through the water profile, causing temperatures at 10 and 15 m to be overestimated. This may be a result of the relative importance of wind direction at the LKR. Here wind direction changes considerably over short time periods, of three weeks, as is the case for the period prior to water column prior stratification in 2005 (13 October and 7 November 2005) and 2006 (15 November and 5 December 2006) (Fig. 3.7.3).

**Table 3.9** Statistical comparison between model simulations and observed data for temperature.

| | RSME | | R | |
|---|---|---|---|---|
| | Calibration | Validation | Calibration | Validation |
| 0 m | 0.972 | 0.902 | 0.978 | 0.980 |
| 5 m | 0.682 | 0.802 | 0.988 | 0.981 |
| 10 m | 1.081 | 0.986 | 0.945 | 0.954 |
| 15 m | 1.221 | 1.069 | 0.905 | 0.930 |

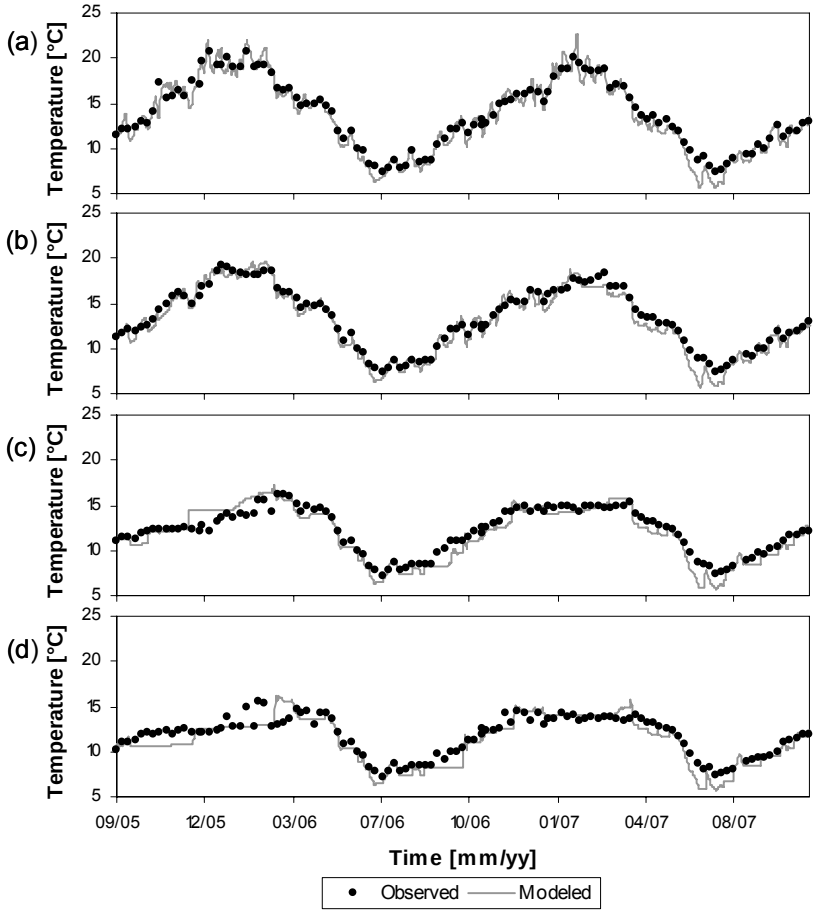


**Figure 3.7.1:** Observed and modeled water temperatures in the Lower Karori Reservoir at (a) 0 m, (b) 5 m, (c) 10 m and (d) 14 m.

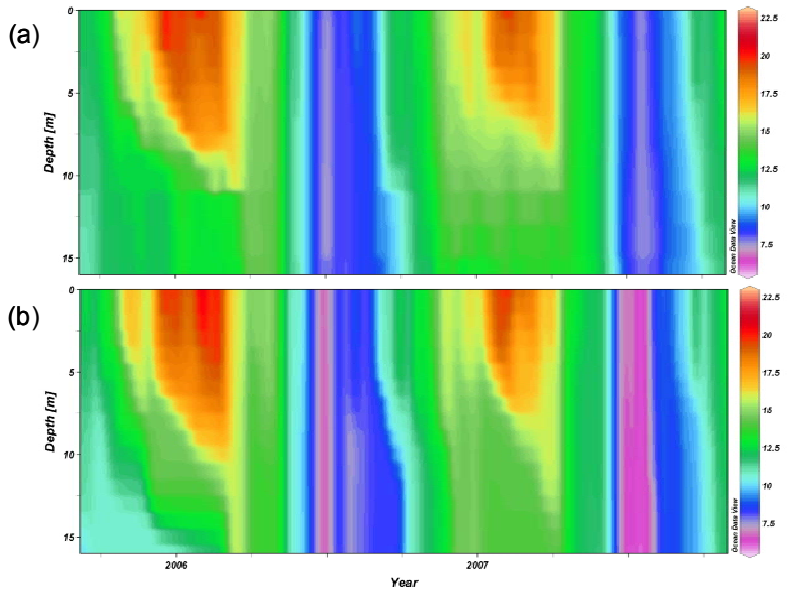


**Figure 3.7.2:** (a) Observed and (b) modeled temperature [°C] profiles in the Lower Karori Reservoir between 5 September 2005 and 29 October 2007.

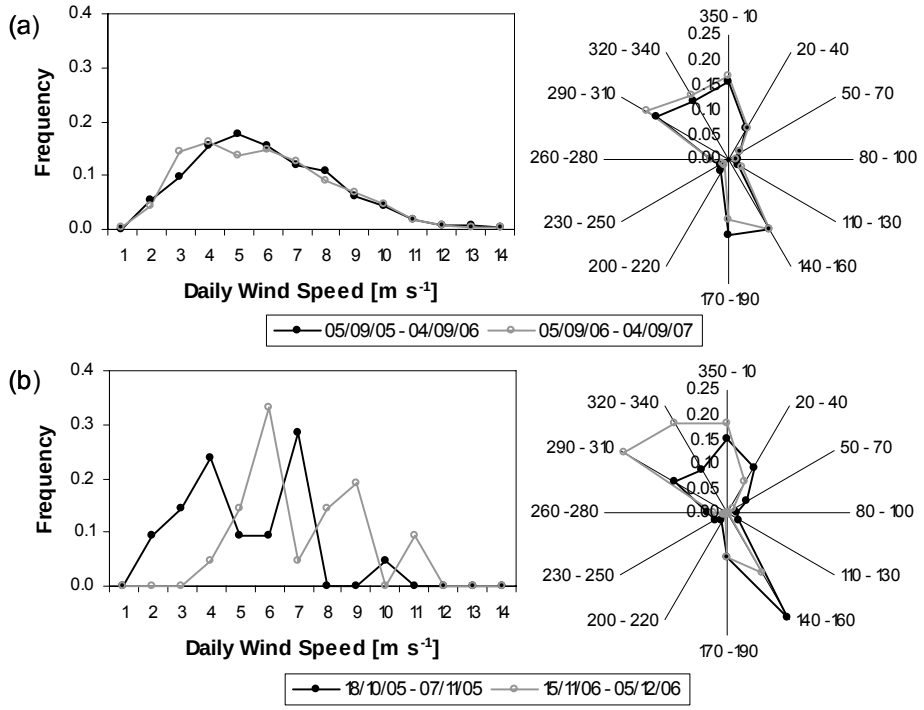


**Figure 3.7.3:** Daily wind speed (left) and prevailing wind direction (right) between (a) 5 September 2005 and 4 September 2006 and 5 September 2006 and 4 September 2007 and (b) comparable three week periods during the onset of stratification in 2005 (13 October and 7 November 2005) and 2006 (15 November and 5 December 2006).

## 3.7.2 Dissolved oxygen

Water column dissolved oxygen was relatively well approximated by the ecological model, CAEDYM, over both time and space (Table 3.10; Fig 3.7.4). Dissolved oxygen was simulated more accurately at depth, in relation to the surface where the model failed to pick up some of the large fluctuations over time. The model did not predict the high degree of anoxia at 5 m during occasional periods over December and January (Fig. 3.7.4b). It also under predicted the duration of anoxia during stratified conditions in the validation year (Fig. 3.7.4d).

**Table 3.10** Statistical comparison between model simulations and observed data for dissolved oxygen

| | RSME | | R | |
|---|---|---|---|---|
| | Calibration | Validation | Calibration | Validation |
| 0 m | 1.804 | 1.966 | 0.456 | 0.501 |
| 5 m | 1.941 | 1.984 | 0.822 | 0.734 |
| 10 m | 2.833 | 2.727 | 0.796 | 0.791 |
| 15 m | 3.604 | 3.437 | 0.693 | 0.707 |

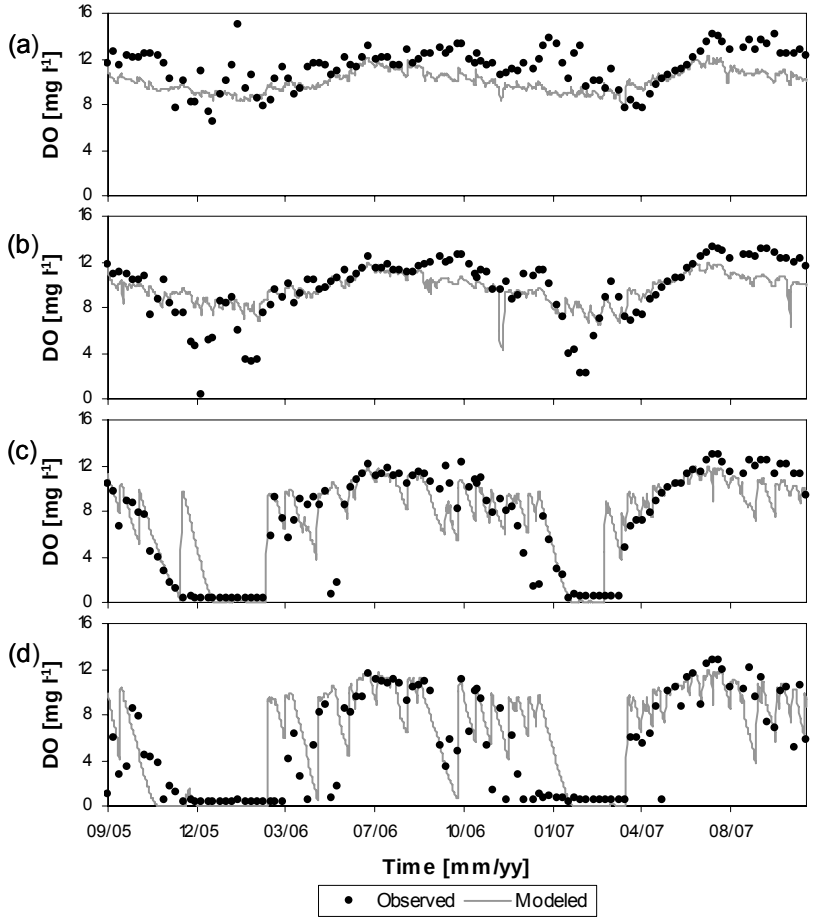


**Figure 3.7.4:** Observed and modeled dissolved oxygen concentrations in the Lower Karori Reservoir at (a) 0 m, (b) 5 m, (c) 10 m and (d) 14 m.

## 3.7.3 Nutrients

Depth concentrations of ammonium and surface concentrations of nitrate were simulated with positive results (Table 3.11; Fig 3.7.5). Although simulations of surface ammonium and depth nitrate were within the correct range, the simulation failed to pick up fluctuations observed in the field data. Although model simulations of the bottom waters predicted the release of ammonium from the sediments during anoxia in the calibration year it was significantly under estimated in the validation year. This under estimation is attributed to the model under estimating the degree of anoxia at a comparable time, thus effecting ammonium release from the sediment. Simulations of total nitrogen at both surface and depth were adequate, although there was a deficit of both dissolved and particulate nitrogen in the modeled system.

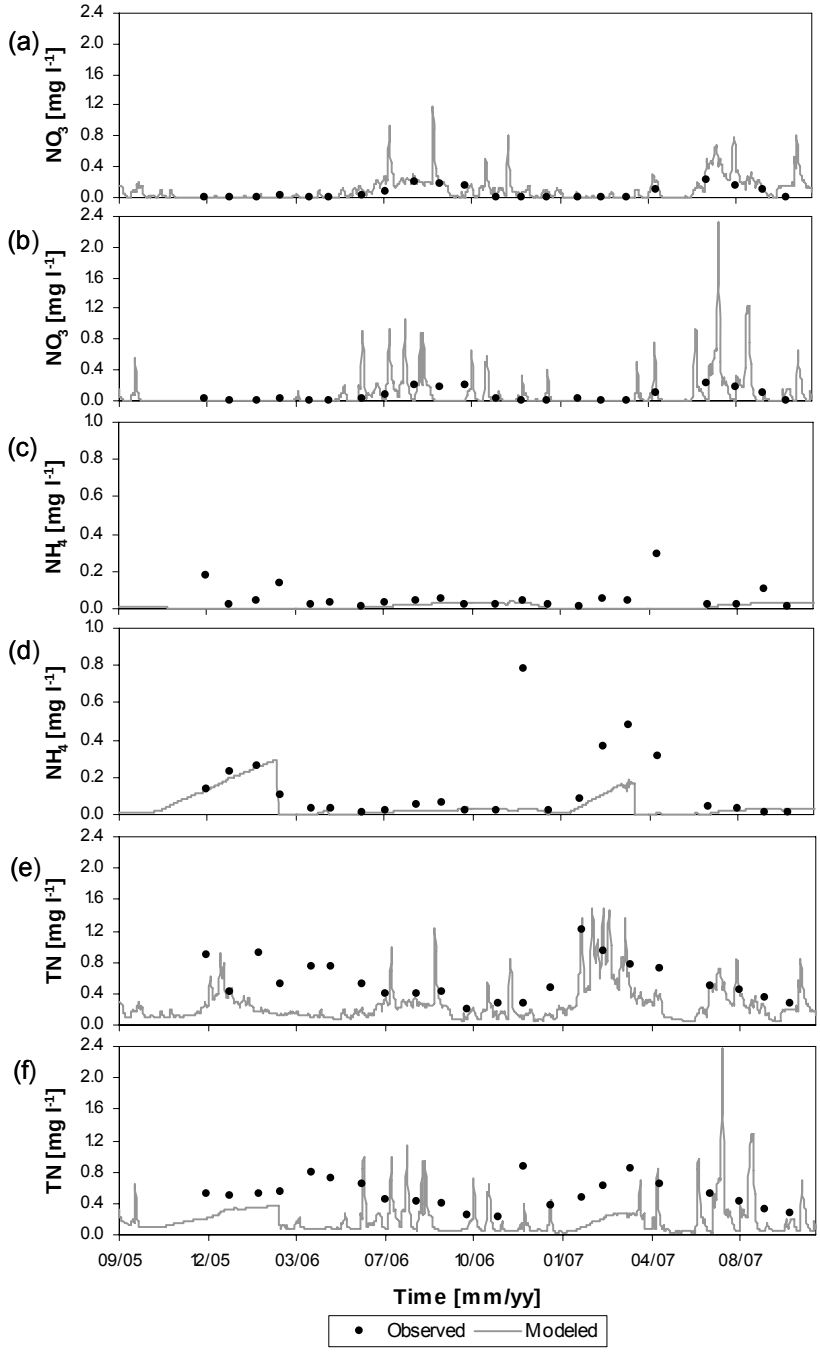


**Figure 3.7.5:** Observed and modeled nitrogen concentrations in the Lower Karori Reservoir, (a) nitrate at 0 m, (b) nitrate at 15 m, (c) ammonium at 0 m, (d) ammonium at 15 m, (e) total nitrogen at 0 m and (f) total nitrogen at 15 m.

**Table 3.11** Statistical comparison between model simulations and observed data for nutrients (nitrate, ammonium, total nitrogen, phosphate and total phosphorus)

| | Surface (0 m) | | | | Depth (15 m) | | | |
|---|---|---|---|---|---|---|---|---|
| | RSME | | R | | RSME | | R | |
| | Calibration | Validation | Calibration | Validation | Calibration | Validation | Calibration | Validation |
| Nitrate | 0.077 | 0.098 | 0.766 | 0.759 | 0.272 | 0.229 | -0.175 | -0.136 |
| Ammonium | 0.079 | 0.084 | -0.184 | -0.213 | 0.041 | 0.112 | 0.956 | 0.709 |
| Total Nitrogen | 0.478 | 0.346 | -0.536 | 0.655 | 0.433 | 0.379 | 0.175 | 0.224 |
| Phosphate | 0.016 | 0.362 | 0.000 | 0.210 | 0.018 | 0.046 | 0.000 | 0.187 |
| Total Phosphorus | 0.051 | 0.057 | -0.562 | -0.324 | 0.048 | 0.050 | 0.513 | 0.121 |

Simulations of both nitrogen and phosphorus involved extensive calibration and the use of some relatively extreme values (Appendix III) to reproduce anything resembling observed data. Unfortunately both phosphate and total phosphorus were still simulated with relatively poor results (Table 3.11; Fig. 3.7.6) and were not simulated with the same accuracy as inorganic and organic nitrogen. Phosphate and total phosphorus at the surface and depth both demonstrated dramatic increases between July and February and only become relatively depleted between February and June. This response appeared related to what was seen in the observed total phosphorus data, while no meaningful trends could be surmised by the observed phosphate data due to a lack of analytical resolution.

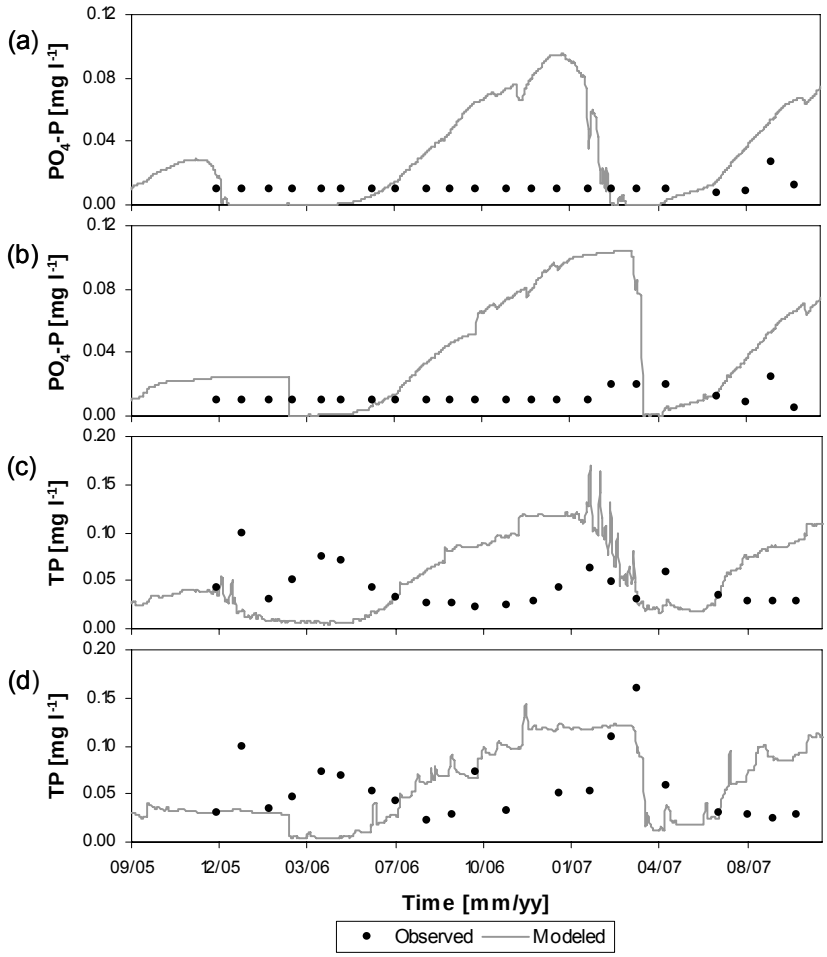


**Figure 3.7.6:** Observed and modeled phosphorus concentrations in the Lower Karori Reservoir, (a) phosphate at 0 m, (b) phosphate at 15 m, (c) total phosphorus at 0 m and (d) total phosphorus at 15 m.

## 3.7.4 Phytoplankton

Cyanobacteria concentrations in the surface were simulated relatively well (Table 3.12; Fig. 3.7.7), capturing both seasonal and inter-annual variability as seen in the observed data. Increases in cyanobacterial concentrations occurred at the onset of stratification. As stratification ended and the surface and bottom waters became fully mixed, cyanobacterial densities began to decrease. Although the magnitude of the 2005/6 bloom was simulated well, the time at which it occurred was not well simulated. The simulations peaked approximately three months before the observed data. The bloom in the calibration year was predicted well, with both the timing and intensity of the bloom captured with great accuracy.

**Table 3.12** Statistical comparison between model simulations and observed data for surface concentrations of *Anabaena planktonica*, *Staurastrum* sp. and chlorophyll *a*

| | RSME | | R | |
|---|---|---|---|---|
| | **Calibration** | **Validation** | **Calibration** | **Validation** |
| *A. planktonica* | 49.755 | 38.316 | -0.333 | 0.641 |
| *Staurastrum* | 0.156 | 0.331 | 0.000 | -0.112 |
| Chlorophyll *a* | 49.501 | 38.780 | -0.099 | 0.679 |

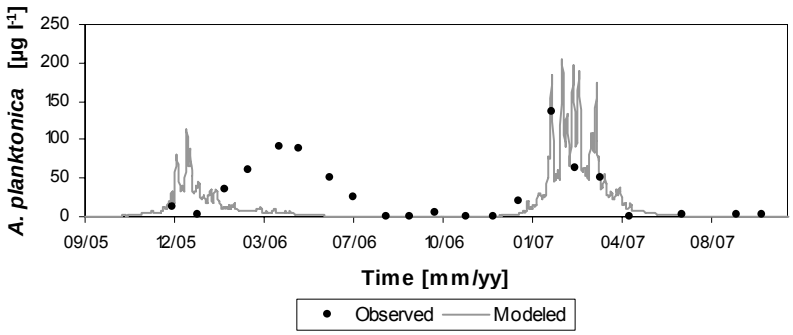


**Figure 3.7.7:** Observed and modeled *Anabaena planktonica* concentrations in the Lower Karori Reservoir at 0 m.

## 3.7.5 Management Scenarios

The greatest reduction in concentrations of *A. planktonica* in DYRESM-CAEDYM occurred through decreasing the residence time of the water in LKR to approximately five days. A 99 % reduction in biomass was achieved. Surface concentrations did not exceed 0.5 µg $l^{-1}$ even though waters remained stratified similar to those with a residence time of over a year. Simulations of artificial destratification were effective in keeping the reservoir from stratifying, although short-lived periods of anoxia still occurred at depths between 14 and 16 m. It also proved effective in reducing *A. planktonica* biomass, with a 94 % reduction over a 2-year period. Surface concentrations also did not exceed 7.5 µg $l^{-1}$ at times when a bloom event would normally have been expected. Simulations with control of the internal load proved largely ineffective in limiting the *A. planktonica* concentrations. Simulations modelling limitation of firstly phosphate and secondly ammonium sediment fluxes showed only a 5.9 and 5.8 % reduction of *A. planktonica* biomass respectively, and the combined phosphate and ammonium limitation showed almost no change. *Staurastrum* sp. only responded in a significant way to the reduction of residence time, with a 13 % reduction in biomass and artificial destratification with a 459 %

biomass increase, although not exceeding concentrations of 5.3 µg $l^{-1}$. The effect of each modeled scenario on total chlorophyll *a* concentrations is shown in Fig. 3.7.8.

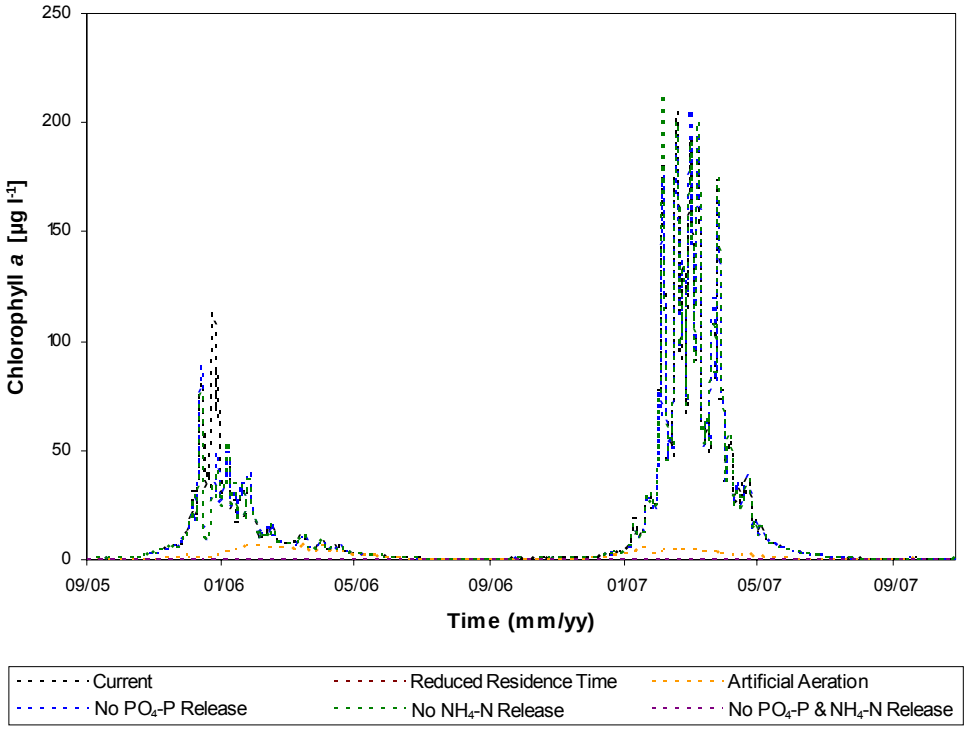


**Figure 3.7.8:** Changes in chlorophyll *a* concentrations as a result of modeled management scenarios.

# 4 Discussion

## *4.1 Phytoplankton composition and environmental variables*

There is a distinct reduction in inorganic nitrogen concentrations in the Lower Karori Reservoir (LKR) when it is thermally stratified. This is a result of *Anabaena planktonica* growth and proliferation under the favorable thermal conditions, leading to the exhaustion of both ammonium and nitrate stores in surface waters. This is also exemplified by the increase of total nitrogen relative to ammonium and nitrate at these times, inferring that the majority of nitrogen in the system during stratified conditions is organic, encapsulated in *A. planktonica* cells. As a result of inorganic nitrogen depleted conditions *A. planktonica* responds physiologically by producing heterocytes through the differentiation of vegetative cells. This physiological adaptation permits *A. planktonica* to fix atmospheric nitrogen dissolved within the water column, a supply that is unlikely ever to be exhausted, under nitrogen depleted conditions (Tandeau de Marsac & Houmard, 1993; Hitzfeld *et al.*, 2000). This adaptation is critical in permitting the dominance of *A. planktonica* in the LKR, as *A. planktonica* is not only able to survive but can thrive even with severe limitation of dissolved inorganic nitrogen.

Elevated levels of ammonium in surface waters compared with nitrate indicate a low oxidation state associated with recycling of large amounts of organic nitrogen (Hicks *et al.*, 2007). Different forms of inorganic nitrogen favor different algal groups, the regime of ammonium dominance in the LKR suits cyanobacteria over eukaryotic phytoplankton, which favor nitrate as their main nitrogen source (Blomqvist *et al.*, 1994; Hyenstrand *et al.*, 1998). Compared with other algae *A. planktonica* is relatively unaffected by the form of total inorganic nitrogen (TIN) (Guerrero & Lara, 1987), owing to their ability to fix atmospheric nitrogen (Reynolds & Walsby, 1975). In the LKR nitrate concentrations exhibit noticeable increases during isothermal conditions, due to reduced denitrification and increased nitrification rates associated with re-oxygenation of the water column. Total phosphorus and total nitrogen have comparable temporal patterns where concentrations tend to increase during periods of

stratification and reduce during periods of isothermy. Such increases of total phosphorus and total nitrogen in surface concentrations are largely attributable to the internal phosphorus and nitrogen stores of the *A. planktonica* population. *Anabaena* spp. have the ability to not only fix atmospheric nitrogen but also store phosphorus in excess of their immediate cellular requirements (Reynolds & Walsby, 1975). Elevated levels at depth are largely a result of phosphate and ammonium release from the sediment-water interface under anoxic conditions (Jeppesen *et al.*, 2005). Reduced levels during isothermal conditions are caused by the system being fully mixed, resulting in thoroughly oxygenated bottom waters and the loss of the adaptive advantage *A. planktonica* had under stratified conditions (Smith, 1983).

Increased temperatures coinciding with stratification help drive cyanobacterial dominance. First by surface waters attaining temperatures near optimal for growth (~ 25 °C) (Robarts & Zohary, 1987) and secondly by strengthening stratification providing a means in which their buoyancy regulation can be used as an adaptive advantage (Paerl, 1988). In growth rate experiments undertaken in this study *A. planktonca* had the highest growth rates at 25 °C (see Section 4.3).

High pH values (~ 10) recorded in surface samples in LKR during stratification are likely to be the result of the elevated photosynthetic activities of *A. planktonica* (Kellar & Paerl, 1980). These high pH values are indicative of carbon dioxide ($CO_2$) depletion, whereby the rate at which $CO_2$ is used exceeds the rate at which $CO_2$ can be resupplied by diffusion at the water-atmosphere interface. These conditions created by *A. planktonica* in the LKR therefore promote their dominance over other phytoplankton as they reduce $CO_2$ concentrations to levels that limit most other phytoplankton (Shapiro, 1997). This is primarily due to their ability to utilize bicarbonate directly; this is the dominant form of inorganic carbon at pH 9 (Paerl, 1988). This response was observed in LKR cell counts; chlorophyte and bacillariophyte concentrations become considerably reduced throughout February, especially at the surface, coinciding with times of pH values exceeding 9. However, it is not possible to discount limitation by phosphorus, for example, at this time.

These results are in agreement with those of Shapiro (1973) who observed cyanobacteria to outcompete chlorophye and bacillariophyte species under similar conditions.

Light attenuation decreased noticeably during bloom conditions due to the high concentrations of *A. planktonica*. *Anabaena planktonica* buoyancy and dominance at the water surface therefore not only permits access to an increased availability and quality of photosynthetically active radiation (PAR), but also indirectly reduces the light climate for other phytoplankton species that may be more evenly distributed through the surface mixed layer (Paerl, 1988; Huisman, 1999). Such conditions also favor *A. planktonica* and other cyanobacteria due to their superior light harvesting systems (Tilzer, 1987; Tandeau de Marsac & Houmard, 1993).

According to Paerl (1988) buoyancy in nitrogen-fixing cyanobacertia such as *Anabaena* spp., is heavily influenced by PAR and inorganic carbon availability. Deficiencies in PAR availability (Walsby & Booker, 1980) and/or inorganic carbon availability (Paerl & Ustach, 1982) cause increased buoyancy. This appears to be the case in LKR as during stratified conditions pH becomes strongly elevated at the surface (indicative of $CO_2$ depleted conditions) and light attenuation is considerably reduced. Buoyancy inferred under such conditions averts sedimentation losses (Reynolds & Walsby, 1975; Reynolds, 1984) but migration to deeper waters overnight, provides access to limiting resources, such as nitrogen and phosphorus in vertically stratified waters (Ganf & Oliver, 1982). Conversely during periods of isothermy, not only is the advantage of vertical migration lost, but pH is also reduced below 9. This results in a reduced dominance of *A. planktonica* relative to other species representing phyla such as chlorophyes and bacillariophytes under such conditions.

The seasonal variation of phytoplankton could be attributed to availability of resources (Carpenter *et al.*, 2000) and species-specific adaptive responses to thermal stratification or lack thereof (Oliver & Ganf, 2000). Cyanobacteria dominated the

assemblage during periods of significant stratification, while several chlorophyte, dinophyte and bacillariophyte species comprised the assemblage during isothermal conditions. This seasonal pattern perfectly demonstrates how cyanobacterial adaptations such as buoyancy regulation and their ability to fix atmospheric nitrogen impart advantages over other species under stratified conditions (Smith, 1983; Paerl, 1988). These advantages are nullified under conditions of isothermy, where mixing of the water column dramatically reduces the advantages of being positively buoyant (Paerl, 1988) and increases nutrients at the water surface, allowing other species to compete better (Smith, 1983).

Multivariate analysis showed that long term variations in the phytoplankton community in LKR were not especially dependent on temperature and that total nitrogen and nitrate were the main correlative factors. Although the ordination failed to recognize the importance of temperature associated with stratified conditions, it roughly split stratified and isothermal conditions over the positive and negative sides of axis 1. The ordination placed the cyanobacterial species *A. planktonica* and *A. circinalis* strongly on the side commonly associated with stratified conditions. The ordination also placed *A. planktonica* near the total nitrogen and total phosphorus vectors, likely owing to their internal nitrogen and phosphorus stores, with the former also related to the ability to fix nitrogen.

Environmental variables explained considerably less variation of phytoplankton assemblages with CCA than in other recent studies. Celik and Ongun (2007) explained 60% and 67% of the variance of the dominant phytoplankton species of two inlets in shallow hypertrophic lake. Stream discharge and secchi depth were shown to be the most important environmental variables in one system and stream discharge and pH in the other. Lopes *et al.* (2005) explained 49% of the variance in the phytoplankton assemblage of a shallow oligotrophic reservoir on axis 1 of a CCA ordination, with temperature revealed as the most important variable in the ordination. This value of Lopes *et al.* (2005), was considerably higher than the 26% of species data explained by the set of variables analysed in the present study.

Although using a similar suite of explanatory variables, the LKR analysis may have explained less of the phytoplankton variance due to a lack of useful variables such as a measurement of light penetration and an accurate dataset for phosphate compared with the studies by Celik and Ongun (2007) and for pH compared with Lopes *et al.* (2005). pH may explain significant amounts of variation in cyanobacteria as elevated pH levels are associated with cyanobacterial blooms and also favour their development (Paerl, 1988).

Application of the *A. planktonica* Taqman QPCR assay developed by Rueckert *et al*. (2008) allowed a large number of samples to be processed in a relatively short period of time. Achieving such high throughput using conventional microscopic counts would have been laborious and time consuming. The assay was sensitive and able to detect low levels of *A. planktonica*. QPCR results highlighted diurnal trends whereby concentrations of *A. planktonica* increased at the surface throughout the course of a day, peaking at 1900 hours, and then decreased again over the course of the evening. Such diurnal variation in surface concentrations is associated with gas vacuolate species such as *A. planktonica*. Diurnal vertical migration has been well documented in species such as *A. circinalis* (Reynolds, 1972) and *Microcystis aeruginosa* (Reynolds & Walsby, 1975). The accumulation of carbohydrate as a result of photosynthesis throughout the course of a day causes a reduction in buoyancy, resulting in low surface concentrations late in the day as they descend deeper in the water column. Throughout the evening their carbohydrate stores are used up, and they again become positively buoyant and return to surface waters (Oliver, 1994; Oliver & Ganf, 2000). Reynolds (1972) reports migration rates for *A. circinalis* of up to 50 m $d^{-1}$. The trend in the LKR seems unusual in that *A. planktonica* appears to peak late in the day rather than early in the morning as would be expected under normal bloom forming conditions (Oliver, 1994; Oliver & Ganf, 2000). This may be a result of the relatively shaded nature of the LKR, where its surrounding topography in relation to the rising and setting of the Sun, limits the amount PAR the system receives on a daily basis. This creates a time lag thus gas-vacuolate species reach

their diurnal peaks in concentration later in the day than would have normally have been expected.

Cyanobacterial blooms only began in LKR when the water residence time went from approximately five days to almost a year (Hicks *et al.*, 2007). Therefore it is likely that high abundances of first *A. lemmermannii* and *A. circinalis*, and later *A. planktonica* in the LKR were enhanced by the increased residence time. Cyanobacteria are more susceptible to lake flushing than other phytoplankton due to their longer generation times (Reynolds, 2002). Celik and Ongun (2007) showed that higher *A. spiroides* concentrations were related to lower discharge rates and longer residence times in the Kocacay Inlet of Lake Manyas, Turkey.

## *4.2 Biomanipulation*

In addition to the physical and chemical influences outlined above, biotic interactions between trophic levels appear to play a significant role in the formation of *A. planktonica* blooms in LKR. Results of the *Perca fluviatilis* removal indicate the possibility of a trophic cascade being initiated within the LKR, although it is not possible to identify in the limited time period of this study if the response of cyanobacteria and zooplankton populations to *P. fluviatilis* removal is a byproduct of normal seasonal trends, or if the *P. fluviatilis* removal was a success. The *P. fluviatilis* removal appeared to have had an immediate effect on cyanobacterial densities within the reservoir, a similar response has been observed in other systems (e.g., Hansson *et al.*, 1998; Lammens, 1999; Gulati & van Donk, 2002).

Zooplankton assemblage changes immediately post-removal were associated with a dramatic decrease in rotifers and an increase in cladocerans (e.g., *Daphnia* sp.). *Daphnia* spp. are considered among the most effective zooplankton species in controlling phytoplankton blooms (Leibold, 1989). This observed increase was probably attributable to reduced predation pressure on the cladocerans through the reduction in *P. fluviatilis* biomass (I. Duggan, pers. comm.). *Perca fluviatilis* as with

most planktivouris fish are known to selectively predate on the large bodied zooplankton such as cladoceans (Gliwicz & Pijanowska, 1989), this is partly due to their larger size (Hall *et al.*, 1976). Reduced predation pressure on cladocerans may have indirectly enabled cladocerans to compete effectively with the rotifer population (Ian Duggan, pers. comm.), who can graze a broader range of phytoplankton size classes and morphologies (Sterner, 1986). This would have resulted in an increased predation pressure on the *A. planktonica* population.

The response of both the zooplankton and phytoplankton assemblages to the *P. fluviatilis* removal tends to support the view that certain zooplankton are in fact large enough to consume filamentous cyanobacteria such as *A. planktonica*. It has been suggested that zooplankton do not predate on cyanobacteria owing to production of toxins by them (Paerl *et al.*, 2001; Ghadouani *et al.*, 2003) or because of their large size, with phytoplankton taxa larger than 30 μm considered inedible for many zooplankton species (Burns, 1968). Recent evidence suggests that cyanobacteria can be consumed by zooplankton, especially large bodied organisms such as *Daphnia* spp. (Work & Havens, 2003). Work and Havens (2003), in a study on eutrophic subtropical Lake Okeechobee, USA, found that all species of macrozooplankton sampled had consumed cyanobacteria, including *A. circinalis* and *M. aeruginosa*. They also demonstrated that consumption of cyanobacteria was most common in *Daphnia* spp. (~70% of phytoplankton consumed were cyanobacteria) and that consumption of filamentous cyanobacteria was greater than that of colonial species. Work and Havens (2003) concluded that regardless of the mechanism, consumption of cyanobacteria may be a common occurrence in other lakes with dense cyanobacteria populations and a low abundance of other food resources. Hairston *et al.* (2001) and Sarnelle and Wilson, (2005) also recently demonstrated phenotypic plasticity of *Daphnia* spp. which adapted to the presence of toxic cyanobacteria in their diet.

The responses of the zooplankton and phytoplankton assemblages to the *P. fluviatilis* removal support the findings of Smith & Lester (2006), who demonstrated a shift in

the relative abundance of zooplankton species between enclosures with and without *P. fluviatilis*. Smith and Lester (2006) found in treatments with *P. fluviatilis* that larger zooplankton species decreased in abundance relative to treatments without *P. fluviatilis*.

Meijer *et al.* (1994) summarized the effects of food web manipulations on three Dutch lakes (Lake Zwemlust, Lake Bleiswijkse Zoom and Lake Noorddiep) and one Danish lake (Lake Væng) over a 4-5 year period. By reducing the biomass of zooplanktivorous fish Meijer *et al.* (1994) noted an initial increase in large *Daphnia* sp., a reduction in phytoplankton biomass and increased water quality. In time as planktivorous fish again began to increase, the systems began to revert to their pre-manipulation state. Hicks *et al.* (2007) suggest that that a concerted effort at reducing the *P. fluviatilis* population in the LKR, in conjunction with ongoing control, via netting and electrofishing could reduce *P. fluviatilis* abundance to a point at which their effect on the zooplankton would be minimal.

## *4.3 Temperature and light growth experiments*

Growth rates of *A. planktonica* in general increased with higher temperatures and light intensities. Highest growth rates were recorded at temperatures of 25 °C. This observation is in agreement with the findings of Imamura (1981) who showed the optimal temperature of *Anabaena* sp. to be 25 °C. Growth rates ranging between 0.08 (20 µmol $m^{-2}$ $s^{-1}$) and 0.25 $day^{-1}$ (25 °C) were in general lower than *Anabaena* spp. growth rates found in other studies. Lee and Rhee (1999) reported growth rates of 0.99 $day^{-1}$ for *A. flos-aquae* and Tsujimura and Okubo (2003) gave growth rates of 0.78 $day^{-1}$ for *A. ucrainica* under optimal conditions. Growth rates were also lower than those reported for other bloom forming cyanobacteria, such as *M. aeruginosa* which are reported by Watanabe and Oishi (1985) to grow at rates of 0.44 $day^{-1}$ at 25 °C.

Interestingly, a drop in temperature from 25 °C to only 10 °C resulted in only a 44% reduction in growth rate and the growth rates at 10 and 20 °C were not markedly

different. This suggests *A. planktonica* has the ability to tolerate and grow at a wide range of temperatures. This may give *A. planktonica* an advantage over other *Anabaena* spp. by enabling it to survive in a pelagic vegetative state throughout the winter and may in part explain why this species has become a dominant bloom forming species throughout the North Island during the past five years (Ryan *et al.*, 2003; Wood *et al.*, 2004). Even during the winter months *A. planktonica* filaments were present in the LKR phytoplankton community and during the two years of sampling, akinetes in *A. planktonica* were only observed for one week in mid-winter. By surviving in a vegetative state this species would have the ability to grow quicker than species that require akinete germination under specific conditions optimal for this process.

The ability of *A. planktonica* to grow at very low irradiance levels may also give it a competitive advantage over other phytoplankton and cyanobacterial species. During summer months when there were dense surface blooms, light did not penetrate far into the water column. It was quite common, however, to find moderate (5,000 – 10,000 cells $ml^{-1}$) concentrations of *A. planktonica* in the samples collected at 10 and 15 m.

Lower concentrations at the stationary phase in the 20 and 40 μmol $m^{-2}$ $s^{-1}$ treatments relative to the 60 and 140 μmol $m^{-2}$ $s^{-1}$ treatments indicate light induced limitation at lower intensities. This may demonstrate that concentrations of *A. planktonica* found in depth samples (i.e. 10 and 15 m) in the LKR, are likely a result of buoyancy regulation providing access to vertically partitioned resources, rather than the depth at which they carry out photosynthesis.

## *4.4 Modelling and bloom control strategies*

The model DYRESM-CAEDYM demonstrated positive results in capturing the seasonal changes of temperature, dissolved oxygen and cyanobacterial dynamics that were influenced strongly by stratification in LKR. Nutrient species, and in particular total phosphorus and phosphate were not replicated with the same success.

The model suggests that *A. planktonica* blooms are strongly associated with periods of thermal stratification, and not by nutrients owing to the relative depletion of inorganic nutrients, especially nitrogen species, at such times. This supports monitored data outlined previously, whereby it is suggested that physiological adaptations of *A. planktonica*, namely buoyancy and nitrogen-fixing capabilities, are driving their dominance.

The model had some problems, with dissolved oxygen and ammonium not well replicated from year to year, during the validation step. Temperature was not especially well replicated at depth, especially at the beginning and break up of stratification. These problems are linked, with the temperature deviations resulting in some difficulties with dissolved oxygen and ammonium fluxes. Some of this effect is probably attributable to the model being unable incorporate the effects of wind direction and the shape of the surrounding topography in relation wind speed, and subsequently the mixing regime. This is problematic in situations like LKR which is within a steep valley, causing northerly or southerly winds to be intensified due to a "funnel-like" effect and easterly and westerly winds to be largely nullified due to sheltering. In essence winds along the main axis of the lake have a long fetch while those from other angles may have a much smaller fetch though these winds may also be modified by the local topography to become more aligned with the lake axis. Simulations of temperature showed that the extent of mixing was underestimated during the onset of stratification in 2005 but less so the following year. Another problem is associated with use of daily mean wind speed as model input. While this is may be practical, it is not accurate as wind speed, unlike other parameters such as shortwave radiation and temperature, affects the process of mixing and stratification over a much shorter time scale (i.e., sub-daily). Other confounding influences may include the use of meteorological data gathered from four different sources and the fact that the time frame in which was used to validate the model included Wellington Airport's coldest December air temperatures since records began (Hicks *et al.*, 2007).

Inflow rates inferred through changes in the UKR water level, and a corresponding shortage of nutrient inflow measurements may have resulted in inaccuracies in nutrient loads entering the system. This may have contributed to the weak relationships between modeled and observed nutrient data.

According to Dokulil and Teubner (2000) although it is generally necessary to reduce the nutrient load from the catchment of the lake to reduce cyanobacterial dominance, management scenarios must also consider the species involved in combination with lake depth and stratification pattern. Therefore my study involved the simulation of in-lake controls as a means to reduce both nutrient levels and cyanobacterial biomass, through the inactivation of nutrients from the system. Here scenarios simulating the effects of reducing internal loading of nitrogen, phosphorus, and both phosphorus and nitrogen through sediment capping all proved ineffective in controlling *A. planktonica* concentrations. This supports the findings of Smith and Lester (2006) who used mesocosm studies to elucidate the effects of nutrient inputs on cyanobacterial densities, and suggested that a removal of *P. fluviatilis* would have a more pronounced effect on the cyanobacterial populations relative to management options associated with nutrient limitation.

Fogg (1969) and Reynolds and Walsby (1975) suggest favorable physical conditions such as stratified waters, act synergistically with nutrient enrichment for maximal bloom concentrations to occur. Although this may be true, several studies have demonstrated strong vertical mixing to significantly reduce cyanobacterial blooms irrespective of the nutrient concentration (Paerl, 1988). This supports the findings of this study, which through model simulations suggest that the implementation of an artificial destratification system would be the most effective and practical means of controlling the cyanobacterial bloom forming species *A. planktonica* within LKR. Visser *et al.* (1996) demonstrated the effects of artificial destratification on hypertrophic Lake Nieuwe Meer, near Amsterdam, which successfully prevented surface *Microcystis* spp. blooms. Mixing in this instance also caused a shift in the species composition to dominance of non-cyanobacterial taxa, as a result of reduced

sedimentation and enhanced silicate availability, which was advantageous to diatom species.

Cyanobacteria with a longer generation time relative to other phytoplankton taxa are generally associated with systems of high residence times and are therefore more susceptible lake flushing (Reynolds, 2002). Model simulations, increasing the inflow of the reservoir and subsequently reducing the water residence time to approximately 5 days, as was the case when it was part of the Wellington water supply (Hicks *et al.*, 2007) reduced cyanobacterial concentrations considerably. Although this method proved even more effective that that of destratification, reinstatement of the original inflow is unlikely to be practical or economical

It is suggested, based on the various management scenarios modeled, that artificial destratification be considered as a means of controlling the *A. planktonica* blooms in LKR. Such methods may be more aesthetically pleasing for a tourist attraction such as the Karori Wildlife Sanctuary than drawing down the reservoir level and poisoning fish (Hicks *et al.*, 2007).

# 5 Conclusions

The phytoplankton assemblage of Lower Karori Reservoir (LKR) shows distinct temporal variations that appear to be primarily driven by thermal structure. Thermally stratified periods coincide with *Anabaena planktonica* dominance. *Anabaena planktonica* has the ability to regulate its buoyancy enabling it to access vertically partitioned resources associated with stratified periods. Results suggest under such a thermal regime *A. planktonica* capitalises on these conditions enabling them to out-compete other phyla. Such responses include; depletion of total inorganic nitrogen as a result of growth, reduction of euphotic depth due to absorption of PAR and increased pH due to enhanced photosynthetic rate. Such conditions created by the large *A. planktonica* biomass are detrimental to other phytoplankton which lack nitrogen-fixing capabilities and are therefore more competitive under nitrogen replete conditions. Other eukaryotic phytoplankton also do not have the additional photosynthetic pigments or buoyancy regulation ability and are thus not able to compete as well under PAR-limitation or reduced inorganic carbon levels at high pH. Under isothermal conditions advantages inferred through buoyancy regulation become considerably reduced owing to increased mixing of the water column and vertically homogenous nutrient concentrations. Thus during isothermal conditions in LKR phytoplankton community is a mixture of phyla, including chlorophytes, bacillariophytes and small flagellated dinophytes. Isothermal conditions also result in a reduction of sedimentation rates and a relative increase in resource availability, such as photosynthetically active radiation (PAR) and nutrients, favouring the mixed phytoplankton assemblage.

In addition to thermal stratification, biotic interactions between trophic levels appear to play a significant role in the formation of *A. planktonica* blooms in LKR. Initial changes in cyanobacteria and zooplankton densities following *Perca fluviatilis* removal suggest the possibility of initiation of a trophic cascade. The removal seems to have resulted in an increase in large Crustaceans (e.g., *Daphnia* sp.) and reduction in *A. planktonica* densities in the months following *P. fluviatilis* removal. Such a response appears to be attributable to reduced predation pressure on large Crustaceans

through the reduction of zooplanktivorus juvenile *P. fluviatilis* within the system. There appears to have been a short term response to *P. fluviatilis* reduction, however, as only a small proportion of the total *P. fluviatilis* population was removed it is therefore unlikely that the effects will be long-lasting. Further *P. fluviatilis* reduction or eradication in the LKR is recommended.

*Ananbaena plantonica* growth experiments showed that this species grew faster at higher temperatures (25 °C) and light intensities (60-140 μmol $m^{-2}$ $s^{-1}$). The growth rates measured under optimal temperatures and light intensities were similar to those measured for other bloom forming *Anabaena* spp. and *Microcystis* spp. Interestingly, however, although there were slight decreases in growth rates, *A. planktonica* could grow reasonably well at low light intensities (20 μmol $m^{-2}$ $s^{-1}$) and temperatures (10 °C). This ability to survive low temperatures may give *A. planktonica* an advantage over other *Anabaena* spp. by enabling it to survive in a pelagic vegetative state throughout the winter. Even during the winter months *A. planktonica* filaments are present in the phytoplankton community and during the 2-year period of sampling, akinetes in *A. planktonica* have only been observed for one week in mid-winter. By surviving in a vegetative state this species would be able to grow quicker than species that require akinete germination, which may occur only when conditions become optimal in spring and summer.

The DYRESM-CAEDYM model simulations also suggested that *A. planktonica* blooms were strongly associated with periods of thermal stratification. Of the five management scenarios simulated using DYRESM-CAEDYM only the scenarios simulating a reduced residence time (> 300 days to 5 days) and implementation of an artificial destratification system emitting air at a rate of 50 $l^{-1}$ $s^{-1}$ were shown significantly reduce *A. planktonica* concentrations. Management techniques associated with reducing internal nutrient cycling proved ineffective. Of the two techniques shown to reduce *A. planktonica* dominance, the most practical is likely to be artificial destratification. Such a technique would prevent thermal stratification and instead result in an isothermal system over summer. Without summer

stratification some of benefits of the physiological adaptations of *A. planktonica* (e.g., buoyancy regulation, nitrogen-fixation) that give it a competitive advantage over other phytoplankton species would be reduced.

# References

Anderson, D. M., Gilbert, P. M., Burkholder, J. M. (2002). Harmful algal blooms and eutrophication: nutrient sources, composition and consequences. *Estuaries, 4B*, 704-726.

Annadotter, H., Cronberg, G., Aagren, R., Lundstedt, B., Nilsson, P.-Å., Ströbeck, S. (1999). Multiple techniques for lake restoration. *Hydrobiologia, 395-396*, 77-85.

Arar, E. J., Collins, G. B. (1997). *In Vitro Determination of Chlorophyll a and Pheophytin a in Marine and Freshwater Algae by Fluorescence*. Cincinnati, Ohio: National Exposure Research Laboratory Office of Research and Development, U.S. Environmental Protection Agency.

Babin, M., Morel, A., Gagnon, R. (1994). An incubator designed for extensive and sensitive measurements of phytoplankton photosynthetic parameters. *Limnology and Oceanography, 39*(3), 694-702.

Badger, M. R., Hanson, D., Price, G. D. (2002). Evolution and diversity of $CO_2$ concentrating mechanisms in cyanobacteria. *Functional Plant Biology, 29*, 161-173.

Benndorf, J. (1990). Conditions for effective biomanipulation; conclusions derived from whole-lake experiments in Europe. *Hydrobiologia, 200/201*, 187–203.

Blomqvist, P., Pettersson, A., Hyenstrand, P. (1994). Ammonium-nitrogen: A key regulatory factor causing dominance of non-nitrogen-fixing cyanobacteria in aquatic systems. *Archiv für Hydrobiologie, 132*, 141–164.

Bolch, C., Blackburn, S. (1996). Isolation and purification of Australian isolates of the toxic cyanobacterium *Microcystis aeruginosa*. *Journal of Applied Phycology, 8*(1), 5-13.

Bruce, L. C., Hamilton, D., Imberger, J., Gal, G., Gophen, M., Zohary, T., Hambright, K. D. (2006). A numerical simulation of the role of zooplankton in C, N and P cycling in Lake Kinneret, Israel. *Ecological Modelling, 193*(3-4), 412-436.

Burch, J. (1997). *The Karori Reservoir Area: A Brief History*. Lower Hutt, Wellington: The Karori Historical Society.

Burns, C. W. (1968). The relationship between body size of filter feeding *cladocera* and the maximum size of particle ingested. *Limnology and Oceanography, 13*, 675-678.

Carmichael, W. W. (1995). The toxins of cyanobacteria. *Scientific American, 270*, 64-72.

Carmichael, W. W. (2001). Health effects of toxin-producing Cyanobacteria: 'The CyanoHABs'. *Human & Ecological Risk Assessment, 7*(5), 1393.

Carpenter, S. R., Ludwig, D., Brock, W. A. (2000). Management of eutrophication in lakes subject to potentially irreversible change. *Ecological Applications, 9*, 751-771.

Carpenter, S. R., Kitchell, J. F., Hodgson, J. R. (1985). Cascading trophic interactions and lake productivity. *BioScience, 35*, 634–639.

Celik, K., Ongun, T. (2007). The relationships between certain physical and chemical variables and the seasonal dynamics of phytoplankton assemblages of two inlets of a shallow hypertrophic lake with different nutrient inputs. *Environmental Monitoring and Assessment, 124*, 321-330.

Chan, T. U., Hamilton, D. P. (1998). Effect of freshwater flow on the succession and biomass of phytoplankton in a seasonal estuary. *Marine and Freshwater Research, 52*, 869-864.

Chorus, I., Bartram, J. (1999). *Toxic Cyanobacteria in Water: A Guide to their Public Health Consequences, Monitoring, and Management*. London: Taylor & Francis.

Clarke, K. R., Ainsworth, M. (1993). A method of linking multivariate community structure to environmental variables. *Marine Ecology Progress Series, 92*, 205-219.

Coles, J. F., Jones, R. C. (2000). Effect of temperature on photosynthesis-light response and growth of four phytoplankton species isolated from a tidal freshwater river. *Journal of Phycology, 36*(1), 7-16.

Coyne, K. J., Handy, S. M., Demir, E., Whereat, E. B., Hutchins, D. A., Portune, K. J., Doblin, M. A., Cary, S. C. (2005). Improved quantitative real-time PCR assays for enumeration of harmful algal species in field samples using an

exogenous DNA reference standard. *Limnology and Oceanography: Methods, 3*, 381-391.

Davies-Colley, R. J. (1988). Measuring water clarity with a black disk. *Limnology and Oceanography, 33*(4), 616-623.

de Bruin, A., Ibelings, B. W., Van Donk, E. (2003). Molecular techniques in phytoplankton research: from allozyme electrophoresis to genomics. *Hydrobiologia, 491*(1-3), 47-63.

Diamond, D. (2000). *QuickChem® Method 10-115-01-1-A, Determination of orthophosphate in waters by flow injection analysis colorimetry*. Lachat Instuments, Milwaukee.

Dokulil, M. T., Teubner, K. (2000). Cyanobacterial dominance in lakes. *Hydrobiologia, 438*(1), 1-12.

Dyble, J., Tester, P. A., Litaker, R. W. (2006). Effects of light intensity on cylindrospermopsin production in the cyanobacterial HAB species *Cylindrospermopsis raciborskii*. *African Journal of Marine Science, 28*, 309-312.

Ebina, J., Tsutsui, T., Shirai, T. (1983). Simultaneous determination of total nitrogen and total phosphorus in water using peroxodisulphate oxidation. *Water Research, 17*, 1721-1726.

Entwisle, T. J., Sonneman, J. A., Lewis, S. H. (1997). *Freshwater Algae in Australia: A Guide to Conspicuous Genera*. Sydney: Sainty & Associates.

Fischer, H. B., List, E. G., Koh, R. C. Y., Imberger, J., Brooks, N. H. (1979). *Mixing in inland and coastal waters*: Academic Press.

Fogg, G. E. (1969). The physiology of an algal nuisance. *Proceedings of the Royal Society of London. Series B, Biological Sciences, 173*, 175-189.

Gal, G., Imberger, J., Zohary, T., Antenucci, J., Anis, A., Rosenberg, T. (2003). Simulating the thermal dynamics of Lake Kinneret. *Ecological Modelling, 162*(1-2), 69-86.

Ganf, G. G., Oliver, R. L. (1982). Vertical separation of light and available nutrients as a factor causing replacement of green algae by blue-green algae in the plankton of a stratified lake. *Journal of Ecology, 70*, 829-844.

Ghadouani, A., Pinel-Alloul, B., Prepas, E. E. (2003). Effects of experimentally induced cyanobacterial blooms on crustacean zooplankton communities. *Freshwater Biology, 48*(2), 363-381.

Glazer, A., Gindt, Y., Chan, C., Sauer, K. (1994). Selective disruption of energy flow from phycobilisomes to Photosystem I. *Photosynthesis Research, 40*(2), 167-173.

Gliwicz, Z. M., Pijanowska, J. (1989). The role of predation in zooplankton succession. In U. Sommer (Ed.), *Plankton ecology: succession in plankton communities* (pp. 253-296). Berlin: Springer-Verlag.

Guerrero, A. G., Lara, C. (1987). Assimilation of inorganic nitrogen. In P. Fay & C. Van Baalen (Eds.), *The Cyanobacteria* (pp. 163-186). Amsterdam: Elsevier.

Gulati, R. D., van Donk, E. (2002). Lakes in the Netherlands, their origin, eutrophication and restoration: state-of-the-art review. *Hydrobiologia, 478*, 73–106.

Gunn, A., Tudhope, K., Cole, D. (2000). Karori Sanctuary – Restoration and environmental ethics. *Planning Quarterly, 138*, 14-16.

Hairston Jr., M. G., Holtmeier, C. L., Lampert, W., Weider, L. J., Post, D. M., Fisher, J. M., Caceres, C. E., J.A., F., Gaedke, U. (2001). Natural selection of grazer resistance to toxic cyanobacteria: evolution of phenotypic plasticity? *Evolution, 55*, 2203-2214.

Hall, D. J., Threlkeld, S. T., Burns, C. W., Crowley, P. H. (1976). The size-efficiency hypothesis and the size structure of zooplankton communities. *Annual Review of Ecology and Systematics, 7*, 177-208.

Hall, R. I., Smoll, J. P. (1992). A weight-averaging regression and calibration model for inferring total phosphorus concentration of diatoms in British Columbia (Canada) lakes. *Freshwater Biology, 27*, 417-434.

Hamilton, D. P., Schladow, S. G. (1996). Prediction of water quality in lakes and reservoirs. Part I - Model description. *Ecological Modelling, 96*(1-3), 91-110.

Hansson, L.-A., Annadotter, H., Bergman, E., Hamrin, S. F., Jeppesen, E., Kairesalo, T., Luokkanen, E., Nilsson, P.-A., Sondergaard, M., Strand, J. (1998). Biomanipulation as an application of food-chain theory: Constraints,

synthesis, and recommendations for temperate lakes. *Ecosystems, 1*(6), 558-574.

Havens, K. E., Phlips, E. J., Cichra, M. F., Li, B. L. (1998). Light availability as a possible regulator of cyanobacteria species composition in a shallow subtropical lake. *Freshwater Biology, 39*, 547-556.

Heid, C. A., Stevens, J., Livak, K. J., Williams, P. M. (1996). Real time quantitative PCR. *Genome Research, 6*, 986-994.

Hicks, B. J., Hamilton, D. P., Ling, N., Wood, S. (2007). Top down or bottom up? Feasibility of water clarity restoration in the lower Karori Reservoir by fish removal: CBER Contract Report No. 54. Report prepared for the Karori Wildlife Sanctuary Trust. Centre for Biodiversity and Ecology Research, Department of Biological Sciences, School of Science and Engineering, The University of Waikato, Hamilton.

Hitzfeld, B., C, Hoger, S., J, Dietrich, D., R. (2000). Cyanobacterial toxins: Removal during drinking water treatment, and human risk assessment. *Environmental Health Perspectives, 108*, 113-122.

Hoare, R. A., Spigel, R. H. (1987). Water balances, mechanics and thermal properties. In W. D. Vant (Ed.), *Lake manager's handbook: A guide to undertaking and understanding investigations into lake ecosystems, so as to assess management options for lakes. Water and Soil Miscellaneous Publication No. 103* (pp. 41-58). Wellington, New Zealand: Water and Soil Division.

Huisman, J. (1999). Population dynamics of light-limited phytoplankton: Microcosm experiments. *Ecology, 80*(1), 202-210.

Humphries, S. E., Lyne, V. D. (1988). Cyanophyte blooms: the role of cell buoyancy. *Limnology and Oceanography, 33*, 79-91.

Hyenstrand, P., Blomquist, P., Pettersson, A. (1998). Factors determining cyanobacterial success in aquatic systems – a literature review. *Special Issues on Advanced Limnology, 51*, 41–62.

Imamura, N. (1981). Studies on the water blooms in Lake Kasumigaura. *Verhandlungen der Internationale Vereinigung fur Theoretische und Angewandte Limnologie, 21*, 652-658.

Jassby, A. D., Platt, T. (1976). Mathematical formulation of the relationship between photosynthesis and light for phytoplankton. *Limnology and Oceanography, 21*(4), 540-547.

Jeppesen, E., Søndergaard, M., Jensen, J. P., Havens, K. E., Anneville, O., Carvalho, L., Coveney, M. F., Deneke, R., Dokulil, M. T., Foy, B., Gerdeaux, D., Hampton, S. E., Kangur, K., Köhler, J., Hilt, S., Lammens, E. H. H. R., Lauridsen, T. L., Manca, M., Miracle, M. R., Moss, B., Nõges, P., Persson, G., Phillips, G., Portielje, R., Romo, S., Schelske, C. L., Straile, D., Tatrai, I., Willen, E., Winder, M. (2005). Lake responses to reduced nutrient loading – an analysis of contemporary long-term data from 35 case studies. *Freshwater Biology, 50*, 1747-1771.

John, D. M., Whitton, B. A., Brook, A. J. (Eds.). (2002). *The freshwater Algal Flora of the British Isles: An Identification Guide to Freshwater and Terrestrial Algae*. Cambridge: Cambridge University Press.

Kellar, P. E., Paerl, H. W. (1980). Physiological adaptations in response to environmental stress during an $N_2$-fixing *Anabaena* bloom. *Applied and Environmental Microbiology, 40*, 587-595.

Kirk, J. T. O. (1994). *Light & photosynthesis in aquatic ecosystems* (2nd ed.). Cambridge: Cambridge University Press.

Kurmayer, R., Kutzenberger, T. (2003). Application of real-time PCR for quantification of microcystin genotypes in a population of the toxic cyanobacterium *Microcystis* sp. *Applied and Environment Microbiology, 69*(11), 6723-6730.

Lammens, E. H. (1999). The central role of fish in lake restoration and management. *Hydrobiologia, 395/396*, 191–198.

Larsen, A., Castberg, T., Sandaa, R., A., Brussaard, C. P. D., Egge, J., Heldal, M., Paulino, A., Thyrhaug, R., van Hannen, E. J., Bratbak, G. (2001). Population

dynamics and diversity of phytoplankton, bacteria and viruses in a seawater enclosure. *Marine Ecology Progress Series 221*, 47–57.

Lee, D., Rhee, G. (1999). Kinetics of growth and death in *Anabaena flos-aquae* (cyanobacteria) under light limited saturation. *Journal of Phycology, 35*(4), 100-709.

Leibold, M. A. (1989). Resource edibility and the effects of predators and productivity on the outcome of trophic interactions. *The American Naturalist, 134*, 922-949.

Lewis, D. M., Brookes, J. D., Lambert, M. F. (2004). Numerical models for management of *Anabaena circinalis*. *Journal of Applied Phycology, 16*(6), 457-468.

Lopes, M. R. M., Bicudo, C., E.M., Ferragut, M. C. (2005). Short term spatial and temporal variation of phytoplankton in a shallow tropical oligotrophic reservoir, southeat Brazil. *Hydrobiologia, 542*, 235-247.

Lynch, J. (1995). Back to the future: Karori - from reservoir to wildlife sanctuary. *Forest and Bird, 275*, 12-19.

Macedo, M. F., Duarte, P., Ferreira, J. G. (2002). The influence of incubation periods on photosynthesis-irradiance curves. *Journal of Experimental Marine Biology and Ecology, 274*(2), 101-120.

Magnhagen, C., Heibo, E. (2004). Growth in length and in body depth in young-of-the-year perch with different predation risk. *Journal of Fish Biology, 64*, 612–624.

Meijer, M. L., Jeppesen, E., van Donk, E., Moss, B., Scheffer, M., Lammens, E., van Nes, E., van Berkum, J. A., de Jong, G. J., Faafeng, B. A., Jensen, J. P. (1994). Long-term responses to fishstock reduction in small shallow lakes: interpretation of five-year results of four biomanipulation cases in The Netherlands and Denmark. *Hydrobiologia, 275/276*, 457-466.

Moore, S. C. (2000). *Photographic Guide to the Freshwater Algae of New Zealand*. Dunedin: Otago Regional Council.

Morrison, S. (1986). *History of Water Supply in the Wellington Region, 1872-1985*. Wellington, New Zealand: Wellington Regional Council.

Oliver, R. L. (1994). Floating and sinking in gas-vacuolate cyanobacteria. *Journal of Phycology, 30*(2), 161-173.

Oliver, R. L., Ganf, G. G. (2000). Freshwater blooms. In B. A. Whitton & M. Potts (Eds.), *The Ecology of Cyanobacteria* (pp. 149-194). Netherlands: Kluwer Academic Publishers.

Paerl, H. W. (1988). Nuisance phytoplankton blooms in coastal, estuarine, and inland waters. *Limnology and Oceanography, 33*(4), 823-847.

Paerl, H. W., Fulton, R. S., Moisander, P. H., Dyble, J. (2001). Harmful freshwater algal blooms, with an emphasis on Cyanobacteria. *The Scientific World, 1*, 76-113.

Paerl, H. W., Ustach, J. F. (1982). Blue-green algal scums: An explanation for their occurrence during freshwater blooms. *Limnology & Oceanography, 27*, 212-217.

Persson, L., Byström, P., Wahlström, E. (2000). Cannibalism and competition in Eurasian perch: Population dynamics of an ontogenic omnivore. *Ecology, 81*(4), 1058-1071.

Pielou, E. C. (1984). *The Interpretation of Ecological Data: A Primer on Classification and Ordination*. New York: John Wiley & Sons.

Pokorný, J., Květ, J. (2004). Aquatic plants and lake ecosystems. In P. E. O'Sullivan & C. S. Reynolds (Eds.), *The Lakes Handbook: Limnology and Limnetic Ecology* (pp. 700). Oxford: Blackwell.

Prescott, G. W., Bamrick, J., Cawley, E. T., Jaques, W. G. (1978). *How to Know the Freshwater Algae*: McGraw-Hill Science/Engineering/Math.

Prokopkin, I. G., Gubanov, V. G., Gladyshev, M. I. (2006). Modelling the effect of planktivorous fish removal in a reservoir on the biomass of cyanobacteria. *Ecological Modelling, 190*(3-4), 419-431.

Prokopy, W. R. (1992). *QuickChem® Method 10-107-06-2-C, Ammonia in surface water, wastewaters.* Lachat Instruments, Milwaukee.

Rasmussen, J. P., Barbez, P. H., Burgoyne, L. A., Saint, C. P. (2008). Rapid preparation of cyanobacterial DNA for real-time PCR analysis. *Letters in Applied Microbiology, In Press*.

Reynolds, C. S. (1972). Growth, gas vacuolation and bouyancy in a natural population of a blue-green alga. *Freshwater Biology, 2*, 87-106.

Reynolds, C. S. (1984). Phytoplankton periodicity: the interactions of form, function and environmental variability. *Freshwater Biology, 14*, 111-142.

Reynolds, C. S. (1997). *Vegetation Processes in the Pelagic: A Model for Ecosystem Theory*. Germany: Ecology Institute.

Reynolds, C. S. (2002). Towards a functional classification of the freshwater phytoplankton. *Journal of Plankton Research, 24*, 417-428.

Reynolds, C. S., Walsby, A. E. (1975). Water-blooms. *Biological Reviews, 50*, 437-481.

Rinta-Kanto, J. M., Ouellette, A. J. A., Boyer, G. L., Twiss, M. R., Bridgeman, T. B., Wilhelm, S. W. (2005). Quantification of toxic *Microcystis* spp. during the 2003 and 2004 blooms in western Lake Erie using quantitative real-time PCR. *Environmental Science & Technology, 39*(11), 4198-4205.

Robarts, R. D., Zohary, T. (1987). Temperature effects on photosynthetic capacity, respiration and growth rates of bloom-forming cyanobacteria. *New Zealand Journal of Marine and Freshwater Research, 21*, 391-399.

Robson, B. J., Hamilton, D. P. (2004). Three-dimensional modelling of a *Microcystis* bloom event in the Swan River estuary, Western Australia. *Ecological Modelling, 174*(1-2), 203-222.

Rueckert, A., Wood, S. A., Cary, S. C. (2008). Development and field assessment of a quantitative PCR for the detection and enumeration of the noxious bloom-former *Anabaena planktonica*. *Limnology and Oceanography: Methods*, In Press.

Ryan, E., Hamilton, D., Burger, D., O'Brien, B., Vant, W. M. (2003). Synchronous blooms of *Anabaena planktonica* in North Island. In N. Miller (Ed.), *Rotorua Lakes 2003, Practical Management for Good Lake Water Quality. Lakes Water Quality Society* (pp. 308-310). Rotorua, New Zealand.

Sarnelle, O., Wilson, A. E. (2005). Local adaptation of *Daphnia pulicaria* to toxic cyanobacteria. *Limnology & Oceanography, 50*, 1565-1570.

Schindler, D. W. (1974). Eutrophication and recovery in experimental lakes: Implications for lake management. *Science, 184*, 897–899.

Schober, E., Kurmayer, R. (2006). Evaluation of different DNA sampling techniques for the application of the real-time PCR method for the quantification of cyanobacteria in water. *Letters in Applied Microbiology, 42*(4), 412-417.

Shapiro, J. (1973). Blue-green algae: Why they become dominant. *Science, 179*, 382-384.

Shapiro, J. (1997). The role of carbon dioxide in the initiation and maintenance of blue-green dominance in lakes. *Freshwater Biology, 37*(2), 307-323.

Shapiro, J., Lamarra, V., Lynch, M. (1975). Biomanipulation: an ecosystem approach to lake restoration. In P. L. Brezonik & J. L. Fox (Eds.), *Water quality management through biological control* (pp. 85-96). Gainesville: University of Florida.

Skovhus, T. L., Ramsing, N. B., Carola Holmström, C., Kjelleberg, S., Dahllöf, I. (2004). Real-time quantitative PCR for assessment of abundance of *Pseudoalteromonas* species in marine samples. *Applied and Environment Microbiology, 70*(4), 2373–2382.

Smith, K. F. (2005). *Trophic interactions promoting dominance by cyanobacteria in a freshwater pelagic food web.* Unpublished MSc thesis, Victoria University, Wellington, New Zealand.

Smith, K. F., Lester, P. J. (2006). Cyanobacterial blooms appear to be driven by top-down rather than bottom-up effects in the Lower Karori Reservoir (Wellington, New Zealand). *New Zealand Journal of Marine and Freshwater Research, 40*, 53-63.

Smith, K. F., Lester, P. J. (2007). Trophic interactions promote dominance by cyanobacteria (*Anabaena* spp.) in the pelagic zone of Lower Karori Reservoir, Wellington, New Zealand. *New Zealand Journal of Marine and Freshwater Research, 41*, 143-155.

Smith, V. H. (1983). Low nitrogen to phosphorus ratios favor dominance by blue-green algae in lake phytoplankton. *Science, 221*, 669-671.

Song, L., Sano, T., Li, R., Watanabe, M. M., Liu, Y., Kaya, K. (1998). Microcystin production of *Microcystis viridis* (cyanobacteria) under different culture conditions. *Phycological Research, 46*(s2), 19-23.

Spigel, R. H., Imberger, J. (1987). A review of mixing processes relevant to phytoplankton dynamics in lakes. *New Zealand Journal of Freshwater Research, 21*, 392–405.

Sterner, R. W. (1986). Herbivores direct and indirect effects on algal populations. *Science, 231*, 605-607.

Tandeau de Marsac, N., Houmard, J. (1993). Adaptation of cyanobacteria to environmental stimuli: new steps towards molecular mechanisms. *FEMS Microbiology Letters, 104*(1-2), 119-189.

Tennessee Valley Authority. (1972). *Heat and mass transfer between a water surface and the atmosphere*: Water Resources Research Laboratory Report 14, Report No. 0-6803.

ter Braak, C. J. F., Similauer, P. (1997). *Biometris-Plant Research International*. The Netherlands: Wageningen.

Tilzer, M. M. (1987). Light-dependence of photosynthesis and growth in cyanobacteria: implications for their dominance in eutrophic lakes. *New Zealand Journal of Marine and Freshwater Research, 21*, 401-412.

Tsujimura, S., Okubo, T. (2003). Development of *Anabaena* blooms in a small reservoir with dense sediment akinete population, with special reference to temperature and irradiance. *Journal of Plankton Research, 25*(9), 1059-1067.

Utermöhl, H. (1958). Zur vervollkommung der quantitativen phytoplankton methodik (Towards a perfection of quantitative phytoplankton methodology). *Mitteilungen der Internationale Vereinigung für Theoretische und Angewandte Limnologie, 9*, 1-38.

Vaitomaa, J., Rantala, A., Halinen, K., Rouhiainen, L., Tallberg, P., Mokelke, L., Sivonen, K. (2003). Quantitative real-time PCR for determination of microcystin synthetase E copy numbers for *Microcystis* and *Anabaena* in lakes. *Applied and Environment Microbiology, 69*(12), 7289-7297.

Vidal, I. L., Frieda Maris-McArthur, G. W. (1973). Limnology of Morton Dam and Upper Karori Reservoir, Wellington, New Zealand. *New Zealand Journal of Marine & Freshwater Research, 7*, 265-300.

Visser, P. M., Ibelings, B. W., van der Veer, B., Koedood, J., Mur, L. R. (1996). Artificial mixing prevents nuisance blooms of the cyanobacterium Microcystis in Lake Nieuwe Meer, the Netherlands. *Freshwater Biology, 36*, 436-450.

Wallace, B. B., Hamilton, D. P. (2000). Simulation of water-bloom formation in the cyanobacterium *Microcystis aeruginosa*. *Journal of Plankton Research, 22*(6), 1127-1138.

Walsby, A. E. (1994). Gas vesicles. *Microbiological Reviews, 58*(1), 94-144.

Walsby, A. E., Booker, M. J. (1980). Changes in buoyancy of a planktonic blue-green alga in response to light intensity. *European Journal of Phycology, 15*, 311-319.

Watanabe, M. F., Oishi, S. (1985). Effects of environmental factors on toxicity of a cyanobacterium (*Microcystis aeruginosa*) under culture conditions. *Applied and Environmental Microbiology, 49(5)*, 1342-1344.

Wendt, K. (2000). *QuickChem® Method 10-107-04-1-A, Determination of nitrate/nitrite in urface and wastewaters by flow injection analysis.* Lachat Instruments, Milwaukee.

Wetzel, R. G. (2001). *Limnology: Lake and River Ecosystems* (Third ed.). California: Academic Press.

Wilhelm, J., Pingoud, A. (2003). Real-time polymerase chain reaction. *ChemBioChem, 4*, 1120-1128.

Wofsy, S. C. (1983). A simple model to predict extinction coefficients and phytoplankton biomass in eutrophic waters. *Limnology and Oceanography, 28*, 1144–1155.

Wood, S. A. (2005). *Bloom forming and toxic cyanobacteria in New Zealand: species diversity, distribution, cyanotoxin production and accumulation of microcystins in selected freshwater organisms.* Unpublished PhD thesis, Victoria University and Massey University, Wellington, New Zealand.

Wood, S., Crowe, A. L. M., Ruck, J. G., Wear, R. G. (2004). New records of planktonic cyanobacteria in New Zealand freshwaters. *New Zealand Journal of Botany, 42*, 479-492.

Wood, S. A., Holland, P. T., Stirling, D. J., Briggs, L. R., Sprosen, J., Ruck, J. G., Wear, R. G. (2006). Survey of cyanotoxins in New Zealand water bodies between 2001 and 2004. *New Zealand Journal of Marine and Freshwater Research, 40*, 585–597.

Work, K. A., Havens, K. E. (2003). Zooplankton grazing on bacteria and cyanobacteria in a eutrophic lake. *Journal of Plankton Research, 25*, 1301-1307.

Yeates, P. S., Imberger, J. (2004). Pseudo two-dimensional simulations of internal and boundary fluxes in stratified lakes and reservoirs. *The International Journal of River Basin Management, 1*, 1-23.

# Appendix I

**Long term data set methods**

On 5 September 2005, Cawthron Research Institute and Waikato University began a long term sampling regime of the Lower Karori Reservoir (LKR). Sampling was carried out from the Valve Tower (Site 1). Water temperature and dissolved oxygen were measured in the field with an YSI Model 58 Meter (YSI Environmental, Yellow Springs, Ohio, USA) at 1 m intervals from the surface to 16 m.

Samples were collected weekly for algal identification and enumeration. These were collected at depths of 0, 5, 10 and 15 m and stored in clean polycarbonate bottles and preserved with lugol's iodine solution (10% (w/v) potassium iodine, 5% (w/v) iodine, 10% (v/v) acetic acid). Every second week (as of 24 July 2006) samples were collected for zooplankton identification and enumeration at depths of 5, 10 and 15 m. Four litres of water from each depth was passed through a 40 µm mesh plankton net and washed into a clean polycarbonate tube using Mill-Q water, and preserved in 95% Ethanol. The three samples were pooled for analysis.

Monthly samples for nutrients (ammonium, nitrate, phosphate, total nitrogen and total phosphorus) and chlorophyll *a* analysis were collected at 0 m and 15 m beginning 12 December 2006.

Algal samples were enumerated and identified by Dr. Susie Wood and Kirsty Smith (Cawthron Institute) using an inverted Olympus microscope (CKX41) and Utermöhl settling chambers (Utermöhl, 1958). Zooplankton samples were identified and counted by Dr. Ian Duggan (Waikato University).

Nutrient samples were analysed by Greater Wellington Regional Council Water Quality Testing Lab between 12 December 2005 and 7 June 2006 and by Environmental Laboratory Services Ltd. from 4 July 2006 to present.

Between 12 December 2005 and 7 June 2006 ammonium was analysed using the APHA 20th Edition 4500-NH3 F method, nitrate the APHA 20th Edition 4110 B method, total nitrogen the Chemiluminescence Gas Analyser method, phosphate the APHA 20th Edition 4110 B method and total phosphorus the APHA 20th Edition 4500-P B&E method. Chlorophyll *a* was measured using the APHA 20th Edition 10200 H Method.

Since 4 July ammonium has been analysed via flow injection analysis following the APHA 21st Edition Method 4500 NH3-G, LAS official test 4.5, 5.10. Nitrate using ion chromatography following USEPA 300.0 (modified), LAS official test 5.13. Total nitrogen using the APHA 21st edition method 4500-NO3 F after being digested in persulphate following APHA 21st Edition 4500-N C. Phosphate using flow injection analysis following the APHA 21st edition method 4500-P F. Total phosphorus using the APHA 21st edition method 4500-P F after digestion in persulphate following the APHA 21st Edition 4500-P B method. Chlorophyll *a* was measured using the APHA 20th Edition 10200 H Method.

# Appendix II

**Preparation of MLA Medium Primary Stock Solutions**

**1.** $MgSO_4.7H_2O$ — 49.4 g $l^{-1}$ $dH_20$
**2.** $NaNO_3$ — 85.0 g $l^{-1}$ $dH_20$
**3.** $K_2HPO_4$ — 6.96 g $l^{-1}$ $dH_20$
**4.** $H_3BO_3$ — 2.47 g $l^{-1}$ $dH_20$
**5.** $H_2SeO_3$ — 1.29 mg $l^{-1}$ $dH_20$
**6.** Vitamins

*Working Stock Solution*
to 100 ml of distilled water, in order, add the following:
Thiamine HCl — 10.0 mg
0.05 ml of the following primary stocks (each made up separately):

*Primary Stocks (per 100 $ml^{-1}$ $dH_20$)*
Biotin — 10.0 mg
Vitamin B12 — 10.0 mg

**7.** Micronutrients

*Working Stock Solution*
to 800 ml of distilled water, in order, add the following (mixing to dissolve each addition):

| | |
|---|---|
| $Na_2EDTA$ | 4.36g (stir on low heat to dissolve) |
| $FeCl_3.6H_2O$ | 1.58g |
| $NaHCO_3$ | 0.60g |
| $MnCl_2.4H_2O$ | 0.36g |

10 ml of the following primary stocks (each made up separately):

*Primary Stocks (per $l^{-1}$ $dH_20$)*

| | |
|---|---|
| $CuSO_4.5H_2O$ | 1.0 g. |
| $ZnSO_4.7H_2O$ | 2.2 g. |
| $CoCl_2.6H_2O$ | 1.0 g. |
| $Na_2MoO_4.2H_2O$ | 0.6 g. |

Finally, make up the micronutrient stock to 1 litre with distilled water. If precipitate forms increase pH up to 7.

Store all primary stock solutions in the refrigerator.

**Preparation of MLA medium Intermediate Stock Solutions**

**1.** Distilled Water — 1 $l^{-1}$
Autoclave to sterilize
**2.** MLA Medium ×40 concentrated nutrients
To 130 ml distilled water add:
$MgSO_4.7H_2O$ — 10 $ml^{-1}$
$NaNO_3$ — 20 $ml^{-1}$

| | |
|---|---|
| $K_2HPO_4$ | 50 $ml^{-1}$ |
| $H_3BO_3$ | 10 $ml^{-1}$ |
| $H_2SeO_3$ | 10 $ml^{-1}$ |
| Vitamin stock | 10 $ml^{-1}$ |
| Micronutrient stock | 10 $ml^{-1}$ |

Filter sterilize using a 0.22µm filter into a sterile 250 ml Schott bottle.

**3.** $NaHCO_3$ 16.9 g $l^{-1}dH_2O$

Autoclave to sterilize

**4.** $CaCl_2.2H_2O$ 29.4 g $l^{-1}dH_2O$

Autoclave to sterilize

Store all intermediate stock solutions in the refrigerator.

**Preparation of MLA medium Solution**

In a sterile 1000 ml Schott bottle add aseptically, mixing well after each addition.

| | |
|---|---|
| **1.** sterile distilled water (**1**) | 964 ml |
| **2.** sterile MLA Medium ×40 concentrated nutrients (**2**) | 25 ml |
| **3.** sterile $NaHCO_3$ (**3**) | 10 ml |
| **4.** sterile $CaCl_2.2H_2O$ (**4**) | 1 ml |

MLA medium is now ready to be decanted aseptically into sterile culture flasks.

# Appendix III

**Appendix Table 1** Physical data parameters used in the DYRESM parameter file.

| Parameter | Value | Unit |
|---|---|---|
| Bulk aerodynamic momentum transport coefficient | 0.0013 | |
| Mean albedo of water | 0.06 | |
| Emissivity of a water surface | 0.96 | |
| Critical wind speed | 20 | $m\ s^{-1}$ |
| Bubbler entrainment coefficient | 0.006 | |
| Buoyant plume entrainment coefficient | 0.083 | |
| Shear production efficiency | 0.06 | |
| Potential energy mixing efficiency | 0.5 | |
| Wind stirring efficiency | 0.3 | |
| Effective surface area coefficient | 130000 | |
| BBL dissipation coefficient | 0 | |
| Vertical mixing coefficient | 430 | |

**Appendix Table 2** Dissolved oxygen parameters used in the CAEDYM data file.

| Parameter | Value | Unit |
|---|---|---|
| Temperature multiplier for sediment oxygen demand | 1.05 | |
| Static sediment exchange rate | 1 | $g\ m^{-2}\ d^{-1}$ |
| Half saturation constant for static DO sediment flux | 0.4 | $mg\ l^{-1}$ |

**Appendix Table 3** Particulate organics, dissolved organics, dissolved inorganics and sediment flux parameters used in the CAEDYM data file.

| Parameter | Value | Unit |
|---|---|---|
| Particulate organics | | |
| Max transfer of POPL to DOPL | 0.02 | $d^{-1}$ |
| Max transfer of PONL to DONL | 0.001 | $d^{-1}$ |
| POML Diameter | 0.000025 | m |
| POML Density | 1050 | $kg\ m^{-3}$ |
| Critical shear stress for POML resuspenison | 0.002 | $m^{-2}$ |
| Dissolved organics | | |
| Max mineralisation of DOPL to $PO_4$ | 0.05 | $d^{-1}$ |
| Max mineralisation of DONL to $NH_4$ | 0.001 | $d^{-1}$ |
| Dissolved inorganics | | |
| Denitrification rate coefficient | 2.5 | $d^{-1}$ |
| Half saturation constant for denitrification | 8 | $mg\ l^{-1}$ |
| Nitrification rate coefficient | 0.003 | $d^{-1}$ |
| Half saturation constant for nitrification | 5 | $mg\ l^{-1}$ |
| Sediment flux parameters | | |
| Release rate of $PO_4$ | 0.000001 | $g\ m^{-2}\ d^{-1}$ |
| Controls sediment release of $PO_4$ via Oxygen | 2 | $g\ m^{-3}$ |
| Release rate of $NH_4$ | 0.005 | $g\ m^{-2}\ d^{-1}$ |
| Controls sediment release of $NH_4$ via Oxygen | 0.5 | $g\ m^{-3}$ |
| Release rate of $NO_3$ | 0 | $g\ m^{-2}\ d^{-1}$ |
| Controls sediment release of $NO_3$ via Oxygen | 0.5 | $g\ m^{-3}$ |